NANO- AND MICROSCALE ANALYSIS OF AMINO ACIDS AND PROTEINS USING CAPILLARY LIQUID CHROMATOGRAPHY AND CAPILLARY ELECTROPHORESIS

By

BRENDAN W. BOYD

A DISSERTATION PRESENTED TO THE GRADUATE SCHOOL
OF THE UNIVERSITY OF FLORIDA IN PARTIAL FULFILLMENT
OF THE REQUIREMENTS FOR THE DEGREE OF
DOCTOR OF PHILOSOPHY

UNIVERSITY OF FLORIDA

1999

ACKNOWLEDGMENTS

I would like to thank my advisor, Dr. Robert T. Kennedy, for his generous support and guidance during my graduate studies, as well as the members of the Kennedy group who also provided me with guidance and created an enthusiastic learning environment throughout my stay at the University of Florida. I am especially thankful for the support provided by my mother throughout this period of my life. I am also thankful for the influence of my grandparents who initiated this journey early in my life with stories about mythology, nature, and history.

TABLE OF CONTENTS

pages

ACKNOWLEDGMENTS ii

ABSTRACT v

CHAPTERS

1 INTRODUCTION 1

Monitoring Neurotransmitter Amino Acids (NTAAs) 2
Quantitative Amino Acid Analysis 3
Amino Acid Derivatization Reagents 5
Quantitative Analysis Using Precolumn Derivatization 11
Detection Limits 12
Role of Separation in Amino Acid Analysis 15
Increasing Concentration Sensitivity 17
Microcolumn Liquid Chromatography 19

2 SUB-NANOMOLAR DETETECTION OF γ-AMINOBUTRYRIC ACID SECRETION FROM SINGLE PANCREATIC ISLETS OF LANGERHANS 32

Introduction 32
Experimental 36
Results and Discussion 39

3 COMPREHENSIVE, SUB-NANOMOLAR ANALYSIS OF NEUROTRANSMITTER AMINO ACIDS: MONITORING DURING *in vivo* MICRODIALYSIS WITH 10 s TEMPORAL RESOLUTION 53

Introduction 53
Experimental 55
Results and Discussion 62

4 AUTOMATED, HIGH SENSITIVITY AMINO ACID ANALYSIS 80

Introduction 80
Experimental 83
Results and Discussion 86

5 PROFILING AMINO ACID SECRETION FROM SINGLE PANCREATIC ISLETS OF LANGERHANS 109

Introduction 109
Experimental 113
Results and Discussion 117

6 RAPID, HIGH SENSITIVTIY ASSAY FOR HUMAN CREATINE KINASE ISOENZYMES USING CAPILLARY ELECTROPHORESIS 128

Introduction 128
Experimental 131
Results and Discussion 134

7 CONCLUSIONS 152

APPENDICES

A CONSTRUCTION OF PACKED CAPILLARY LIQUID CHROMATOGRAPHY COLUMNS 155

B FAMOS USER-PROGRAM 158

C PCR PLATE ADAPTER 160

REFERENCES 161

BIOGRAPHICAL SKETCH 172

Abstract of Dissertation Presented to the Graduate School
of the University of Florida in Partial Fulfillment of the
Requirements for the Degree of Doctor of Philosophy

NANO- AND MICROSCALE ANALYSIS OF AMINO ACIDS AND PROTEINS USING CAPILLARY LIQUID CHROMATOGRAPHY AND CAPILLARY ELECTROPHORESIS

By

BRENDAN W. BOYD

August 1999

Chairman: Robert T. Kennedy
Major Department: Chemistry

In this work, strategies for nano- and microscale analysis utilizing microcolumn separations are presented for the purpose of monitoring changes in amino acid secretion from biological specimens. The trace levels of amino acids in these samples required the development of methods possessing lower concentration limits of detection than those currently available. This was accomplished using a combination of on-column preconcentration, scavenging reactions after derivatization, high sensitivity electrochemical detection, and protocols to minimize amine contamination. Sub-nanomolar detection limits ($0.06 - 0.18 \times 10^{-9}$ M) are obtained for all of the neurotransmitter amino acids, greater than 10-fold lower compared to other conventional or microcolumn methods. The use of high resolution capillary liquid chromatography column and gradient elution permit the separation of 20 amino acids and primary amines from over 40 primary amines found in biological samples. These amino acids include:

the excitatory neurotransmitters aspartate and glutamate, the inhibitory neurotransmitters glycine and γ-amino-n-butyric acid, the suspected neurotransmitters or neuromodulators taurine, β-alanine, and serine, as well as arginine and citrulline which are indicators of the nitric oxide production. The sensitivity and resolving power of this method permitted amino acid secretion to be profiled during *in vivo* microdialysis, from single, pancreatic islets of Langerhans, and during the early stages of cellular development and differentiation.

This method was used to reduce temporal resolution for *in vivo* microdialysis 60-fold compared to conventional methods. The ability to monitor all of these amino acids during *in vivo* studies allows the interaction between different neurotransmitter systems to be observed. Utilizing fraction collection and 10 s sampling, 200 nL dialysate samples were collected for analysis using this high sensitivity technique. To facilitate sample manipulation, the 200 nL fractions were diluted to 2 μL prior to analysis. Changes in amino acid secretion were monitored during potassium-induced depolarization as well as during a selective uptake inhibition of γ-amino-n-butyric acid using a pharmacologically active reagent. All of these studies were performed with 10 s temporal resolution. The precision was improved by automating the sample manipulation and injection system and the separation time was reduced to 7 min using the linear solvent strength theory.

CHAPTER 1
INTRODUCTION

The determination of amino acids in complex, biological samples requires high sensitivity detection and high resolution separation methods capable of detecting trace levels of these compounds from a large number of endogenous compounds found in living systems. Due to the wide variety of roles that amino acids play in protein structure, metabolism, development, and neurochemistry, the development of systems to analyze this class of analytes has received significant attention since the introduction of the first amino acid analyzer (Spa58). As interest in analyzing amino acids has grown in several areas of biology and chemistry, the methods used to analyze amino acids have been pushed to their limits both in terms of resolving power and sensitivity.

With the development of microscale analytical systems, the mass sensitivity of amino acid analysis has been increased to a level where the amino acid content of single cells can be analyzed (Ken89a, Oat90, Gil95). However, since these microscale methods provide concentration sensitivity similar to conventional scale methods, specialized sample handling and micro-injectors techniques were required to prevent excessive dilution of the nanoliter samples (Ken89a, Oat90, Gil95).

In this work, microscale analytical techniques are used in conjunction with sample preconcentration to obtain very low mass and concentration limits of detection for nanoliter, biological samples. Sample manipulation was performed using conventional

microdispensors and injection valves by diluting the samples to microliter volumes prior to analysis. This approach required the development of quantitative methods for analyzing amino acids at sub-nanomolar concentrations. To enhance the concentration sensitivity of the microanalytical system used in this work, sample preconcentration of 500 nL volumes from 2 μL samples was used to obtain the necessary concentration sensitivity. With this level of concentration sensitivity, it was necessary to minimize both amine contamination and the chemical background resulting from the derivatization chemistry. Once optimized, this method was used to increase the temporal resolution for monitoring changes in amino acid neurotransmitter level during *in vivo* microdialysis studies (a 60-fold increase) and to profile amino acid secretion from single pancreatic islets of Langerhans, which has not previously been demonstrated.

Monitoring Neurotransmitter Amino Acids (NTAAs)

The amino acid neurotransmitters are subdivided into two groups, the excitatory neurotransmitters aspartate (ASP) and glutamate (GLU) which cause depolarization of cells expressing receptors specific for these molecules, and the inhibitory neurotransmitters, glycine (GLY), taurine (TAU), and γ-amino-n-butyric acid (GABA) that result in hyperpolarization of cells expressing their receptors. These amino acids have been demonstrated to play significant roles in several neurochemical processes such as memory and learning, as well as diseases such as Parkinson's, Alzheimer's, and epilepsy (Smi96a). Of these NTAA's, the major excitatory and inhibitory neurotransmitters are GLU and GABA, respectively (Figure1-1). Analytical methods

used to monitor the NTAA's must possess sufficient selectivity to resolve these molecules from the numerous other small, primary amines in the brain (Figure 1-2).

To monitor NTAA changes in living systems, *in vivo* sampling techniques such as microdialysis are used. Microdialysis is a sampling technique used to monitor extracellular concentrations of neurotransmitter in living brains with both temporal and spatial resolution (Ung84). These time-resolved measurements allow the neurobiological function of neurotransmitters to be studied and correlated to either pharmacological or behavioral stimulation. The neurotransmitters and all other small molecules present in the extracellular space of the brain are sampled by concentration dependent diffusion across a small dialysis membrane (Figure 1-3). In addition to sampling the extracellular neurotransmitters, these probes can also be used to introduce reagents directly into the extracellular space to monitor the pharmacological response by supplementing the artificial cerebrospinal fluid (aCSF) with the pharmacological agent as it is perfused through the probe. To prevent neurotransmitter depletion and to reduce disturbances to the tissue, the probe is perfused at low volumetric flow rates (0.5-3.0 μL/min). The effluent from the probe can be coupled directly to on-line microscale analyzers or collected for off-line analysis. Using conventional methods to analyze for amino acid content, the sampling time or temporal resolution is typically limited to 10-30 min to collect sufficient mass and volume of sample for analysis.

Quantitative Amino Acid Analysis

High sensitivity methods of amino acid utilize derivatization reactions to enhance the detectability of the amino acids. These derivatization reactions also impart similar

detection characteristics to the amino acids. Originally, in the work of Spackman, Stein, and Moore, the amino acids were separated using ion-exchange chromatography followed by post-column derivatization using ninhydrin and absorbance-based detectors (Spa58). However, the absorbance detector used in this work obtained only nanomole sensitivity and the gradient elution, ion-exchange chromatography required very long separation times. The detection limits have been improved somewhat using fluorogenic reagents that are not fluorescent until reacted with an amine, and fluorescence detection, but the sensitivity of this method is limited by the post-column derivatization scheme. Since derivatization reagent is added after the separation, post-column reactions inherently dilute sample zones eluting from the chromatography column decreasing sensitivity (increasing detection limits). Also, these detectors suffer from a large, continuous background fluorescence caused by trace level amines present in the mobile phases and derivatization buffer that also decrease sensitivity. While some post-column detection schemes have been reported using microscale separations to improve the mass sensitivity of amino acid analysis, the sensitivity for amino acid analysis is relatively poor (Old97, Cob98, Pen88, Ros88).

Another method of analyzing amino acids is based on pre-column derivatization followed by separation of the derivatized amino acids and high sensitivity detection. This allows the use of either fluorogenic or fluorescent labeling reagents, since the excess reagent is separated after the labeling reaction eliminating any chemical background. The mode of separation used in conjunction with pre-column derivatization is typically reversed-phase chromatography since the majority of fluorogenic or fluorescent labeling reagents utilize organic fluorophores. The use of gradient or isocratic elution depends on

the number of amino acids that are to be analyzed. For many biomedical applications such as plasma analysis, where several amino acids are analyzed, the use of gradient elution is required since the derivatized amino acids have a wide range of hydrophobicities (Lin79, God84). For applications where only a few amino acids are monitored, isocratic elution can be used. In similar applications to those using isocratic analysis, capillary zone electrophoresis (CZE) separations and high sensitivity detection have been used to obtain impressive mass detection limits for some amino acids. While the theoretical separation efficiencies for CZE are higher than those for liquid chromatographic-based techniques (Gid91), the ability to resolve the large number of amino acids present in biological samples is difficult since many of the amino acid derivatives possess similar electrophoretic mobilities (Smt97). A significant exception is in the analysis of ASP and GLU, which are easily resolved from each other and virtually all the other amino acids due to their large, negative, electrophoretic mobilities (Lad97). The use of micellar electrokinetic chromatography (MEKC) has been used to increase the resolution of the other NTAAs by introducing a hydrophobic partitioning mechanism in capillary electrophoresis, however, the ability to resolve all the NTAAs from the numerous amines commonly found in biological samples has not been demonstrated (Beq94, Smt97). Amino acid derivatives are more easily resolved in liquid chromatography since several different separation parameters can be optimized to achieve the necessary selectivity and resolution (Lin79, Jar86). The detection method used in pre-column derivatization based methods is dependent on the absorbance, fluorescent, electrochemical, or chemiluminescent properties of the derivatization reagent used.

Amino Acid Derivatization Reagents

In a survey of the literature and recent reviews on amino acid analysis, over 40 reagents cited in well over 1000 articles (Institute for Scientific Information, ISI, www.webofscience.com) have been used for amine derivatization (Bar97, Bov94, Ohk94, Fek96). A majority of these reagents are fluorescent labeling reagents that use an amine reactive moiety such as an isothiocyanate or succinimidyl ester to link a highly fluorescent reporter group such as fluorescein or rhodamine to the amino acid (Figure1-7). This produces highly fluorescent amino acid derivatives that can be detected at the zeptomole levels in diluted solution using a sheath flow cuvette and high sensitivity laser-induced fluorescence (Che88). While these reagents produce highly fluorescent derivatives, they are not widely used in quantitative analysis because the excess derivatization reagent and side-products are also highly fluorescent making trace level analysis difficult due to the large fluorescent background (Arr95, Lau98). While it has been recently reported that succinimidyl ester-based fluorescent labeling chemistry produces fewer side products relative to isothiocyanate-based labeling reagents, there remains a 300-fold discrepancy between the detection limits between *in situ* derivatized samples and instrumental detection limits determined using derivatized, diluted standards (Lau98).

Fluorogenic reaction chemistry was developed to minimize the background fluorescence of the derivatization reagent for high sensitivity detection of the highly fluorescent, derivatized amino acids. At the present time, all the fluorogenic reagents that have been used in quantitative analysis are amine reactive. Fluorescamine, a fluorogenic reagent, reacts rapidly (<1 s) with a primary amine in basic solutions to form fluorescent

and unstable pyrrolinone lactones (Figure 1-7, Und72). The fluorescamine reagent rapidly hydrolyzes in aqueous solutions on a similar timescale, requiring this reagent be stored in 100% organic solution prior to use. An apparent side reaction of the pyrrolinone lactones is intramolecular conversion to pyrrolinone acid alcohols that result in two peaks for each amino acid when separated using reversed phase separations (Mch76). As a result of its instability in aqueous solution and the formation of multiple products, this reagent is not widely used in amino acid analysis with precolumn derivatization.

Another class of amine reactive, fluorogenic reagents is based on the *o*-phthalaldehyde (OPA) reagent introduced by Roth in 1971 (Rot71). In OPA derivatizations, the dialdehyde rapidly reacts with a nucleophile and primary amine in basic solution to form a highly fluorescent and electroactive isoindole (Sim78a, Jos83) (Figure 1-6). Originally, organic thiols such as β-mercaptoethanol (β-ME) and ethanethiol were used as the nucleophile, however the use of these thiols produce isoindole derivatives of some amino acids that are highly unstable and decompose rapidly to non-fluorescent and non-electroactive products (Sto83). It was found that the amino acids with straight, unbranched side chains (β-alanine, γ-amino-n-butyric acid) degraded at significantly higher rates than amino acids with branched side chains (alanine and β-amino-n-butyric acid) and that the degradation rate increased proportionally with the OPA concentration (Sto83). Since it has been demonstrated that a 200-fold excess of OPA relative to the total amine content of the sample is required for a reproducible, quantitative reaction for biological samples, reducing the OPA concentration to decrease the degradation rate is not a viable approach (Lin79). In a search for thiols that convey

an increased stability to these derivatives relative to β-ME, it was observed that *tert*-butyl thiol, produced γ-amino-n-butyric acid derivatives that demonstrated a decay half-life of 410 min, 42-fold longer than the corresponding β-ME-based derivative (Jac86). While the derivatives of *tert*-butyl thiol are highly stable, the fluorescence yield has been reported to be 10-fold lower than that of the β-ME derivatized amino acids (All84). However, the electrochemical properties of the isoindoles were unaffected by the bulkier thiol, indicating that the electrochemical properties of these derivatives are not as sensitive to structural changes as fluorescence. After this work, a wide variety of alternative thiols and nucleophiles have been used for OPA-based derivatization schemes including sulfite and cyanides with greater stability relative to β-ME (Table 1-1, references within). The fluorescent (F) properties of many of these reagents have been found to be quite similar; however, the electrochemical (E) properties of many of these derivatives have not been explored. Chiral thiols have also been used with this reagent to react with chiral amino acids to form diasteromers that can be separated using traditional reversed-phase chromatography or micellar electrokinetic chromatography (Table 1-1, references within).

Table 1-1: Nucleophiles used in OPA reaction

Nucleophile	**Det.**	**Chiral**	**Ref.**
β-mercaptoethanol (β-ME)	F,E	No	Sim78a, Joe83
Ethanethiol	F	No	Sim77
3-mercaptopropinoic acid (3-MPA)	F	No	God84
2-methyl-2-propane thiol (tert-butyl)	E	No	All84
Sulfite	F,E	No	God97, Jac87
Cyanide	F	No	Dem87
N-acetyl-L-cysteine	F	Yes	Asw84
Boc-L-cysteine	F	Yes	Buc84
N-acetyl-D-penicillamine	F	Yes	Buc87
N-isobutyryl-L-cysteine	F	Yes	Bru89
2,3,4,6-terta-O-acetyl-1-thio-β-D-glucopyranose	F	Yes	Ein87

A series of fluorogenic reagents that produce amino acid derivatives possessing either enhanced fluorescence properties relative to OPA derivatives or whose excitation wavelengths more closely match commercially available lasers have recently been introduced (Dem87, Bea90, Liu91). These reagents also form isoindoles with a modified structure but similar stability to OPA derivatives based branched thiols such as 3-MPA (Figure 1-7, Table 1-2). Naphthalene-2,3-dicarboxaldehyde (NDA), a dialdehyde similar to OPA but incorporating a naphthalene backbone, was developed to provide fluorescent products with greater stability to OPA; however, it was found that the fluorescent yield of the amino acid alanine derivatized with NDA and cyanide (CN^-) was 2.85-fold higher than alanine derivatized using OPA/β-mercaptoethanol (Dem87). The reagents 3-(2-furoyl)quinoline-2-carbaldehyde (FQ) and 3-(4-carboxybenzoyl)-2-quinolinecarboxaldehyde (CBQ) are aroylaraldehydes that also use CN^- and were developed to produce fluorescent amino acid derivatives with excitation maxima closer to the helium-cadmium (442 nm) and argon-ion (488 nm) lasers (Bea90, Liu91). At the present time, there is insufficient information to compare either the relative fluorescent yield or quantum yield (Φ) of CBQ derivatized amino acids to NDA or OPA derivatives. However, from the difference in quantum yield for the glycine derivative of both NDA/ CN^- and FQ/ CN^- (both in an aqueous matrix), it is not obvious that an increase in fluorescence properties was obtained by the modification of this reagents. This group of reagents requires significantly longer reaction times relative to OPA (Table 1-2). It is also important to note neither NDA, CBQ, nor FQ can be in solution with CN^- until initialization of the derivatization reaction. This is required to reduce CN^--catalyzed degradation of NDA, benzoin condensation, and cyanohydrin formation (Dem87, Bea90,

Liu91, Roa87, Arr95). The formation of small crystals in the microliter samples has also been observed using NDA which can be disastrous for microcolumn separations (Oat90, Boy98). Interestingly, the alkane thiol derivatives of these derivatives are highly unstable preventing their use with chiral thiols for chiral analysis (Dem87).

Table 1-2: Properties of fluorogenic reagents and derivatives in aqueous solution

Reagent	Reaction Time (min)	λ_{ex} (nm)	λ_{ex} (nm)	Φ	Ref.
Fluorescamine	<0.01	381	470	0.1	Che79
o-Phthalaldehyde (OPA)	< 1	340	450	0.4	Sim78, Che79
Naphthalene-2,3-dicarboxaldehyde (NDA)	15	420	490	0.75	Dem87, Mat87
3-(2-Furoyl)quinoline-2-carbaldehyde (FQ)	45 (37° C)	480	590	0.3	Bea90
3-(4-Carboxybenzoyl)-2-quinolinecarboxaldehyde (CBQ)	60	450	550	N.A.	Liu91

Recently, a new class of strictly electrogenic reagents has been described that are reactive towards both primary and secondary amines (Ros99). The homogentisic γ-lactone tetrahydropyranyl ether (HLTE) acylates primary or secondary amines at basic pH to form amide intermediates that are transformed into the hydroquinone-amine derivative by an acidification step to cleave (via hydrolysis) the tertahydropyranyl protecting groups (Figure 1-8). The *p*-nitrophenyl 2,5-dihydroxyphenylacetate, bis-tetrahydropyranyl ether (NDTE) reagent reacts with both primary and secondary amines to form a similar final product. Neither reagent was observed to have native electrochemical activity at electrode potentials less than +0.55 V at a carbon disk electrode (vs. Ag/AgCl), however, once reacted with the primary amine the hydroquinone moiety is freed from the protecting groups via acidification and can be detected at +0.35 V. However, the HLTE reagent reacts slowly producing final yields of less than 2-5%

for a 30 min reaction time. The NDTE reagent is substantially more reactive than HLTE (generating a 95% yield for a 30 min reaction), but is technically not electrogenic since the excess reagent is converted into an electrochemically active homogentisic acid that is electrochemically active in the same potential window as the final NDTE derivatized amines. Since these reagents are hydroquinone-based, the electrochemical reaction is reversible, making signal amplification possible using recycling electrochemical detectors.

Quantitative Analysis Using Precolumn Derivatization

There is a considerable number of methods for the precolumn derivatization of amino acids, and determining the appropriate method from this vast body of articles can be challenging (Table 1-4). Of the large number of method papers for each derivatization reagent, there are several that are the most heavily cited (Table 1-5).

Table 1-4: Citations for methods using different reagents

Reagent	**Citations (1977-present)**	**Ref.**
OPA	> 1000	ISI
NDA	93	ISI
FQ	1	ISI
CBQ	6	ISI

Table 1-5: Citations for different methods used for amino acid analysis

Reagent	**Ref.**	**Citations (1977-present)**
OPA-βME	Lin79	1055
OPA-βME	Jon81	473
OPA-βME	Jon83	358
OPA/tert-butyl thiol	All84	165
OPA/3-MPA	God84	150
NDA	Dem79	140

When first introduced for amino acid analysis, methods based on precolumn derivatization were validated against assays using traditional amino acid analyzers (Lin79, God84). Several important observations regarding the derivatization reaction were made that are worthy of note. Since the total amine content of the samples in precolumn derivatization is considerably higher than individual amino acid zones eluting from an ion exchange columns, the amount of derivatization reagent needed for precolumn derivatization is considerably higher than post-column methods (Lin79). For post-column derivatization with OPA/β-ME, the concentration of OPA and thiol after post-column mixing are greater than 1 mM (Har80). This large amount of derivatization reagent is required for fast, pseudo-first order reaction kinetics (Lin79). Even using derivatization solutions containing 62.5 mM OPA (after derivatization) was found to be insufficient for directly analyzing biological fluids such as urine, plasma, or cerebrospinal fluids that contained large concentrations of amino acids, proteins, and other primary amines (Lin79, God84). This required the total amine content of the sample be lowered by dilution prior to sample derivatization (Lin79, God84). Using a 200-fold excess of OPA to total primary amine content, intra-assay validation between ion-exchange chromatography and precolumn derivatization was achieved (Lin79, God84), however when this ratio fell to below 100, discrepancies of 5-30% were seen between the pre-column and post-column methods (Lin79). When this protocol is not followed, it is not uncommon for methods using lower ratios to report low values for some amino acids or that certain amino acids are not present in the sample all together (Jon83, Uhe91).

Detection Limits

When reviewing detection limits reported in the literature, several factors should be taken into account. Since microscale techniques are inherently more mass sensitive, the methods utilizing conventional or microbore columns (0.32 – 4.6 mm inner diameter columns) are listed in Table 1-5 while methods based on microscale columns (0.62 – 75 μm inner diameter) are listed in Table 1-6. The methods are listed in descending concentration sensitivity and the range of detection limits for the NTAAs analyzed by these methods are also included. The detection limits are reported using a signal-to-noise ratio of 3, and were recalculated if necessary. In addition to the NTAAs, ARG and CIT, the substrate and product of the nitric oxide (NO) producing enzyme that can be used to estimate changes in NO, were also included. For the methods in Table 1-5, both isocratic and gradient liquid chromatography are used. The isocratic methods (Table 1-5) are typically selective for ASP and GLU or GABA, while the gradient methods include at least one addition amino acid (GLY, TAU, or GABA).

The popularity of the OPA-based methods (14 of 15) is due to the large body of work regarding retention mechanism of these isoindoles (Lin79, Jar86, All84) and compatibility with automation (one reagent addition, short reaction time). The lowest concentration limits of detection (CLOD) are obtained using the NDA/CN^- reagent; however, the detection limits obtained in this study were made by derivatizing a 50 μM amino acid solution and then diluting with distilled water prior to analysis for the purpose of eliminating any background (Roa87). While valid for assessing analyte detectability or instrumental limits of detection, this methodology is not useful for quantitative analysis. As expected, the methods utilizing microbore columns (Qu98, Smo95, Keh98a,

Keh98b, God97, Fur90) obtained lower MLODs relative to the methods using conventional bore columns.

Table 1-5: Detection limits using conventional and microbore separation columns

Reagent	Det.	Analytes	MLOD (fmol)	CLOD (nM)	Times Cited	Ref.
1. NDA/CN	F	ASP, GLU, GLY	0.16-0.01	0.01-0.05	90	Roa87
2. OPA/tert-butyl thiol	E	ASP, GLU, GLY, TAU, GABA	1-60	0.1-6.0	0	Qu98
3. OPA/tert-butyl thiol	E	GABA	10	1	13	Smo95
4. OPA/3-MPA	F	ASP, GLU, TAU, GABA	28-64	1.7-3.2	0	Bia99
5. OPA/β-ME	F	ASP, GLU	20-30	2.0-3.0	1	Keh98a
6. AQC	F	ASP, GLU, GLY, GABA	66-150	3.3-7.6	0	Liu98
7. OPA/β-ME	F	ASP, GLU, GLY, TAU, GABA	50	5.0	1,055	Lin79
8. OPA/β-ME	F	ASP, GLU, GLY, TAU, GABA, ARG	50	10	478	Jon81
9. OPA/sulfite	E	GABA	1.3	5.2	0	God97
10. OPA/3-MPA	F	ASP, GLU, GLY	6	6.0	83	Fur90
11. OPA/tert-butyl thiol	E	ASP, GLU, GLY, TAU, GABA	60-1000	6.0-100	13	Smo95
12. OPA/β-ME	F	ASP, GLU	80	8.0	13	Smo95
13. OPA/tert-butyl thiol	E	ASP, GLU, GLY, TAU, GABA	30-150	30-150	165	All84
14. OPA/β-ME	F	GABA	1.7	34	0	Keh98b
15. OPA/3-MPA	F	ASP, GLU, GLY, TAU, GABA, ARG, CIT	800	40	150	God84
16. OPA/3-MPA	F	ASP, GLU, GLY, TAU, GABA, ARG, CIT	180	180	83	Fur90

The amino acids derivatized with OPA/β-ME, OPA/3-MPA, OPA/*tert*-butyl thiol, and NDA/CN$^-$ have been demonstrated to produce isoindoles with very similar fluorescent and electrochemical sensitivity (Che79, God84, All84, Chap 4, Roa87,

Dem87, Mat87) with the exception of LYS which is double-labeled using all these reagents (Che79, God84, All84, Roa87). Interestingly, the double-labeling is observed to cause a significant decrease in fluorescence yield that has been attributed to intramolecular quenching (Che79, God84) but a two-fold increase in electrochemical signal (Pal87). While some differences for inter-assay detection limits of amino acids are expected, the large variations (17- to 60-fold) seen for some methods is unexplained (Qu98, Smo95). The large variations in detection limits could be due to background peaks co-eluting with the derivatives that artificially increase detector response, however, since blanks are not included in for a majority of these studies (exceptions, Liu98, Keh98a, Keh98b) it is impossible to determine if background peaks contribute to this problem. Another possible factor for these results is the low concentration of OPA used to directly derivatize samples without dilution. For these methods, the final concentration of OPA was 2.5 mM (Qu98, Smo95) directly in the sample compared to 3.75 mM in 20-fold diluted samples (Lin79, God84) or 20-33 mM in undiluted samples (All84, Jar86). In several methods, the final OPA concentration ranged from ~0.7 to 1.42 mM for direct derivatization of microdialysis samples (Bia99, Keh98a, Keh98b); however, since these are isocratic methods it is unclear if this had an affect on the reaction for other amino acids.

Role of Separation in Amino Acid Analysis

The resolving power of the separation also plays an important role in amino acid analysis. For any separation used in amino acid analysis, it is necessary to validate the separation against a sample representative of the samples that are to be analyzed. In the

analysis of physiological samples, plasma or microdialysate, while it is impossible to account for all the possible components in complex samples, there are amino acids standards that contain 44 primary amines found in many physiological samples (Fek96). However, many of the used separations used for microdialysis work are not tested against complex standards (Qu98, Smo95, Bia99, Liu98) that include non-protein amino acids such as CIT, β-aminoisobutyric acid, α-amino-n-butyric acid, or *O*-phosphoethanolamine that have been demonstrated to be present in microdialysates. Failure to properly validate the separation with sufficiently complex samples can lead to erroneous results.

Table 1-6: Detection limits using microscale separations

Reagent	Det.	Analytes	MLOD (amol)	CLOD (nM)	Times Cited	Ref.
1. CBQ/CN	F	ARG	0.009	0.026	17	Arr95
2. OPA/tert-butyl thiol	E	ASP, GLU, GLY, TAU, GABA, ARG, CIT	16-45	64-181		Chap4
3. OPA/tert-butyl thiol	E	GABA	50	0.1	0	Boy98
4. OPA/β-ME	F	ASP, GLU	486	0.27	12	Rei94
5. CBQ/CN	F	ASP, GLU, GLY, GABA, ARG	2.8-601.8	0.43-102	21	Beq94
6. FITC	F	ASP, GLU	3.75	3.75	6	Tuc97
7. NDA/CN	F	ASP, GLU	0.33-0.61	4.2-7.9	12	Ber96, Rob96
8. NDA/CN	E	ASP, GLU, GLY	36	5.0	43	Oat89
9. Fluorescamine	F	ARG,GLU	52.3-3800	5.2-3800	6	Flo98
10. NDA/CN	E	ASP, GLU, GLY	20.6-217	10.5-1200	0	Swa98
11. OPA/β-ME	F	GLY	110	94	2	Old97
12. CBQ/CN	F	ARG	>34	>100	17	Arr95
13. Fluorescamine	F	GLU, GLY	0.022-0.033	169-253	1	Wei98

In this list of high sensitivity microscale techniques, there are several differences compared to the previous table. A majority of these methods use CZE or MEKC instead of liquid chromatography (Boy98, Oat89), only 4 use OPA, and only the methods

presented in Chapters 3 and 4 is demonstrated to be capable of resolving all the NTAAs as well as ARG and CIT from physiological amino acid standards. Comparing the high sensitivity detection of ARG using CBQ/CN derivatization, MEKC, and LIF detection using the sheath flow cuvette, there is a 3800-fold difference between the instrumental and method detection limits (Table 1-6:Arr95). In this study, a concentrated ARG solution that was derivatized and extensively diluted (Table 1-6:1) was compared to a sample that was derivatized *in situ* (Table 1-6:12). Due to the large, fluorescent background encountered using this reagent, trace level quantitative analysis was impossible (Arr95). Surprisingly, sub-nanomolar detection limits (0.42 nM) were achieved for GABA using CBQ; however, the same method resulted in a 102 nM CLOD for ARG, which is similar to the previously described method. The authors attribute this 243-fold difference in detection limits to inherent differences in detectability for the different CBQ-derivatized amino acids, however, the original work using this reagent noted only a 7-fold difference in detectability for the amino acid derivatives (Beq94, Liu91). The total amino acid content of the cerebrospinal fluid, which was directly analyzed, using this method was ~ 0.55 mM after dilution with reagent however the reagent concentration was only 2.73 mM. This creates a ~5 fold excess of derivatization reagent far below the ratio established by Lindroth (Lin79), in actuality, this is ratio is less due to the protein content of these samples. Large variations in detection limits are also seen for other microscale methods (Flo98, Swa98). In the FITC-based method, it was determined that only 50 FITC molecules in excess of the total amine content was required for quantitative derivatization (Tuc97). Of the physiological methods cited in

Table 1-6, only two were validated against complex, amino acid standards (Chapter 4, Ber96, and the similar method Rob96)

Increasing Concentration Sensitivity

While a majority of these methods obtained MLODs in the low attomole range, many obtained concentration detection limits in the low nanomolar range similar to the conventional methods outlined in Table 1-5. This is because as the separation methods are miniaturized, the sample injection volumes must be proportionally reduced to maintain the high separation efficiency. For many of these microcolumn techniques, the sample injection volume must be less 10 nL to prevent excessive broadening. To increase the concentration sensitivity of conventional scale chromatographic techniques, the sample injection volume can be increased providing the sample matrix is a weak mobile phase (Kar74). During preconcentration, the sample molecules partition into the stationary phase and accumulate at the column inlet providing the sample matrix is a weak solvent (mostly aqueous) to prevent partitioning between the stationary and mobile phase. The use of sample preconcentration techniques with microscale sample is not compatible with conventional analytical systems since these methods require at least 10 μL of sample for analysis.

Preconcentration can be used with microcolumns providing that either the sample components are efficiency stacked into a narrow zone in the column by chromatographic partitioning or the large sample zone on the column can be compressed using electrophoretic zone compression methods such as isotachophoresis (Rei94). Using on-column derivatization in which the derivatization reagent is a component of the

electrophoresis buffer, 0.27 nM detection limits were obtained using 1.8 μL injection volumes of dilute amino acid standards, isotachophoretic (ITP) zone compression, and laser induced fluorescence detection (Rei94). However, to reduce the background peaks associated with the reagent, an OPA concentration of 0.7 mM was used for the derivatization reaction, diminishing the quantitative ability of this technique (Rei94). In a much simpler approach, the hydrophobic nature of the OPA/*tert*-butyl thiol amino acid derivatives was used to perform efficient, large volume injections onto 50 μm i.d. packed capillary liquid chromatography columns to obtain impressive detection limits (Boy98). However, it was found that the background peaks associated with this reagent prevented larger sample preconcentration from being used (Boy98, Chapters 3,4).

The current limitation in obtaining sub-nanomolar CLODs using precolumn derivatization chemistry is the fluorescent and/or electroactive side-products caused by the large concentrations of derivatization reagent required to obtain a quantitative reaction (Boy98, Kwa90, Mol98, Mol99, Arr95, Rei94, Sai94, Alv89, Hos86, Dai97, God84, Cob98, Pen88, Old97, Rob95, Phi97, Orw91, Dem87, Mif89, Dem90, Kil98, Pal87, Bou91, Row95). Invariably, one or more of these neurotransmitters co-elutes or co-migrates with a background peak, making the sensitivity of the method limited by the reproducibility of the background peaks (Sko84). This can result in detection limits that are significantly higher compared to instrumental noise limited measurements (Boy98, Arr95, Lau89). To obtain sub-nanomolar detection limits, strategies that reduce the number and intensity of the background are needed (Orw91, Boy98, Kil98, Kwa90, Rob95).

Microcolumn Liquid Chromatography.

Fused silica capillary columns (20-50 μm i.d.) packed with porous stationary phase particles (5 μm) enables the analysis of nanoliter or sub-nanoliter samples with high mass sensitivity (Ken89a, She97, Boy98). An additional benefit of miniaturization is enhanced chromatographic efficiency resulting from a more uniform packing density due to favorable column wall effects that decrease the range of mobile phase velocities in the column (Ken89b).

The use of microscale columns also requires the development of high efficiency, low dispersion microscale detectors to maintain the high efficiency obtained using microcolumn separations. One of the first microscale detectors developed for open-tubular liquid chromatography in 9-15 μm i.d. columns was an electrochemical detector based on a cylindrical, 9 μm carbon fiber microelectrode inserted into the outlet of the separation column (Kne84, Stc85). The thin annular region between the inner column wall and electrode surface create a high oxidation efficiency detector (Figure 1-9) that can obtain detection limits of 1 amol once optimized (Ken89c).

Microscale separation systems also require the use of low-dispersion sample injection valves to prevent loss of separation efficiency. This has been accomplished previously using either a static split injector (Figure 1-10) or a pneumatic microinjector (Kne84, Jor83, Ken89c). The static split injector requires significantly larger sample volumes (> 10 μL) than those injected into the capillary column (5 nL) to thoroughly flush out the tee-connectors used to split the mobile phase (Figure 1-10). An alternative approach to this injector is the pneumatic microsyringe that can dispense the required injection volume (4-5 nL) directly into the chromatography column without waste

(Ken89b). However, neither method is easily automated, a requirement for high throughput analysis.

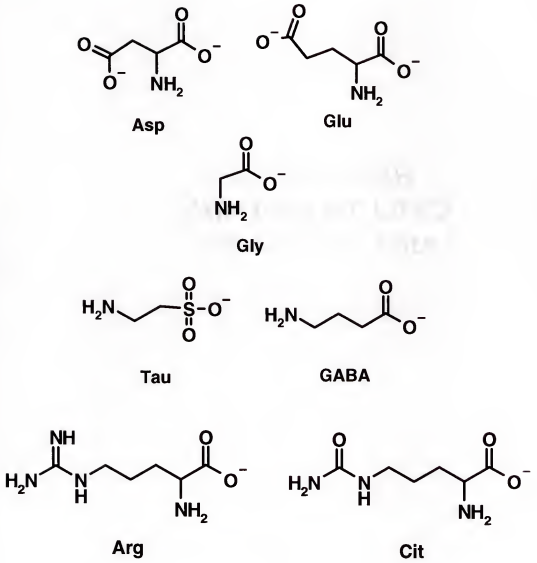

Figure 1-1: Major neurotransmitter amino acids: ASP, GLU, GLY, TAU, and GABA. Also displayed are the substrate (ARG) and product (CIT) of the nitric oxide producing enzyme.

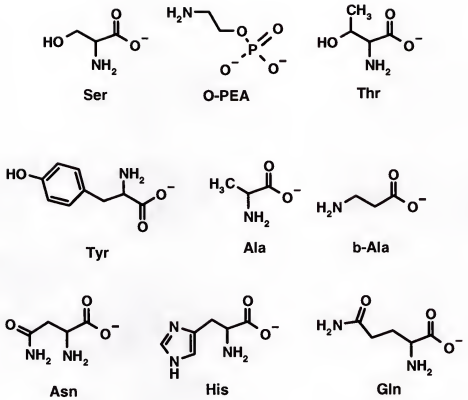

Figure 1-2: Other primary amines and amino acids found in many physiological samples: Ser (serine), O-PEA (*O*-phosphoethanolamine), Thr (theronine), Tyr (tyrosine), Ala (alanine), b-ALA (β-alanine), ASN (asparagine), His (histidine), and Gln (glutamine)

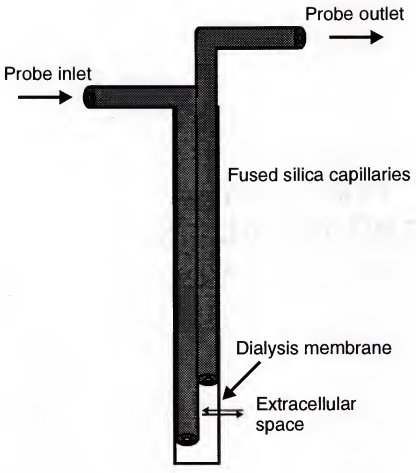

Figure 1-3: Representation of a side-by-side microdialysis probe. The fused silica capillary (40 μm inner diameter) perfuses an articifical cerebrospinal fluid (aCSF) through the active area covered by the dialysis membrane. The dialysis membrane possesses a molecular weight cutoff.

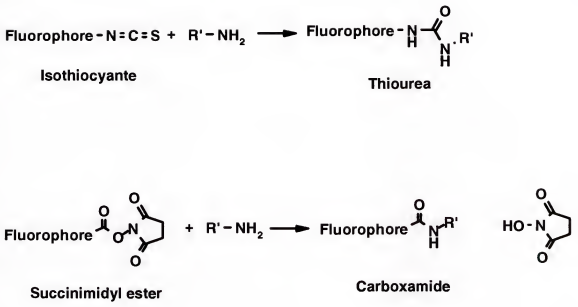

Figure 1-7: Common fluorescent labeling reactions

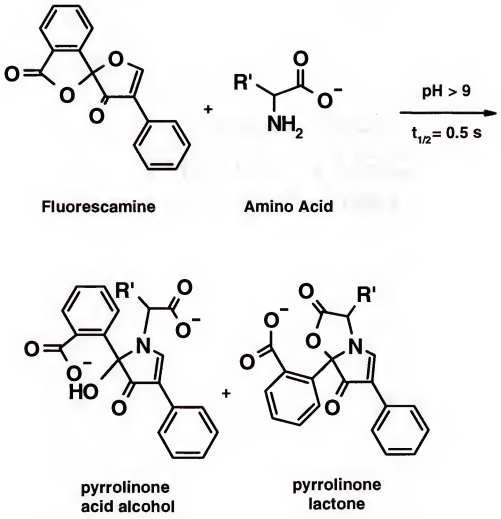

Figure 1-7: Reaction of fluorescamine.

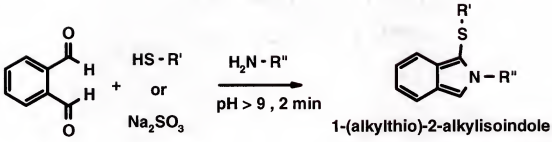

Figure 1-6: Reaction of *o*-phthalaldehyde (OPA)

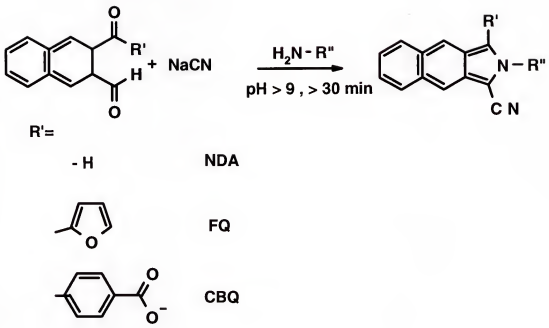

Figure 1-7: Reaction of naphthalene-2,3-dicarboxaldehyde (NDA), 3-(2-furoyl)quinoline-2-carbaldehyde (FQ), 3-(4-carboxybenzoyl)-2-quinolinecarboxaldehyde (CBQ)

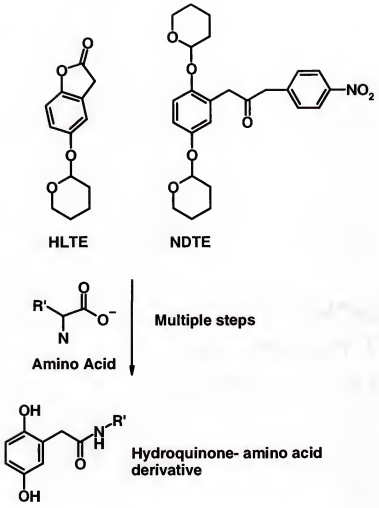

Figure 1-8: Reaction of homogentisic γ-lactone tetrahydropyranyl ether (HLTE) and *p*-nitrophenyl 2,5-dihydroxyphenylacetate, bis-tetrahydropyranyl ether (NDTE)

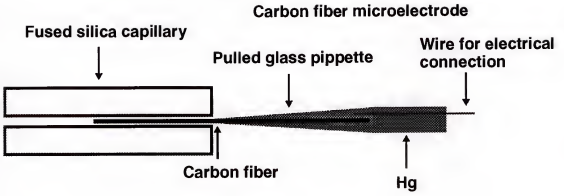

Figure 1-9: Carbon fiber microelectrode-based electrochemical detector for microcolumn separations. The cylindrical carbon fiber (9 μm outer diameter) protrude 1-2 mm past the oriface of the pulled glass pipette and is inserted in the outlet of the column (9 – 50 μm inner diameter) using a x-y-z stage micromanipulator. The electrical connection between the carbon fiber and silver wire (connected to the current amplifier) is made using Hg.

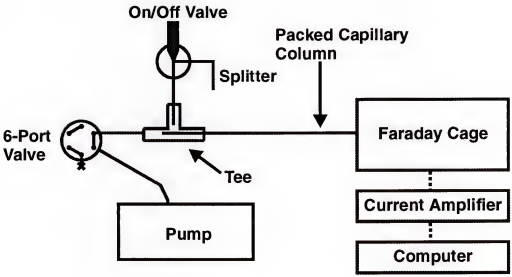

Figure 1-10: Static split system used for open-tubular and packed capillary liquid chromatography. This system is based on the use of a standard HPLC pump operating at 1 mL/min. The tee is required to split the high volumetric flowrate from the pump (~ 100 μL/min) to a flow rate compatible with the microcolumn (less than 0.25 μL/min). An electrochemical detector is shown here with a Faraday cage to reduce the ambient electrical noise. Small volume injections are made by filling the tee with sample using a syringe, closing the on/off valve, and pressurizing the system using the pump for a short amount of time to inject the sample. The chromatographic run is started by opening the on/off valve which flushes excess sample from the tee at a high volumetric flow rate.

CHAPTER 2
SUB-NANOMOLAR DETECTION OF γ-AMINOBUTRYIC ACID SECRETION FROM SINGLE PANCREATIC ISLET OF LANGERHANS

Introduction

Quantification of amino acids at trace concentrations in complex biological samples is a challenging analytical problem. Most current methods of amino acid analysis incorporate pre-column derivatization of the amino group followed by a chemical separation with either fluorescence or electrochemical detection. Perhaps the most popular derivatization chemistries are 2,3-naphthalenedicarboxyaldehyde (NDA) and *o*-phthalaldehyde (OPA) which react with amines in the presence of a nucleophile (usually CN^- for NDA and a thiol for OPA) to form electroactive and/or fluorescent isoindole derivatives (Rot71, Sim78a, Jos83, Dem87, Oat89). These derivatives can be detected at extremely low concentrations. For example, the NDA derivative of serine has been reported to have a concentration limit of detection (CLOD) of 8.3 pM by HPLC with laser-induced fluorescence (LIF) detection and the OPA derivative of glutamate has been reported to have a detection limit of 350 pM with similar instrumentation (Roa87). To date, detection limits this impressive have usually only been achieved when analyte is derivatized at a higher concentration and then diluted prior to separation and detection.

When detection limits are expressed as the concentration of analyte that can be derivatized and detected, they tend to be considerably worse. One of the best detection

limits reported using NDA/CN^- derivatization was for determination of catecholamines by capillary zone electrophoresis (CZE)-LIF. In this study, Renaud's group reported noradrenaline derivatized at 1 nM concentration yielded a signal to noise ratio (S/N) of 8.1 for a CLOD of 0.38 nM. However, they also reported that derivatization of lower concentrations was not successful resulting in an effective detection limit of 1 nM (Rob95) and that extension of the technique to amino acids resulted in even higher detection limits (4.2 nM) (Ber96a). Best cases for OPA derivatization with fluorescence or electrochemical detection are 5-30 nM if the signal is compared to background peaks (Smo95, Keh88, God97, Dur88, Bou91, Row95, Phi97). One exception was a 35 pM detection limit which was obtained for the interesting case of derivatizing γ-glutamyl (sulfhydryl-containing) peptides to form fluorescent cyclodeca[*a*]indenes without the need for an added thiol (Orw94).

The higher detection limits for derivatization at trace levels compared to detection of derivatives that are formed at higher concentrations and then diluted can largely be attributed to the many interfering substances that are formed during derivatization. Most analytical methods use 10^{-3}-10^{-4} M concentrations of derivatization reagent to obtain rapid, pseudo-first order reaction kinetics and short reaction times (10-30 minutes for NDA, 1-3 minutes for OPA) (Dem87, All84). Unfortunately, the large excess of derivatization reagent can lead to numerous spurious peaks in the chromatogram which overlap or co-elute with analyte peaks. This is particularly well documented in GABA analysis (Smo95, Kehr88, Keh98a, God97, Dur88, Pal87, Jac86, Bou91, Row95, Phi97). These spurious peaks are generally attributed to derivatization of impurities in the reagents or sample solvents (Row95), side-products formed during derivatization

(Bour91), and degradation products of the primary reaction or side reaction(s). Several strategies have been used to minimize background signals in OPA derivatization including: 1) extensive purification of the dialdehyde (Orw94, Oat90), 2) scavenging of the initial reactants (Rob95, Smo95), 3) acid hydrolysis of undesired derivatives (Orw94), 4) photodestruction of unwanted derivatives (Orw94), or 5) electrochemical scavenging (or coulombic preoxidation) of reaction side products or reagents (Bour91, Phi97, Orw91). The first two strategies can be universally applied; however, the latter methods can only be used in applications where the analytes have greater stability than the interfering peaks. Even with these background reducing measures, only rarely is the sensitivity truly limited to the root-mean-square (RMS) noise of the detector.

In this work we examine the derivatization and detection of γ-aminobutyric acid (GABA), at sub-nanomolar concentrations. For an analysis system we use capillary LC with electrochemical detection (ED). Capillary LC/ED typically has mass limits of detection (MLOD) of 1-40 amol (She97, Ewi94) corresponding to concentration limits of detection (CLOD) of 1- 40 nM with 1 nL injection volumes; however, on-column preconcentration allows CLODs to be improved to the picomolar level with no effect on MLOD. For example, we have achieved 20 pM detection limits for the electroactive peptide met-enkephalin by injecting 1 μL samples onto a 25 μm i.d. capillary column (She97). As with LIF detection, preconcentration with ED detection will not allow low CLOD in real samples unless the derivatization conditions are improved since preconcentration also concentrates the interfering substances formed during derivatization. In our work we found that scavenging the derivatization reaction with excess amine and scavenging excess thiol, greatly reduced the number and size of most

interfering background peaks allowing the sensitivity to be limited by instrumental noise. This allowed detection limits of 100 pM to be obtained with a 0.5 μL injection volume without extensive reagent purification or elaborate detection strategies.

As a demonstration of the utility of this method, it was used to measure GABA secretion from single islets of Langerhans. Islets are pancreatic microorgans that contain approximately 3,000 cells including α-cells that secrete glucagon and β-cells that secrete insulin. Secretion of these peptide hormones during different metabolic states are largely responsible for glucose homeostasis. Recently, attention has focused on the possible intercellular interaction of α-and β-cells mediated by GABA. One hypothesis is that GABA is released from β-cells and interacts with α-cells causing inhibition of glucagon secretion (Ror89, Ree91, Tho93). This hypothesis is supported by several lines of evidence including: 1) GABA is found in high concentration in pancreatic islets (Bri72), 2) islet GABA and its synthesizing and metabolic enzymes are found predominantly in β-cells which are in close proximity to α-cells within islets (Bri72, Gar79a), 3) GABA has been shown to be localized within synaptic-like microvesicles that are present in β-cells and are similar in morphology to secretory microvesicles found in neurons (Tho93), and 4) exogenous GABA has been shown to inhibit glucagon secretion in isolated pancreatic islets and in isolated α-cells by activating a $GABA_A$-receptor (Ror89). Attempts to demonstrate regulated secretion of GABA from islets or β-cells have been hampered by the difficulty of assaying GABA in the low nM range.

Experimental

Reagents. Amino acid standards, OPA, and buffers were purchased from Sigma (St. Louis, MO) and *tert*-butyl thiol (2-methyl-2-propanethiol) was obtained from Aldrich (St. Louis, MO). Kreb-Ringer buffer (KRB) consisted of 120 mM NaCl, 4.8 mM KCl, 1.2 mM in $MgCl_2$ and Na_2HPO_4, 3 mM D-glucose, 2.5 mM $CaCl_2$, and 24 mM NaH_2CO_3 at pH 7.4 which was maintained by continual sparging with 95/5% air/CO_2 mix at 37° C. Borate buffers were made from boric acid and solid NaOH. All solutions were made with deionized water obtained from a Milli-Q system (Millipore, France) and filtered using 0.2 μm nylon filters (MSI, Westboro, MA).

Capillary liquid chromatography. Columns were prepared by packing 50 μm i.d. fused silica capillaries (Polymicro Technologies, Phoenix, AZ) with 5 μm Alltima C-18 particles (Alltech, Deerfield, IL) using previously described techniques (Ken89a). The method development studies used a 22 cm column, while a 30 cm column was used for the islet secretion experiments. The lifetimes of these columns was greater than one month without neutralizing the sample prior to large volume injections. During the lifetime of these columns, very little change in retention time was observed and the column was discarded only when the outlet frit was broken or the column clogged. The capillary LC injection and separation system is similar to that described previously (She97) with the exception that a Isco 100 DM syringe pump (Lincoln, NE) was used for mobile phase delivery (Figure 2-1). All experiments were performed in a constant pressure mode (13.8 MPa) and volumetric flow rates were typically 0.3 μL/min.

Mobile phases. All mobile phases were mixed and degassed by sparging with He for 10 minutes prior to loading the syringe pump. The mobile phase for all OPA/*tert*-butyl thiol experiments was 0.15 M phosphate pH 5.4 with 50% (v/v) acetonitrile.

Electrochemical detection. Electrochemical detection was accomplished using a 1 mm long x 9 μm diameter carbon fiber cylinder electrode, fabricated in lab as described elsewhere (Kaw89), and inserted into the outlet end of the LC column as the working electrode (She97, Kne84). The outlet of the column was mounted in an electrochemical cell containing 0.1 M KCl as a supporting electrolyte and fitted with an Ag/AgCl reference (all voltages are versus this reference). Between chromatographic runs the electrode potential was swept from 0 to +1.8 V at 1 V/s for 30 seconds to obtain a reproducible signal and maintain a low background current (Oat89). When stored in the supporting electrolyte and swept for 2 minutes at the beginning of the day, the average lifetime of these electrodes exceeded seven days. The electrode was poised at +0.8 V for detection, the potential found to give the optimal S/N. Current was amplified using an Keithly 428 current amplifier and electrode potential was applied via an external source. Data was collected at least 8 Hz and low pass filtered at 3 Hz. Chromatograms were analyzed using a statistical moments programs written in-house. Median filtering (Moo93) to remove baseline drift and Savitzky-Golay smoothing were performed using locally written software.

OPA derivatization and scavenging reactions. An OPA/*tert*-butyl thiol solution of 30 mM was made with a 50% methanol/borate buffer (pH 11.5 before addition of methanol) containing 17.9 μL of *tert*-butyl thiol (final concentration 40 mM). The OPA/*tert*-butyl thiol scavenging solution was 0.4 M glycine made in borate buffer and the *tert*-butyl thiol

scavenger solution was 0.5 M iodoacetamide (IAA) in the 50% methanol/borate buffer solution. All reagents were stored at room temperature in darkened glass vials except for glycine. Derivatization began by adding 1.5 μL of the OPA/*tert*-butyl thiol solution to 15 μL of sample and allowing the quantitative derivatization to take place for 2 minutes in the dark. OPA/*tert*-butyl thiol scavenging was performed by adding 1.5 μL of the glycine solution and letting this reaction take place for 2 min. The excess *tert*-butyl thiol was scavenged by adding 1.5 μL of the IAA solution and allowing to react for 4 min before injection.

For all analyses, glass vials used to store derivatization reagents were washed in 50% nitric acid and left to soak over night before being rinsed with deionized water, absolute ethanol and then dried under a nitrogen stream. Polypropylene centrifuge tubes were washed briefly in nitric acid, but otherwise treated in a similar manner. Significant losses of GABA, presumably via adsorption, were experienced when glass vials were used to store GABA standards. Polypropylene centrifuge tubes (Row95) reduced this adsorptive loss and were used for sample storage and derivatization.

Islet experiments. Mouse and rat islets were isolated and cultured using previously described techniques (Hua95). Islets were cultured in RPMI 1640 cell culture media supplemented with 10% fetal bovine serum, 1% penicillin, and 1% streptomycin. For single islet experiments, individual islets were washed with KRB and pre-incubated in KRB (3.0 mM glucose) for 60 min prior to islet incubation. For determination of GABA, single islets were incubated for 20 minutes in 20 μL of: KRB, or KRB with 16.7 mM glucose, or KRB with 60 mM KCl (with NaCl reduced to maintain the same ionic strength). The supernatant (19 μL) was removed and stored at -80 ^{o}C until analysis.

Before analysis, 1 μL of a borate buffer (0.5 M, pH 11.5) was added to the supernatant, which was then centrifuged at 1,000 g for 5 minutes at 4 °C. From this solution 15 μL was removed and derivatized as described above. All incubations were performed with quiescent solution in an incubator with 95/5% air/CO_2 at 37 °C.

Results and Discussion

Characterization of the detector. The detection system was initially evaluated using 4-methyl catechol (4-MC), which is natively electroactive, as a test analyte. The mass limit of detection for 4-MC was 8 amol when using a 9 μm diameter carbon fiber microelectrode and a 50 μm i.d. capillary at a volumetric flow rate of 0.3 μL/min. This mass corresponded to a signal 3 times the root-mean-square (RMS) noise of the detector which was consistently between 14 and 30 fA for a 0-3.3 Hz bandwidth. These results are comparable to what has been reported previously for carbon fiber detectors in capillary separations (She97, Ewi94).

Preconcentration with OPA and NDA derivatives. When the sample volume is large enough, it is possible to improve the CLOD over that determined above by preconcentrating on-column. To preconcentrate on a column, it is necessary that the analyte have a high capacity factor (k) under the injection conditions. If this condition is not met, the analyte will partition into the mobile phase and be transported down the column during a large volume injection resulting in band broadening or, in an extreme case, breakthrough. Development of high k on a reversed-phase column requires that the analyte is hydrophobic and the sample solution is a weak mobile phase. In pilot experiments, OPA was found to be more suitable than NDA for preconcentration for two

reasons. First, OPA/*tert*-butyl thiol derivatives were more hydrophobic than the NDA/CN^- derivatives resulting in *k*'s that were typically at least two times greater. The second reason was that the OPA/*tert*-butyl thiol reaction could be performed using less than 5% organic in the final sample solution since OPA itself is fairly soluble in aqueous solution, while NDA/CN^- required more than 45% organic to prevent precipitation of the NDA stock. The lower organic content of the OPA derivatization solution made it a weaker injection solvent which was more effective for retaining analyte during preconcentration.

To evaluate the extent of band broadening for the OPA/*tert*-butyl thiol derivative of GABA during large volume injections, the zone variance for this derivative as a function of injection volume was determined (Figure 2-2). This data shows that increasing the injection volume up to 2 μL (~6.7 column volumes) did not affect the peak width demonstrating complete retention of the GABA derivative during injection. A plot of injection volume versus peak height increased linearly ($r^2 > 0.98$) from 0.02 to 2.0 μL also indicating complete capture of the analyte and control of the volume injected. The relative standard deviation (RSD) for peak height for both 0.02 and 2.0 μL injections of the GABA derivative (200 nM) was < 5 %.

Pre-column derivatization using the OPA/*tert*-butyl thiol reaction. An inherent difficulty of using preconcentration injection techniques for trace analysis is that any retained compound, including electroactive impurities and side-products, will also be preconcentrated. An example of this problem is shown in Figure 2-3 which compares chromatograms from OPA/*tert*-butyl thiol derivatization of purified water (blanks) to samples of 10 nM GABA with and without preconcentration. The off scale current

reading prior to the void time (~1.2 min) is due to unretained, electroactive components of the sample. While preconcentration clearly increases the signal for GABA, it also increases the height of a plethora of background peaks that are present even in the absence of intentionally added amines. Particularly troubling for GABA determination are the peaks at approximately 6.9 and 7.2 min that overlap with GABA. We estimated the CLOD for GABA under these conditions as the concentration that would yield a signal as large as the mean blank signal plus three times the standard deviation of the blank (Sko92). Using this criteria, the CLOD was 760 pM corresponding to a MLOD of 0.38 fmol. These detection limits are over an order of magnitude worse than what would be expected for this injection volume based on the sensitivity of the detector clearly indicating the adverse effect of the background peaks, which had RSD's in height and area >50%, on detection limits.

Pre-column derivatization using the OPA/*tert*-butyl thiol reaction with scavenging and scavenging reactions. In order to fully capitalize on the sensitivity of capillary LC-ED, it was necessary to investigate the source and possible reduction of the background peaks. To determine if these peaks were due to electroactive species present within the reagents, each component of the derivatization was injected individually onto the column. Neither borate, methanol, OPA, or de-ionized water, as individual standards or combined (without *tert*-butyl thiol) produced these peaks. The *tert*-butyl thiol was found to be responsible for one of the background peaks (see below). Use of different lots and vendors of OPA as well as OPA purified by recrystallization (3 times) in n-heptane (Orw91) in these experiments did not reduce or eliminate any of the interfering peaks under these separation conditions. The background peaks were also present in deionized

water and in the KRB, indicating that these peaks were not the result of endogenous amines in the water or buffer salts. These results suggested that most of the peaks were due to reactions involving OPA and *tert*-butyl thiol that form electroactive products even without intentionally added amines. The formation of OPA/thiol conjugates such as hemithioacetyls or cyclic hemithioacetyls and cyclic OPA hydrates has been postulated by others as non-productive reaction pathways (Sim78b, Won85, Alv89).

One potential method of eradicating undesirable products is to scavenge the derivatization reaction by adding an excess of a primary amine after the analyte has been derivatized. To be practically useful the scavenging reagent must form a stable product that is undetectable or unretained. In this work, glycine was used as the OPA/*tert*-butyl thiol scavenger because it is: 1) soluble at high concentrations in basic, aqueous solutions, 2) unretained (in either form) with 50% acetonitrile at pH 5.4, and 3) forms a stable OPA/*tert*-butyl thiol derivative (All84). In Figure 2-4A, no scavenging reaction was used, and the two peaks that interfere with GABA at 6.9 and 7.2 minutes are apparent. When 0.4 M glycine is added to scavenge the derivatization reagents the interfering peak at 6.9 minutes is eliminated, along with another background peak (5.25 minutes), as seen in Figure 2-4B.

The remaining peak that interfered with GABA detection was found to be due to excess *tert*-butyl thiol. The peak due to this reagent was eliminated by scavenging with iodoacetamide (IAA), which reacts with sulfhydryl groups. This sulfhydryl-scavenging reaction has been used to remove excess *tert*-butyl thiol previously in amino acid analysis (Smo95). After a 4 minute reaction with 0.4 M IAA following the glycine reaction, the *tert*-butyl thiol peak was eliminated from the chromatogram as shown in Figure 2-4C.

The results in Figure 2-4 show that it is possible to virtually eliminate the electroactive background peaks from an OPA/*tert*-butyl thiol derivatization by scavenging the amine reaction with excess amine (glycine in this case) and scavenging the excess thiol with IAA. In situations where glycine or other less retained amino acids (ex. aspartate, glutamate, taurine) are the analyte(s), we have found that cysteic acid is also effective at scavenging excess OPA/*tert*-butyl thiol (preliminary results). With these precautions, no background peaks interfere with GABA detection and the CLOD is limited by the detector noise as demonstrated in Figure 2-4D. The peak for GABA in Figure 2-4D has a S/N of 69 for a 360 amol injected (10 nM concentration in 0.05 μL volume). The chemical drawings of these reactions are displayed in Figure 2-5.

With elimination of background peaks it was possible to improve concentration detection limits by preconcentrating larger sample volumes on column. Figure 2-6 shows chromatograms resulting from injecting a 0.5 μL sample of 250 pM GABA in KRB that had been derivatized using the improved derivatization method. A well-resolved peak was obtained (Figure 2-6A, top trace) for GABA and the blank is free of contaminating peaks (Figure 2-6A, bottom trace). Using a Savitsky-Golay smooth (15 point), the S/N was increased to 7.5 in Figure 2-6B (top trace) corresponding to a CLOD of 100 pM (50 amol in 0.5 μL) based on a signal-to-noise ratio of 3. This chromatogram represents the lowest, derivatized concentration of amino acid published in the literature. The linear dynamic range of this method was found to be > 3 orders of magnitude (0.25 - 500 nM) with a correlation coefficient > 0.999.

The MLOD of 50 amol obtained here is comparable to that achieved in similar sized columns for LC-ED with derivatization (Oat89); however, the important advantage

of this technique is the low CLOD which is achieved as a result of using injection volumes that are 1000-fold greater than typical. This improvement in CLOD with preconcentration is only possible when the background peaks have been controlled. An advantage of capillary LC columns is that large preconcentration can be used even with sample volumes less than 1 μL. As a result this technique can achieve amol/μL detection limits for real samples.

Detection of GABA release from islets. As a demonstration of this technique, we investigated the secretion of GABA from single rat and mouse islets of Langerhans stimulated by high K^+ and 16.7 mM glucose compared to the basal condition of 3.0 mM glucose. Figure 2-7 displays chromatograms for single islets from the three different incubation solutions while quantitative results of both rat and mouse islets studies are summarized in Table 2-1.

Table 2-1. Summary of GABA Secretion Data from Single Islets of Langerhans

Islet Species	**Test Stimulant in KRB**	**fmol GABA/ min ± 1 S.E. (n) * ($p < 0.01$)**
rat	3.0 mM glucose	40 ± 12 (13)
	16.7 mM glucose	51 ± 8.0 (13)*
	60 mM potassium	190 ± 41 (5)*
mouse	3.0 mM glucose	13 ± 1.1 (5)
	16.7 mM glucose	8.2 ± 1.8 (3)*
	60 mM potassium	19 ± 8.2 (3)

The difference in secretion rates between rat and mouse islets is proportional to the difference in islet GABA content for the different species (Mic92). For both species, it was found that incubation with K^+ substantially increased GABA secretion while secretion decreased when glucose was increased from 3.0 to 16.7 mM. The increased secretion with K^+ depolarization is expected as β-cell lines have given similar results (Tho93). It is not clear if K^+-induced secretion is due to exocytosis or reverse transport

of the amino acids. The decrease in GABA secretion with higher glucose is surprising since the hypothesis that regulated secretion of GABA inhibits glucagon secretion would require that GABA secretion increase as glucose levels increase since glucagon secretion is suppressed by high glucose. Although this result is surprising, the only other study on GABA secretion from primary β-cell cultures reported that with prolonged exposure (24 h) to high glucose (16.7 mM), GABA secretion decreased relative to lower glucose (Gas96). This difference was attributed to the decrease in total GABA content in β-cells that occurred as a result of the change in metabolism in the cells (Smi97). Further studies using a wider range of glucose concentrations and showing the time dependency of GABA secretion will be required to fully understand the regulation of GABA and its possible role in islet function. Such studies will be aided by the high sensitivity method reported here.

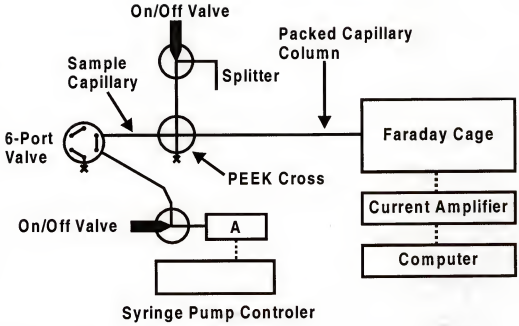

Figure 2-1: Isocratic LC-EC system.

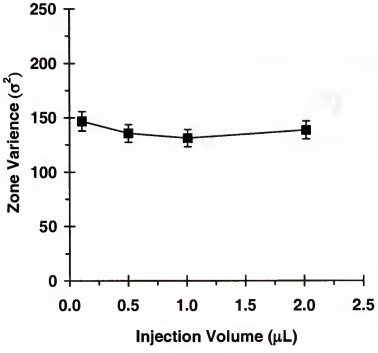

Figure 2-2: Plot of 200 nM GABA peak variance versus injection volume (n=3).

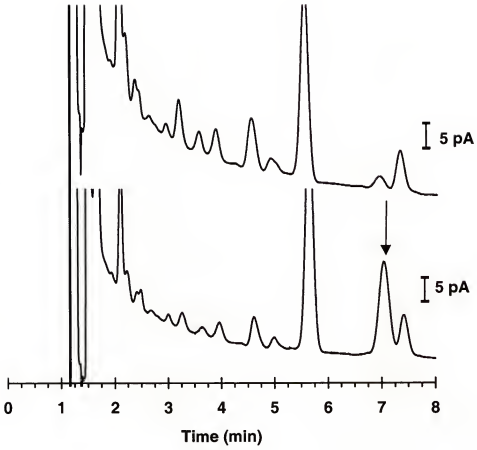

Figure 2-3: Chromatograms of preconcentrated samples using only OPA/*tert*-butyl thiol derivatization. The top trace in A and B are derivatized de-ionized water blanks and the bottom traces are derivatized 10 nM GABA (arrow). Injection volumes were 0.5 µL.

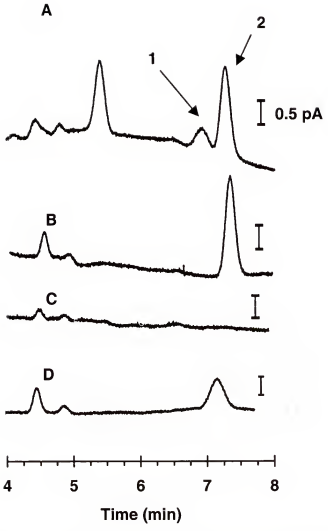

Figure 2-4: Chromatograms from injection of 50 nL of derivatized samples using: (A) blank sample with OPA and *tert*-butyl thiol only, (B) blank sample with OPA and *tert*-butyl thiol derivatization followed by glycine scavenging, (C) same as B plus IAA scavenging, and (D) 10 nM GABA sample derivatized identically to C.

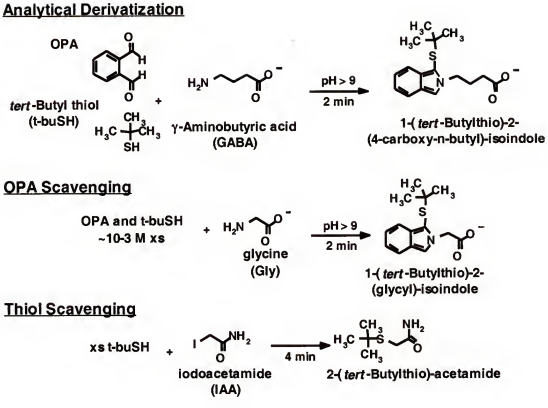

Figure 2-5: Chemical drawings of the analytical and scavenging reactions.

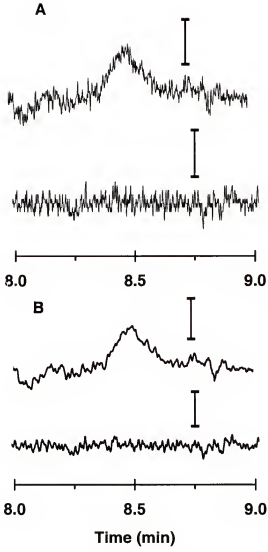

Figure 2-6: Chromatogram from large volume injection (0.5 µL) of 250 pM GABA in KRB (top trace) and blank (bottom trace). Median filtered data (A) and Savitsky-Golay 15 point smooth (B).

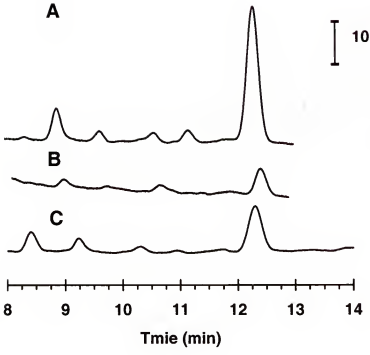

Figure 2-7: Chromatograms showing GABA peak from incubation of a single mouse islet of Langerhans for 20 min in KRB with following modifications: (A) 60 mM K^+, peak corresponds to 33.0 nM GABA, (B) 16.7 mM glucose, corresponds to 5.7 nM GABA, and (C) KRB, corresponds to 12.3 nM GABA.

CHAPTER 3
COMPREHENSIVE, SUB-NANOMOLAR ANALYSIS OF NEUROTRANSMITTER AMINO ACIDS: MONITORING DURING *in vivo* MICRODIALYSIS WITH 10 s TEMPORAL RESOLUTION

Introduction

In vivo microdialysis is a sampling technique used to monitor extracellular concentrations of neurotransmitter in living brains with both temporal and spatial resolution (Ung84). Such measurements allow the neurobiological function of neurotransmitters to be studied by correlating neurotransmitter levels to either pharmacological manipulation or behavior. Of particular interest are the amino acid neurotransmitters which have been implicated in many physiological roles as diverse as learning, movement, and hunger as well as several diseases including Alzheimer's, Parkinson's, and epilepsy (Smi96a). High temporal resolution in microdialysis studies is desirable to decrease experiment time and to monitor fast changes in neurotransmitter levels. Temporal resolution in microdialysis is usually limited by the mass sensitivity of the analytical method used to quantitate analytes so that fraction collection times must be long enough to collect a detectable amount of analyte. Using conventional methods of amino acid analysis, detection limits of 5-60 femtomole are obtained and temporal resolution is limited to 5-10 min for aspartate (ASP) and glutamate (GLU) (Smo95, Qu98, Keh98a), the main excitatory neurotransmitters, and 10-30 min for γ-aminobutyric

acid (GABA), the main inhibitory neurotransmitter, which is present at lower concentrations in dialysate (Keh98b, Smo95). At this temporal resolution, the total experiment time can be several hours to collect samples for control and experimental conditions (Row95).

Temporal resolution has been improved to 5 s for ASP and GLU using on-line microdialysis with fast capillary zone electrophoresis and laser-induced-fluorescence detection (CZE-LIF)(Lad97); however it is desirable to have a means to monitor all the amino acid neurotransmitters to examine possible interaction of these systems. This goal requires a method capable of analyzing sub-microliter samples with high sensitivity and sufficient resolving power to separate the trace-level neurotransmitters from the large number of endogenous amines found in the extracellular space. In this work, we explore a strategy of collecting fractions at 10 s intervals (200 nL volume), diluting the fractions to microliter volumes to facilitate sample manipulation, derivatization, and injection, preconcentrating the derivatized samples onto capillary liquid chromatography columns, and separating the derivatized amines using gradient elution. While the dilution step facilitates sample handling, it also increases the sensitivity necessary for detection. In fact, trace level amino acids such as GABA could not be analyzed using existing methods of amino acid derivatization.

Success of this strategy requires sub-nanomolar detection limits in order to quantify the low level neurotransmitters. For this project we chose to utilize *o*-phthalaldehyde (OPA) and *tert*-butyl thiol which has frequently been used for neurotransmitter analysis (All84, Jac86, Smo95, Qu98). Like other reagents a large excess of reagent is required to obtain a rapid and quantitative reaction; however, the

excess reagent forms numerous detectable compounds that interfere with detection of analytes. To reduce the chemical background associated with the OPA and naphthalene-2,3-dicarboxyaldehyde (NDA) reactions, several strategies have been employed including purification of the dialdehyde, chemical scavenging, and electrochemical scavenging or coulombic preoxidation, as described in the previous chapter. Recently, we reported that scavenging reactions significantly reduce the number of background peaks produced by the OPA/*tert*-butyl thiol reaction in an assay for GABA (Boy98). Scavenging involved reacting the OPA with a hydrophilic amine, glycine, which formed an electroactive product well resolved from GABA, and reacting the *tert*-butyl thiol with iodoacetamide, which formed a non-electroactive product (Ein84). Using these scavenging reactions, on-column sample preconcentration on 50 μm i.d. packed capillary columns, and high sensitivity electrochemical detection, a concentration limit of detection (CLOD) of 100 pM for γ-aminobutyric acid was obtained for a 500 nL injection volume; however, this procedure was only useful for GABA. A modification of these reactions that permits the major neurotransmitter amino acids to be determined is reported here.

Experimental

Reagents. Amino acids, iodoacetamide (IAA), *o*-phthalaldehyde (OPA, >99% purity), 2-methyl-2-propanethiol (*tert*-butyl thiol), nipecotic acid, and boric acid were of the highest purity grade from Sigma or Aldrich (St. Louis, MO). All buffer salts and solvents were obtained from Fisher (Fairlawn, NJ). The phosphate buffer salts were enzyme grade while other salts were certified A.C.S. grade. Water and methanol were HPLC grade. Artificial cerebrospinal fluid was made to the following specifications: 145 mM NaCl,

2.68 mM KCl, 1.01 mM $MgSO_4 \bullet 7H_2O$, and $CaCl_2 \bullet 2H_2O$. The high potassium made similarly except KCl was 145 mM and NaCl was 2.68 mM. All solutions were made in clean glassware and filtered (see below).

Borate buffer. Borate buffer was made to 0.4 M at pH 10.6 $\pm$ 0.1 using 12.37 g boric acid and 7.53 g NaOH (s) and 0.5 L HPLC grade water. This produced a solution buffered at the appropriate pH without needing further adjustment. This was done after it was determined that the pH electrode was a source of amino acid contamination. This buffer was used for up to one week with daily filtering (see below).

Phosphate buffer. The phosphate buffered mobile phase was made by mixing 4.73 g NaH_3PO_4, 4.22 g $Na_2H_2PO_4$, and 0.372 g ethylenediaminetetraacetic acid (EDTA) in 1 L of HPLC grade water. This made a solution of 0.05 M phosphate buffered at pH 6.51 which was filtered once (see below) and then stored in a capped glass flask at room temperature. This solution was then used for one week and then discarded.

Mobile phases. Mobile phases for gradient elution were made from the phosphate buffer daily and degassed by ultra-pure He(g) sparging for 10 min prior to use. During sparging, the 100 mL glass mobile phase reservoirs were covered with parafilm to prevent solvent evaporation. Mobile phase A was 100 % phosphate buffer. Mobile phase B was 35% phosphate buffer and 65% HPLC grade acetonitrile.

o-Phthalaldehyde Purification. OPA was recystallized from n-heptane (60° C) two times. OPA was placed in a glass test tube and hot heptane added in aliquots (~ 1 mL) and decanted via glass Pasteur pipette to a petri dish (also at 60° C). After several extractions, a dense, very dark yellow solution remained at the bottom of the test tube which was then discarded. The solubility of OPA in this solvent at this temperature is quite low which

required large amounts of solvents to be used (~ 10 mL) and produced recoveries of less than 50%/recrystallization. The mother liquor was allowed to recrystallize at room temperature in a glass petri dish for 15 min, vacuum filtered at room temperature with a 0.22 μm nylon filter, and washed with room temperature heptane. After two recrystallizations this product was removed and stored in a capped brown borosilicate glass vial until use. Great care must be taken to avoid contamination during this purification procedure.

OPA derivatization solution. A solution with 40 mM OPA and 50 mM *tert*-butyl thiol was made in a borate buffer containing 50% methanol (both solvents were used after filtration). This solution was made by directly weighing 53.6 mg recystallized OPA into a cleaned glass vial followed by 5 mL methanol, 56.2 μL *tert*-butyl thiol , and then 5 mL borate buffer. This solution was mixed by shaking, and the pressure was released shortly afterward. This solution remained in a capped, darkened, borosilicate vial in the dark at room temperature.

IAA- thiol scavenging solution. A 1 M IAA solution was made by weighing 0.925 g IAA into a darkened, borosilicate vial and adding 5 mL methanol. This solution was also kept in the dark at room temperature.

CA/sulfite –OPA scavenging solution. A solution of 0.1 M cysteic acid and Na_2SO_3 was made in 5 mL of borate buffer in a darkened, borosilicate vial.

Derivatization. All samples were derivatized in polypropylene vessels. The reagents were added in a 1:5 ratio to the total sample volume. All samples were derivatized in cleaned polypropylene vials using a Eppendorf microdispensor and gel-loading pipette tips (Fisher). The samples (2 μL) were derivatized as follows: 0.4 μL of OPA/*tert*-butyl

thiol was added and allowed to react for 2 min, then 0.4 μL of IAA was added and allowed to scavenge excess thiol for 4 min, and then 0.4 μL of the cysteic acid/sulfite solution was added and allowed to react for 10 min. The final sample volume was 3.2 μL.

Polypropylene microvials. Microvials (10 μL total volume) were made from 1000 μL pipette tips (Fisher Scientific, Fairlawn, NJ). The procedure to make these vial was as follows, the small orifice was sealed by melting (not burning) using a Bunsen burner and solidifying on a cold, clean metal surface. These vials were then cut to a height of ~ 0.5 cm and then cleaned as described below.

Cleaning procedures- glassware. Volumetric flasks were washed in 1 N HCl followed by rinses in HPLC grade water and then absolute ethanol. These flasks were then dried under nitrogen stream and capped until use. Reagent vials were soaked in a bath of 50% 5 N NaOH and HPLC grade methanol. Prior to use these vials were then rinsed and dried as described above. An emphasis must be placed on capped glassware after cleaning as it was noticed that dust and other particulates quickly adsorb to the surface of clean glassware.

Cleaning procedures- polypropylene. All centrifuge tubes and pipette tips were rinsed thoroughly with 1 N HCl, HPLC water, and absolute ethanol then dried under nitrogen prior to use.

Solution filtering. All solutions were filtered using 0.22 μm Teflon (hydrophobic) membranes (MSI, Fisher Scientific, Atlanta, GA) prior to use. The glass vacuum filtration system (cleaned as described above) and TFE membrane were conditioned with HPLC methanol which was then discarded. The solutions were then filtered in the following

order: methanol, phosphate buffer, and then borate buffer. Between each solution the glassware and membrane surface was rinsed with HPLC grade water. After filtering, solutions were quickly decanted into cleaned glass flasks and capped. If particulates or dust were observed in the solutions they were immediately discarded and then re-made.

Capillary Liquid Chromatography. Fused silica capillary of 48 μm i.d. x 40 cm (Polymicro Technologies, Phoenix, AZ) was used to prepare packed capillary column using previously describe techniques (Ken89a). A slurry of 10 mg/mL of Alltima C8 particles (5 μm, 100 nm pore) was prepared in acetone. Columns were packed at 4000 psi using a pneumatic amplifier (Alltech) and fully packed within 20 min. Prior to use the columns were flushed with a 90% acetonitrile solution and cut to a final length of 32 cm. A schematic of the pumping and injection system is shown in Figure 3-1. Mobile phase pumping was accomplished using two ISCO (Lincoln, NE) 100 DM syringe pumps controlled by a gradient controller set to deliver a proportioned mobile phase at 8 μl/min. The mobile phase exited the pumps through two on/off valves (V, VICI, Houston, TX) through two high pressure check valves (C, Alltech, Deerfield, IL) and 0.2 μm fritted filters (F, VICI). The mobile phases were mixed in a 0.75 mm bore stainless steel tee (S_1, VICI) and transported in 0.02" x 4 cm stainless steel tubing (Alltech) to the first splitter (27 μm x 170 cm fused silica capillary, Polymicro Technologies, Phoenix, AZ). This shunted 6 μL/min of flow, generating a backpressure of 2100 psi. The remainder of the flow was transported to the 6-port injection valve (UW6, VICI) via a 0.005" x 4 cm stainless steel tubing. The ~ 1 cm of polyimide from the injection end of the capillary column was removed using a scalpel and inserted into the 0.4 mm bore pilot hole of the injection valve until the column end was very slightly recessed (~0.05 mm) from the

inner valve body/rotor housing (Figure 3-2). This alignment was done with the aid of a stereomicroscope. This thin annular region around the column inlet allowed flow (~1.7 µL/min) around the column head and through the 0.02" x 4 cm stainless steel tubing to a second stainless steel tee (S_2, 0.75 mm bore, VICI). This flow was then transported to a third on/off valve (V, VICI) and second splitting system (21 µm x 140 cm fused silica capillary). This post-injection valve splitting system was turned off during sample injection to conserve volume limited samples such as the microdialysates and the turned on prior to starting the gradient run. This post-injection splitting system generated system dwell times of less than 30 s which is important in maintaining gradient integrity. Without the second splitter, excessively long dwell times (> 10 min) and poorly defined gradient profiles were observed. All connections involving fused silica capillary (360 µm outer diameter) were made using 381 µm i.d., 1/16 o.d. x 4 cm PEEK tubing (Upchurch Scientific) and stainless steel nuts and ferrules. These fitting held the capillary in place to pressures up to 4000 psi which out leaking. Note that careful positioning of the column head is important to prevent scratching of the rotor surface and inner wall of the valve body. If the column protrudes even slightly from the inner wall of the rotor housing permanent damage will occur to the valve!

Sample injection. Samples (3.2 µL) were removed from the polypropylene microvials using a 10 µL HPLC syringe (Hamilton), and loaded in to the UW6 valve equipped with a 5 µM loop that was filled with mobile phase A. When the contents of the syringe were injected into the valve, a small air bubble introduced by inserting the syringe into the syringe guide on the valve, was observed to move through the sample loop that was made from fused silica capillary. The rotor slot volume was estimated to be 500 nL, therefore,

the entire sample was injected from the volume element of the rotor slot, not the injection loop. To injection the sample into the column, the on/off valve connected to the second splitter was closed and the sample valve switched to the inject position quickly. The valve remained in this position until the injection was done, then the valve was switched back to the load position, the on/off valve was re-opened, and the gradient program was started.

Gradient elution. The ISCO pumps were operated in the concentration gradient/constant flow mode. Prior to initialization of the gradient program, the pumps were pressurized to 2300 psi. The total mobile phase flow rate was 8 μL/min generating a backpressure on each pump of 2300 psi. The gradient program was as follows: initial = 35% B, then a constant change of 2% B/min until 70% B (17.5 min), a wash off step of 100% B for 5 min, and 10 min re-equilibration step at 35% B.

Electrochemical detection. Cylinder carbon fiber microelectrodes of 9 μm o.d. x 1.5 mm were fabricated published methods (Kaw93). Prior to use, an electrochemical pretreatment was applied (0-+1.8 V, at 1 V/S for 30 s) (Stc85). Background current for these electrodes was typically ~ 16-20 pA after treatment. The electrochemical detector and collection electronics have been described in detail elsewhere (Boy98, Kne84). A notable exception in the detection system was the use of a Stanford SR-570 low-noise current preamplifier (Sunnyvale, CA).

Microdialysis. *In vivo* experiments were performed in male Sprague-Dawley rats as described previously (She97). Microdialysis sampling was performed using side-by-side 4 mm probes constructed in-house. The artificial cerebrospinal fluid (aCSF, Reagent section) was perfused at 1.2 μL/min using a microliter syringe pump (Harvard Apparatus

553206, South Natwick, MA). The microdialysis probe was placed in the striatum (AP=+0.2, ML=+3.0, DV=-6.5). Prior to collection of samples, the rat was allowed to recover until basal levels were constant (~ 2 hr). 10 s microdialysis fraction were collected into microvials containing 1.8 μL of aCSF. After collection, the microvials were covered using parafilm and stored at –20 °C until assayed, typically within 12 hours of collection. Longer term storage resulted in noticeable loss of sample by sublimation.

Results and Discussion

Choice of derivatization reagent. The OPA/*tert*-butyl thiol reagent was used in this study due to the hydrophobicity of the final amino acid derivative that made it ideal for preconcentration onto reversed-phase columns (Boy98). Since this reagent is also highly soluble in aqueous solutions, the derivatized sample matrix is a weak mobile phase and permits sample injection volumes of up to 2 μL be used without loss in chromatographic efficiency (Boy98). Other thiols, including β-mercaptoethanol, were tested, however, the derivatives of the polar amino acids (ASP and GLU) did not preconcentrate as well as the *tert*-butyl thiol derivatives. The NDA/CN reagent was also tested, however, due to the large amount of organic needed to solubilize sufficient amounts of NDA for quantitative derivatization, the final sample matrix is a strong mobile phase and required dilution prior to injection (Roa87, Oat89). The NDA/CN reaction also formed very small crystals that clogged these packed capillary columns and could not readily be removed from the 3.2 μL samples (Oat90).

High sensitivity electrochemical detection of OPA/*tert*-butyl thiol derivatives. To select the optimal potential setting for this electrochemical detector, the electrochemical signal,

root-mean-square noise, and drift caused by the gradient were all measured as a function of electrode potential (Figure 3-3). The electrochemical response of selected amino acid OPA/*tert*-butyl thiol derivatives was similar to results obtained by others using a glassy carbon electrode (All84) for most of the amino acids except ARG which demonstrated a slight decrease in signal at the carbon fiber microelectrode at higher electrode potentials (Figure 3-3A). It is not clear if this effect is due to the difference in electrode material (glassy carbon vs. carbon fiber) or due to the structural effects of the ARG derivative. The RMS noise of the detector increased from 33 fA at 0.65 V to 400 fA at 1.0 V, a trend has been noted before (Ken89c), and has been attributed to the EDTA present in the mobile phase which serves to chelate metal ions leeched from the stainless steel syringe cylinders and tubing of the mobile phase pumping system (Figure 3-3B). The plot of signal-to-noise ratio (Figure 3-3C), demonstrates that a range of +0.7 to 0.8 V would be suitable for high sensitivity detection. However, in addition to signal and noise considerations, the drift in baseline current associated with gradient elution and electrochemical detection should also be considered. The magnitude of gradient drift was calculated as the difference in baseline current from the position of the last eluting amino acid (GABA) and the first eluting amino acid (ASP) and as seen in Figure 3-3D, this effect become appreciable at higher electrode potentials making high sensitivity detection difficult. Since the signal-to-noise curve for GABA (the amino acid expected to be in the lowest concentration in the extracellular space) levels off in the range of +0.7 to +0.8 V and the gradient drift does not increase dramatically until +0.8 V, an electrode potential of +0.75 V was used for all subsequent experiments.

Optimization of derivatization conditions. In this study, the OPA concentration in the derivatization solution was adjusted to yield a final concentration of 8 mM after addition to the sample, which proved to be sufficient OPA to quantitatively derivatize the diluted microdialysate samples while creating minimal background. When the OPA concentration fell below 8 mM in the sample, the ASP and GLU peaks decreased considerably in height. This discrimination seemed to occur primarily against ASP and GLU, an observation that has been made previously for both OPA and NDA (Chapter 1). Since a majority of OPA exists in a hydrated, unreactive form in aqueous solutions (Alv89), it has been suggested that at least a 200-fold excess of OPA to the total amine content of the sample be used for quantitative derivatization (Lin79, God84).

When blanks, samples derivatized that contained no intentionally added amines were run, the resulting chromatogram was littered with peaks (Figure 3-4A). The source of these peaks could be from only two sources: contaminating amines or products from side reactions of OPA and *tert*-butyl thiol. The use of scavenging reactions has been reported to be useful in removing excess reagent peaks for high sensitivity work (Orw91, Rob94, Smo95). Previously, we described a series of scavenging reactions that remove excess OPA and then excess *tert*-butyl thiol that was highly successful, however, the primary amine added in the first scavenging reaction was glycine, a inhibitory neurotransmitter, which limits the use of this amino acid as a scavenger to cases where glycine is not an analyte (Boy98). Several hydrophilic primary amines were tested for use a scavengers, however, the hydrophobicity of the *tert*-butyl group made all of these amines preconcentrate during sample injection, which is undesirable. To prevent the *tert*-butyl group from being incorporated into the final isoindole, the thiol scavenger

iodoacetamide (IAA) was used to remove the excess thiol after sample derivatization. The excess OPA was then scavenged by adding cysteic acid, a highly polar amino acid, and sodium sulfite, a nucleophile that can be used to make OPA-based N-alkyl-1-isoindole sulphonates (Figure 3-5)(Jac87). The cysteic acid based isoindole sulfonate was so hydrophilic it could not be retained on a C18 column in 100% aqueous mobile phase (data not shown), making it ideal for these studies. A large number of the peaks present in the OPA/*tert*-butyl thiol blank were greatly diminished after these reactions (Figure 3-4B), however, some interfering peaks such as those that co-elute with SER and GLY could not be removed by the scavenging reactions and are due to amine contamination of the reagents, vials, pipette tips, or sample matrix. When a 50 nM amino acid solution is derivatized and then the excess reagent scavenged, a majority of the derivatives were free from interference (Figure 3-4C). The ASP derivative is partially resolved from a large peak a 7.5 min that is the OPA/*tert*-butyl thiol derivative of cysteic acid and the TAU derivative is obscured by an amino contaminant introduced during the IAA reaction. The ASP peak was resolved more from the cysteic acid derivative by adjusting the mobile phase pH from 6.8 (pH used in this figure) to 6.5 which reversed the elution order of the two peaks and increased their resolution. The amine interfering with TAU was absent in other batches of iodoacetamide.

Several other attempts were made to reduce the chemical background that merit mention. One approach to reducing background peaks that originate from amino acid contamination is to age the derivatization solution prior to use (Jon81). Proponents of this approach typically use the OPA/β-mercaptoethanol reaction, which forms isoindoles that are inherently more unstable than *tert*-butyl thiol derived isoindoles. When similar

aging experiments were attempted using the OPA/*tert*-butyl thiol reagent, no change in the number or intensity of the background or contaminant peaks was observed after aging the solution 24 hours. Since NDA derivatization requires the separate addition of nucleophile and aldehyde to prevent the benzoin condensation (Roa87, Dem87), experiments were performed in which the OPA and *tert*-butyl thiol solution were added separately to the sample in an attempt to reduce the background, however, this did not result in a decrease in the intensity or number of the background peaks. Experiments were also performed in which reagents were kept at 4° C, but no different in the background was observed. It was observed that the background peaks were considerably larger when more acidic mobile phases were used.

Nano- and Microscale Derivatization. When the sample handling and derivatization steps were miniaturized in preparation for the microdialysis studies, amine contamination became problematic. Experiments with microvials of different aspect ratios demonstrated a strong correlation between surface-area-to-volume ratio and the degree of contamination, indicating surface contamination. When cleaning procedures were used, a majority of the contamination peaks were eliminated except for those interfering with SER and GLY which remained constant through out these experiments (Figure 3-6, bottom trace). Polypropylene was used throughout these studies since it was found to be much easier to clean relative to glass microvials and did not appear to be adsorb the amino acids.

Detection limits. The use of scavenging reactions and 250 nL injection volumes allowed detection limits of 90 to 3401 pM to be obtained for several amino acids based on a signal-to-noise ratio of 3 (Table 3-2). When injection volumes greater than 250 nL were

used, several additional peaks appeared in the chromatogram that were not removed with the scavenging reactions. Most of the amino acids whose signal are measured against the RMS noise of the detector fall in the range of 302-341 pM. With the exception of ARG and CIT (see below), most of the other amino acids possess similar detection limits, suggesting that no discrimination took place during the reaction. The similarity in detection limits also indicates that most of these amino acids are free of side product interference which would artificially increase the derivative signal, resulting in lower calculated detection limits as seen in Table 3-2 for GLY. Quantitation of GLY near the detection limit is background limited (Sko92), however, since the GLY levels in diluted dialysate are near 200 nM, the background contribution (<5 nM) is negligible. The lower detection limit for ARG and CIT relative to the other amino acids is attributed to structural or charge differences in these analytes which display higher electrochemical sensitivity (Figure 3-3A) compared to the other amino acids.

Table 3-2: Detection Limits using OPA/*tert*-Butyl Thiol Derivatization and Scavenging Reactions

Analyte	CLOD (pM)	Background without scavenging
ASP	340	Yes
GLU	340	Yes
CIT	160	Yes
ARG	90	Yes
GLY	170 (background)	Yes
TAU	320	No
GABA	300	No

High temporal resolution monitoring during *in vivo* microdialysis. Basal level measurements of all the amino acid neurotransmitters, were detected in the 10 s microdialysis fraction (Figure 3-7A). Peak identification was performed by matching peak retention times between microdialysate samples and known standards. In addition

to the amino acids that were used in method development, several additional peaks (unlabeled in Figure 3-7) appear in the dialysate. When tested against a 44 amino acid standard, α-aminobutyric acid and β-amino-isobutyric acid were identified as 2 of the 3 peaks eluting at 16 min while MET and VAL were determined to be 2 of the 3 peaks eluting at 18 min. The identity of the remaining peaks is unknown, but were only present in the microdialysis samples. Due to the high resolving power of the chromatography system, these additional peaks are easily resolved from TAU and GABA. Despite careful cleaning of the syringe used perfuse the microdialysis system, a small ASP contaminant was observed during some microdialysis experiments.

As a demonstration during *in vivo* microdialysis, the aCSF was supplemented with 0.5 mM nipecotic acid, an uptake inhibitor selective for GABA transporters (And90). Once perfused through the microdialysis probe into the extracellular space, the extracellular concentration of GABA 2.2-fold ($p > 0.001$) relative to the basal level (Figure 3-7B), which corresponds well to literature values for GABA uptake inhibition in the striatum (Bia99). The levels of the other amino acids remained constant during the uptake inhibition experiment, as observed by others (Bia99). The results of these studies for three different rats are displayed in Figure 3-8.

In another set of experiments performed on the same rat, the aCSF was changed to 150 mM potassium supplemented aCSF. This level of potassium should cause depolarization of the neuronal membrane and inhibit uptake, resulting in elevated levels of amino acid neurotransmitters. As seen in Figure 3-7C, the change in amino acid neurotransmitter levels is significant only for ASP, GLU, SER, GLY, L-ALA, β-ALA, TAU, and GABA, all of the neurotransmitter and neuromodulator candidates. The

increase in extracellular amino acid levels corresponded to the duration of the potassium stimulation (Figure 3-9), except for TAU, which remained elevated even after the stimulation. This behavior has not previously been observed, but would not be noted due to long sampling times (15-30 min) traditionally used in microdialysis studies. Also presented in Figure 3-9 are the values for several other endogenous amino acids that did not change during the potassium stimulation. The results from all the potassium stimulation data is presented in Figure 3-8. The values obtained in these studies are in agreement with previously published reports of extracellular amino acid concentration in rat striatum (But87a, But87b, Uch94, And90, Tot93, Shi95, Shi93, Sem95, And92, Mor91). Interestingly, all of these experiments were performed in less time (120 s) than it would take to collect one sample in using conventional analytical methods (900 s).

Manually collecting these 10 s fractions did lead to some sampling error that resulted in artificially low levels of neurotransmitter levels being reported, such as fraction 8 (80 s point, Figure 3-9) collected during the time-resolved potassium stimulation. Error of this sort arose when the probe outlet was not smoothly transferred into the filled microvial or if the probe outlet was bumped against the side of the microvial during transfer from well to well. Automation of both the fraction collection and derivatization steps are currently being addressed to minimize this error.

In conclusion, we have presented a method capable of quantitative analysis of all the neurotransmitter amino acids in 200 nL microdialysis fractions collected at 10 s intervals. This represents a 60-fold improvement in temporal resolution. In order to achieve these detection limits, amino acid contamination must be eliminated by thorough cleaning procedures, quantitative derivatization conditions used, detection settings

optimized, and background peaks from excess reagents must be minimized to the fullest extent possible. Further improvements in the method are being developed, including automation of the fraction collection, derivatization, and sample injection as well as decreasing separation time by optimizing the gradient, using smaller stationary phase particles and higher pressures. While well suited for high temporal resolution monitoring during *in vivo* microdialysis studies, this approach to nanoscale amino acid analysis could enable the analysis of nanoliter volumes containing single cells with conventional, commercially available microdispensors without the use of specially constructed microdispensors (Ken89), laser tweezers (Chi98), or microfabricated devices. In addition, the high resolution separation would enable comprehensive profiling of amino acids secretion from single cells with similar temporal resolution to other recently described methods such as channel electrophoresis (Liu99) or enzyme assays (Wan97).

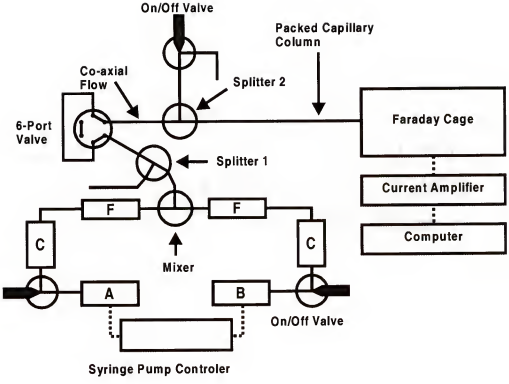

Figure 3-1: Capillary LC-EC Instrument. Abbreviations are listed in the text of the Experimental section. Inset: Close up view of the placement of the packed capillary column and injection loop capillary in the injection valve. During sample injection, the on/off valve after the second splitter was closed to conserve sample.

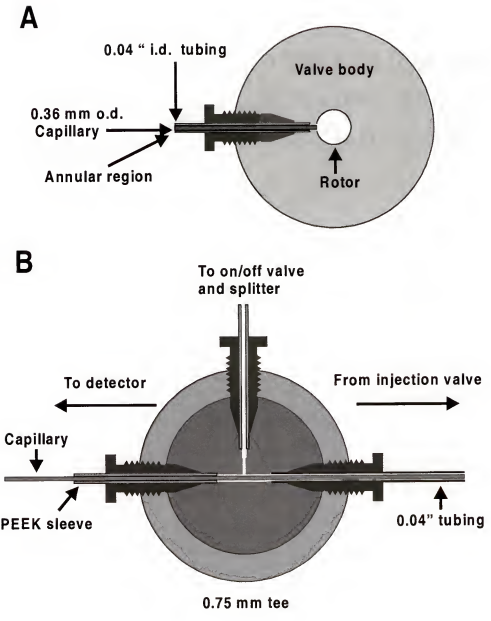

Figure 3-2: Capillary LC-EC Instrument. A: Close up view of the placement of the packed capillary column and injection loop capillary in the injection valve. B: Positioning of the packed capillary within the second splitter tee.

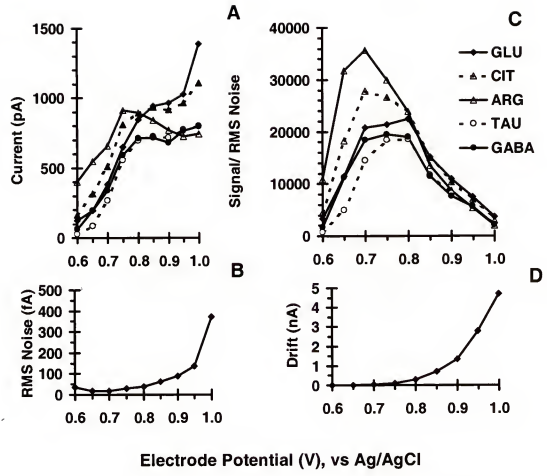

Figure 3-3: Electrochemical Characteristics of OPA/*tert*-butyl thiol derivatized amino acids and carbon fiber microelectrode. All amino acids were 1 μM using 100 nL injections, mobile phase contained 1 mM EDTA. A: hydrodynamic voltammogram of amino acid derivatives. B: root-mean-square noise of the electrochemical detector. C: Signal-to-RMS noise. D: Electrochemical drift.

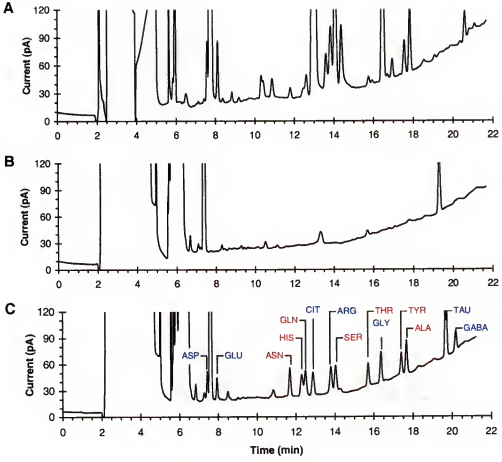

Figure 3-4: High sensitivity blanks. All injection volumes were 100 nL. A: sample without intentionally added amines after OPA/*tert*-butyl thiol derivatization only. B: sample after derivatization followed by scavenging reaction using IAA and then cysteic acid/sulfite. C: 50 nM amino acid standard derivatized and scavenged as in B.

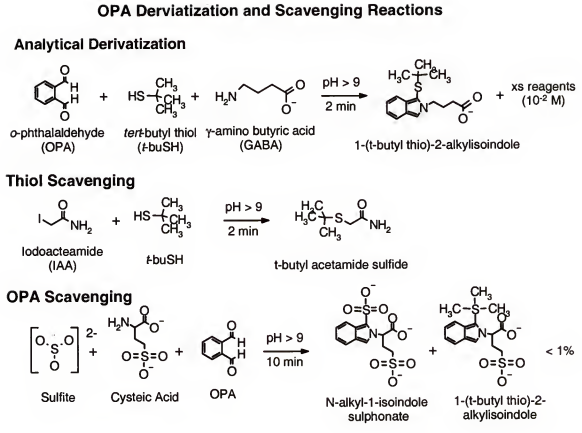

Figure 3-5: Chemical drawings of the 3-step derivatization

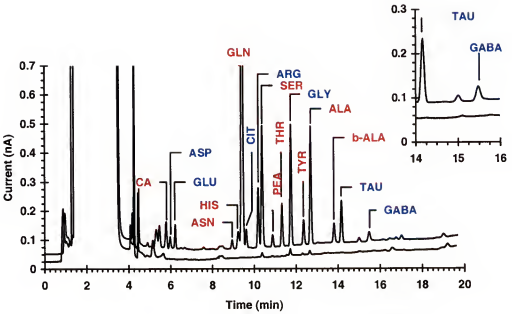

Figure 3-6: Microscale derivatization. Derivatization of aCSF (bottom trace) and an amino acid standard (top trace). 2.0 µL samples were derivatized in a polypropylene microvial, and then 250 nL was preconcentrated onto the capillary column.

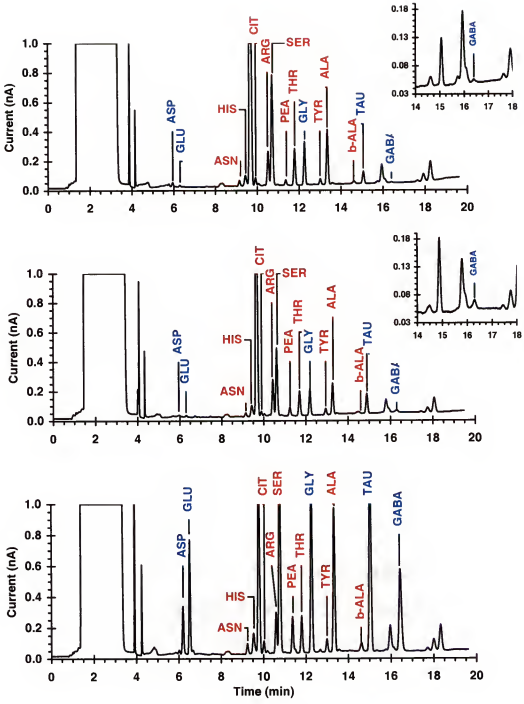

Figure 3-7: 10 s monitoring during *in vivo* microdialysis. 200 nL microdialysis fraction diluted to 2.0 µL prior to derivatization and scavenging. Top trace: aCSF, basal . Middle trace: aCSF with 0.5 mM nipecotic acid . Bottom trace: aCSF with 150 mM potassium.

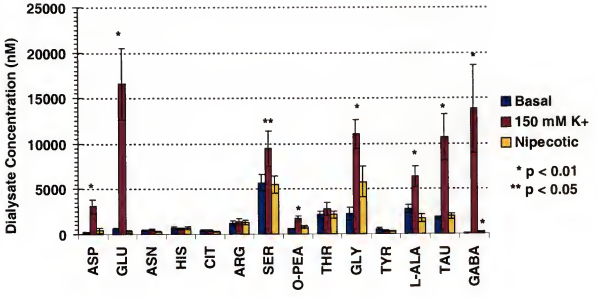

Figure 3-8: Results of 10 s monitoring during *in vivo* microdialysis of the striatum. Data collected from 3 anesthetized animals, significant changes ($p < 0.01$) are listed. Basal levels correspond to aCSF (see experimental section) being perfused through the probe. For nipecotic aid data, aCSF was supplemented with 0.5 mM nipecotic acid. For potassium stimulation, the potassium concentration was elevated to 150 mM (see experimental section).

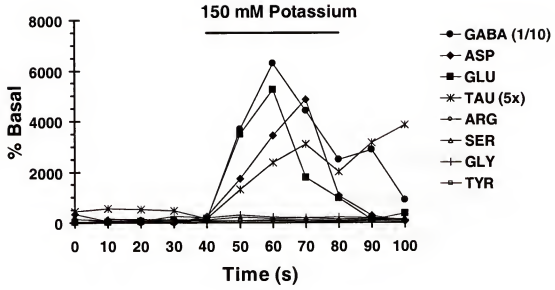

Figure 3-9: Changes in extracellular amino acid levels during potassium stimulation. Data presented as % basal. Note that the GABA scale was reduced 10-fold and TAU scale enhanced 5-fold. Potassium supplemented aCSF reached the probe at 40 s and was removed at 80 s.

CHAPTER 4
AUTOMATED, HIGH SENSITIVITY AMINO ACID ANALYSIS

Introduction

Comprehensive, microscale analysis of neurotransmitter amino acids in biological samples requires analytical methods possessing both high mass sensitivity and high resolving power to separate the large number of endogenous, primary amines found in these samples. Extending this approach to nanoscale analysis typically requires the construction of specialized instrumentation to precisely manipulate and injection sub-microliter samples for quantitative analysis (Ken89c, Gil90). Capillary electrophoresis-based analyzers are compatible with such nanoliter sample manipulation using on-line analyzers (Lad97), microfabricated devices (Jac94a, Jac94b), or laser-tweezers (Chi98), however, the lack of available methods for comprehensive neurotransmitter amino acid (NTAA) analysis has limited this approach to only a few of the NTAAs. A open-tubular liquid chromatography (OTLC) method using 15 μm inner diameter columns has been described for the analysis of 17 protein amino acids in single cells using a pneumatic microdispensor, however, neither GABA, TAU, or CIT were determined (Oat89).

A different approach for quantitative amino acid analysis of nanoscale samples has recently been presented in which sub-microliter fractions are diluted to microliter volumes to permit sample handling and injection using conventional microdispensors and

microsyringes (Chapter 3). However, the dilution of the sample reduces the concentration of trace level neurotransmitters to levels below the detection limits of most conventional methods for amino acid analysis. To obtain the necessary sensitivity a method capable of sub-nanomolar detection of the NTAAs was developed that used precolumn derivatization, chemical scavenging of the excess derivatization reagents to greatly reduce the number of background peaks, and sample concentration onto 50 μm inner diameter chromatography columns packed with 5 μm reversed-phase particles. The major neurotransmitter amino acids (ASP, GLU, GLY, TAU, and GABA) as well as ARG and CIT, the substrate and metabolite of the nitric oxide producing enzyme, were well resolved from other endogenous amines found in microdialysis samples.

While the sensitivity of this method was impressive, improvements in sample handling and derivatization are needed to improve the reproducibility which varied from 5-8 % for the range of amino acids. The improvement in reproducibility is necessary to determine small, significant changes in neurotransmitter levels of biological systems. Automation of the analysis steps should improve the precision of reagent handling and minimize the volume of derivatized sample consumed. This cannot be accomplished using conventional autosamplers for liquid chromatography due to the relatively large sample volume requirement (10-20 μL for derivatization and injection) and large dead volume introduced by the microinjection valve of the autosampler and connection tubing (Table 4-1). While the dead volumes of these systems are nominal for micro-(0.32-1.8 mm) and conventional (4.6 mm) bore systems using 1-1000μL/min flowrates, even 10 μL dead volumes can cause over-injection and excessively long gradient dwell times in capillary columns. Recently, a micro-autosampler using a low dead volume injection

valve has been demonstrated to precisely manipulate sample volumes as low as 1.0 μL in isocratic studies using 0.32 mm bore columns (Vis97).

Table 4-1: Figures of merit for microscale, amino acid analyzers

Amino Acids	Minimum V_{sample} (μL)	Reagent	On-line	Injection V (μL)	% RSD	Ref.
ASP, GLU	0.1	OPA/β-ME	YES	~ 8.3 pL	1-6	Lad97
ASP, GLU	1.0	NDA/CN	YES	N.A.	10.8	Rob98
ASP, GLU	10	OPA/β-ME	YES	41.67	5	Keh98a
ASP, GLU	2.0-10	OPA/β-ME	NO	16	3-11.4	Keh98a
GABA	10-20	OPA/β-ME	NO	9-20	6.4	Keh98b
GABA	10	OPA/tert-butyl thiol	NO	10	2.66	Smo95
ALL 5 NTAA	10	OPA/tert-butyl thiol	NO	10	1.5-4.9	Smo95
ALL 5 NTAA	10	OPA/tert-butyl thiol	NO	10	4.6-8.3	Qu98
ALL 5 NTAA	10	AQC	NO	4-20	1.4-6.0	Liu98

In this work, the direct coupling of a 50 μm i.d. capillary column and micro-autosampler is described for use in microscale analysis of 2 μL biological samples. The direct connection of the column to the autosampler is established without the use of post-injection valve splitting greatly simplifying this design over those previously described. This is accomplished by minimizing the mobile phase transfer lines from the gradient mixer and splitter to the autosampler using fused silica capillaries and results in acceptable gradient dwell times (< 2 mins). The sample injection procedure is optimized to consume only 1.0 μL of sample per 0.25 μL injection and the precision of the autosampler is optimized and to obtain relative standard deviations of less than 5 % for the NTAAs as well as ARG and CIT in both amino acids standards and in biological samples permitting small, significant changes in amino acid secretion to be observed. The automated method is then evaluated over a four day period of continuous use to

evaluate the ruggedness of the system. Once sample derivatization and injection are optimized, the gradient separation is optimized to reduce analysis time and improve both resolution of a critical pair of amino acids and to improve the detection limits by decreasing zone variance.

Experimental

Reagents. Amino acids, iodoacetamine (IAA), *o*-phthalaldehyde (OPA, >99% purity), 2-methyl-2-propanethiol (*tert*-butyl thiol), and boric acid were of the highest purity grade from Sigma or Aldrich (St. Louis, MO). All buffer salts and solvents were obtained from Fisher (Fairlawn, NJ). The phosphate buffer salts were enzyme grade while other salts were certified A.C.S. grade. Water, acetonitrile, and methanol were HPLC grade.

Cleaning procedures. Volumetric flasks, centrifuge tubes, pipette tips, and microvials were washed using 1 N HCl followed by rinses in HPLC grade water and then absolute ethanol. These items were then dried under nitrogen stream and capped until use. Darkened, borosilicate reagent vials were soaked in a bath of 50% 5 N NaOH and HPLC grade methanol overnight prior to cleaning.

Buffers and mobile phases. All buffers were made to be self adjusting in pH after it was determined that the pH meter contaminated the buffers with low levels of amino. Solutions were filtered using a using 0.22 μm Teflon (hydrophobic) membranes (MSI, Fisher Scientific, Atlanta, GA) and a cleaned glass vacuum filtration system. Borate buffer used for derivatization was made to 0.4 M at pH 10.6 $\pm$ 0.1 using 12.37 g boric acid, 7.53 g NaOH (s), and 0.5 L HPLC grade water. The phosphate buffered mobile phase was made to 0.05 M phosphate buffered at pH 6.51 by mixing 4.73 g NaH_3PO_4,

4.22 g $Na_2H_2PO_4$, and 0.372 g ethylenediaminetetraacetic acid (EDTA) in 1 L of HPLC grade water. Mobile phase A was 100 % phosphate buffer while mobile phase B was phosphate buffer with 65% (v/v) acetonitrile. Mobile phases were prepared daily and degassed by He(g) sparging for 10 mins prior to use.

Derivatization solutions. A solution with 40 mM OPA and 50 mM *tert*-butyl thiol was made in a borate buffer containing 50% methanol (both solutions were filtered previously) by directly weighing necessary amounts of recystallized OPA into a cleaned, glass vial prior to addition of the solvents. The iodoacetamide was made to 1 M in methanol. All solutions were stored in darkened, borosilicate glass vials to prevent degradation of the solutions by ambient lighting. All samples were derivatized in cleaned polypropylene vials. The samples (2 μL) were derivatized as follows: 0.4 μL of OPA/*tert*-butyl thiol was added and allowed to react for 5 mins, then 0.4 μL of IAA was added and allowed to scavenge excess thiol for 4 mins. The final sample volume was 2.8 μL. In these studies, the thiol scavenging reaction was sufficient for removing a majority of the background peaks. Note: if any buffer, solvent, or derivatization solution were observed to have particulates or dust, the solution was immediately discarded and re-made.

Capillary Liquid Chromatography. Fused silica capillaries of 48 μm i.d. x 40 cm (Polymicro Technologies, AZ) were fitted with end frits and packed with Alltima C8 particles (5 μm, 100 nm pore) in an acetone slurry (10 mg/mL) at 4000 psi using a pneumatic amplifier pump (Alltech). Columns packed fully within 20 mins, were flushed with 90% (v/v) acetonitrile/water. Upon installation onto the LC system, the columns

were trimmed to 36 cm and flushed with 100 % B for 10 mins prior to use. One gradient cycle was needed to clean the column after packing.

A FAMOS well plate micro-autosampler was obtained from LC Packings, INC (San Francisco, CA). The major components of the autosampler are present in Figure 4-1. The low dispersion valve (VICI C2 6-port valve, Houston TX) was fitted with a 1 μL injection loop constructed in-house using 100 μm i.d./360 μm o.d. fused silica capillary (Polymicro Technologies, Phoenix, AZ) using 381 μm i.d./ 1/16" o.d. PEEK sleeves and stainless steel ferrules and nuts (VICI). The 0.25 μL polypropylene, tapered microvials used in this work were obtained from Sun International (Wilmington, NC). Experiments were also performed using a 384 well, polypropylene microtiter plate obtained from MJ Research (Framingham, MA). In order to use these PCR plates with the FAMOS an adapter plate was made from stainless steel (Appendix C). The reagent vials (10 mL headspace vials with silicone/TFE septa) were obtained from Sun, and both were cleaned prior to use.

Electrochemical detection. Preformed as described in Chapter 3.

Results and Discussion

Automated instrument. An earlier instrument used for microscale injection and gradient elution used a UW6 port valve with a conical rotor and 0.4 mm bore ports (Chapter 3). Initial attempts to directly couple a 50 μm i.d. column to the UW6 valve resulted in very long dwell times of ~10 mins as determined by monitoring the baseline current until the drift associated with the mobile phase gradient was observed. It is also suspected that the dead volume of the valve (~2.3 μL) distorted the gradient profile. Therefore, in order to

use the UW6 valve, it was necessary to develop a post-injection valve splitting system to rapidly sweep out the dead volume of the injection valve. However, due to the very limited sample volume (~3 μL), it was necessary to install an on/off valve on the post-injection valve splitter to prevent the sample from being split during sample injection.

The FAMOS autosampler is equipped with a model C2 6-port injection valve that uses a flat, plate rotor and 0.25 mm bore ports resulting in an internal volume of ~200 nL. Using 0.25 μL/min flowrates, the dwell volume of the injection valve is flushed in 48 s. To further decrease the dwell volume, the transfer lines from the gradient mixer and mobile phase splitter were replaced with fused silica capillaries (Figure 4-1). Using a 75 μm i.d. by 30 cm length of capillary, the volume from the mixer (~ 300 nL) to the mobile phase splitter was reduced to 1.3 μL. The combined flow rate from the high pressure syringe pumps is 8 μL/min therefore the dwell time in this part of the mobile phase system is 9.75 s. After the mobile phase split (1:160 split), the flow rate is reduced to the column flow rate (0.25 μL/min at 3600 psi). To minimize this volume, the transfer line from the mobile phase splitter to the injection valve was made from 50 μm i.d. by 14 cm capillary (~275 nL). The created a dwell volume of ~475 nL which was swept by the column flow rate in 1.9 mins, which is an acceptable dwell time.

Minimizing sample consumption. Three pre-programmed methods for sample injection are included in the FAMOS, however, a user-defined injection sequence was designed to minimized sample consumption and dwell volume (Appendix B). In these studies a final derivatized sample volume is 2.8 μL. In the previous study, we determined that injection volumes of 0.25 μL allow the greatest degree of preconcentration while minimizing

background peaks not removed by chemical scavenging after sample derivatization. The capillary dimensions required for a 250 nL injection loop are 50 μm i.d. by 12.76 cm, which places a large backpressure on the internal syringe pump of the autosampler, making full loop injections of this volume impossible. Partial loop injections switch the injection valve for a set period of time and then return to the load position, both removing the valve the mobile phase transfer lines (adding no dwell volume) to permit injection volumes smaller than the injection loop to be injected onto the column. However, the entire sample is consumed using this injection. The micro-pickup injection sandwiches a small plug of sample between large plugs of a transport solution, minimizing sample consumption. However, this injection method requires a 10 μL sample loop adding considerable dwell volume to the mobile phase transport lines. In order to minimize sample consumption and dwell volume, a user-defined injection sequence was made that combines the features of partial loop and the micro-pickup injections. In this method, the autosampler needle, injection loop (1 μL), and valve is filled with mobile phase A. The fused silica sample needle (100 μm i.d.) is then placed in the sample vial and a preset volume of sample is aspirated into the end of the sample needle. The sample zone is transferred to the injection loop by placing the capillary inlet into a vial containing mobile phase A and then aspirating a volume equal to the fused silica sample needle (2.4 μL). In reality the needle volume is slightly less than 2.4 μL, but this additional volume clears out the ports and rotor slot connecting the sample needle and injection loop. The valve is then switched into the inject to load the sample onto the column head. The volume injected into the column is the product of the column flowrate (0.25 μL/min) and

injection time. After this injection time has expired the valve is switched back into the load position, removing the sample loop from the mobile phase flow path.

Table 4-2: Injection Methods for FAMOS Autosampler

Injection Method	Added dwell volume (μL)	Injection volume (μL)	Volume consumed per injection (μL)
Full loop	1.0 (loop)	1.0	2.8
Partial loop	0.0	< 1.0	2.8
Micro-pickup	10.0 (loop)	1.0	1.0
User-defined	0.0	0.3	0.3

To determine the reproducibility of the user-defined injection method, 2 μL samples containing a 16 component, 100 nM amino acid standards were derivatized (see below) and injected onto a 50 μm i.d. capillary column. Using the user-defined method is was possible to consume only 0.3 μL per 0.25 μL injection with RSD's (n=4) ranging from 3.0 to 8.4% for neurotransmitter amino acids and CIT (Table4-3). Due to the age of this column, ARG and SER were not resolved, therefore the ARG data is not presented. When 1.0 or 2.0 μL of sample is used to flush and fill the injection valve prior to injection, the RSD's for a majority of the amino acids improves to 1.9 to 3.0% (n=4). This is due to a more thorough rinsing of the internal volume of the C2 valve (~200 nL), part of which is a dead volume that originates from a mismatch in inner diameter of the 100 μm i.d. sample needle and 250 μm bore port leading to the valve rotor. In subsequent studies, 1.0 μL of sample was removed for each injection to achieve the maximum injection reproducibility with minimum sample waste.

Table 4-3: Injection Reproducibility of 0.25 µL Injection Consuming Different Sample Volumes

Analyte	0.3 µL	1 µL	2 µL
ASP	7.8	1.8	6.4
GLU	8.4	2.2	1.8
GLY	3.0	2.5	1.5
TAU	3.4	4.1	3.7
GABA	4.1	3.0	4.0
ARG	n.d.	2.9	1.6
CIT	5.7	2.6	1.4

Automation of derivatization. A user defined derivatization method was developed for derivatization of 2.0 µL samples by reacting 0.4 µL of OPA/*tert*-butyl thiol followed by addition of 0.4 µL of iodoacetamide reagent with one mixing step after addition of each reagent. Initial experiments without the mixing step resulted in peak area RSD's (n=3) from 7.6% (L-ALA) to 59% (HIS), and decreased for some amino acids to 1.6% (CIT) to 56.2% (HIS) when one mixing step was used after each reaction. For each of these studies, a 2 min OPA reaction time was used. The mixing efficiency using the autosampler is not as thorough as manual mixing using a microdispensor, so the OPA reaction time was increased to 5 mins. Using the longer OPA reaction time, the RSD's fell to 1.4% (ARG) to 6.4% (ASP) (Figure 4-2A, Day 1). Throughout these initial studies, it was observed that the RSD's for ASP and GLU (peak retention time, height, and area) were typically higher than the other amino acids. After this study, it was discovered that a very small leak (1-2 µL/min) had developed on the piston seal of the high pressure syringe pump A, which contained the weak mobile phase (50 mM phosphate pH 6.51 with 1 mM EDTA). Under these gradient conditions, ASP and GLU elute from the column under semi-isocratic conditions using the initial gradient mobile phase (35% B= 22.75 % acetonitrile) and a small leak from pump A caused the mobile

phase strength to be proportionally stronger (24% acetonitrile for a 2 μL/min leak in pump A). The irreproducible initial mobile phase conditions caused not only variations in chromatographic properties (retention time, peak variance, peak height) but also decreased the efficiency of preconcentration which caused variations in peak height and area.

Long term use of the automated system. To test the ruggedness of the autosampler, mobile phase delivery system, capillary column, and electrochemical detector, the system was run for 4 consecutive days during which a set of amino acids standards was assayed followed by biological samples. When standards or samples were not being analyzed, the gradient system was operated in a continuous loop to determine what effect, if any, constant exposure to the mobile phase had on the resolving power of the column. Since each high pressure syringe pump has a 100 mL mobile phase reservoir and the total flow rate from the system for these experiments was 8 μL/min, the pumps could be operated for roughly 17 days without refilling. At the beginning of this study a new carbon fiber microelectrode was installed at the column outlet and was then operated continuously for the 4 day period without physical or electrochemical pretreatment. The derivatization reagents were made fresh daily.

The automated method yielded RSD's (n=3-4) below 5% for GLU, GLY, TAU, GABA, CIT, and ARG over the 4 day period (except for ASP as discussed above). The resolving power of the column remained constant over the entire testing period for a majority of the amino acids except for ARG and SER (Figure 4-2B). On day 1 and 2, the resolution between ARG and SER was 0.82-0.84, but by day 3, the resolution had degraded to less than 0.5, which adversely affects quantitative analysis of these two

important amino acids (Figure4-2A). The peaks neighboring ARG and SER (CIT and O-PEA) maintained the same resolution from the co-eluting peak as from either ARG or SER, respectively. The cause for the loss in resolution between these amino acids is probably the result of a slow degradation in column performance caused by either the phosphate-based mobile phase or the high pH (~9.6) sample both of which have been observed to slowly dissolve silica-based stationary phase particles that could effect the column efficiency or selectivity. In studies where the column is stored in an organic solution (65% mobile phase B) when not being used, the useful lifetime of the column can approach one week (data not shown). This indicates that the mobile phase may play a faster role in degrading the column than the high pH samples. During this study, cell conditioned media was analyzed after the system precision was measured and detector calibrated and at not time was column clogging observed. In fact, throughout the 4-month period the automated system was used, no columns ever became clogged. Since the column resolving power currently limits the long term, unattended use of this system to 2 days, the use of pH- and phosphate buffer stable stationary phase particles was investigated.

Alternative stationary phase particles. In an attempt to increase the useful lifetime of these capillary columns the use of pH and phosphate stable stationary phase particles was explored. Reversed-phase, 5 μm particles were obtained from MetaChrome and Phenomenex. The MetaCapsil C8 particles are silica-based, porous particles (12 nm) that are encapsulated in silicon and then have the stationary phase bonded to this silicone base. With the silica base encapsulated and the stationary phase bonded through Si-C bonds instead of siloxane bonds, a stationary phase resistant to aggressive solvents and

high pH is formed. The slurries formed using acetone and the Metacapsil particles were not stable for more than 30 mins with particle aggregates forming even during stirring that prevented packing columns to the same length as the Alltima particles. A test mixture of the 16 amino acid standard used in the 4 day study was derivatized, preconcentrated and separated on the Metacapsil column (Figure 4-3B). The same gradient (35-63% B slope = 2%B/min) was used on this column as the 4 day old Alltima column (Figure 4-3A). The new Metacapsil column performed similarly to a new Alltima column, offering less than baseline resolution for the ARG-SER pair. Compared to the Alltima column, the Metacapsil column was unable to resolve the ASN-HIS pair and provided less resolution for O-PEA-THR and TAU-GABA which prevented this column from being used in further studies, since at least 3 peaks (α-aminobutyric acid, β-iso-aminobutyric acid, and an unknown) elute between TAU and GABA in biological samples. The Phenomenex Luna C5 particles was made from high purity silica that provides high surface bonding of the stationary phase. The capacity of this C5 phase was greater than that of either C8 phase (Alltima or Metacapsil) and required a longer gradient (35-70% B, slope=2%B/min) to elute GABA (Figure 4-3C). This column provided a substantial increase in resolution for the ARG-SER peaks, however, resolution between ARG-CIT and TAU-GABA is decreased relative to the Alltima particles making this column unacceptable for biological samples. Interestingly, the peak elution order was the same on all columns. In amino acids analysis using both NDA/CN and OPA/β-mercaptoethanol, the resolution between GLY and THR is difficult on C18 columns using acetonitrile/phosphate mobile phases similar to those used here. In these studies, the authors used tetrahydrofuran (THF) as a modifier (5% v/v) in the acetonitrile mobile

phase to resolve GLY-THR. In a similar strategy to help improve the resolution between ARG-SER in this separation, mobile phase B was remade to be 60/30/5% (v/v) acetonitrile/phosphate/THF. However, using the older Alltima column and this mobile phase did not increase the resolution between ARG-SER. Instead, it was observed that THF in mobile phase B increased the gradient drift. It was also observed that the chromatography system backpressure increased (~100 psi) during the gradient run before returning to initial levels, whereas the backpressure typically falls slightly (50 psi) during one chromatographic run. This indicates that the small amount of THF added to the acetonitrile/phosphate mobile phase significantly increases the viscosity of the mobile phase. This could be useful maintaining consistent backpressure in low-pressure mixing and splitting capillary chromatography systems, where the backpressure typically fluctuates greatly (500 psi) when aqueous/acetonitrile gradients are used.

Decreasing Analysis Time. The gradient used in prior work for the amino acids utilizes a linear gradient from 35-63% B and a change of 2%B/min in slope, resulting in a gradient separation time of 14 min. This separation was found to be capable of resolving the neurotransmitter amino acids from the endogenous amino acids and primary amines found in physiological samples and was used without further optimization. To determine if the separation time could be decreased without loss in resolution of the neurotransmitter amino acids, the gradient was optimized using the Linear Solvent Strength (LSS) theory proposed by Snyder (Sny79). The gradient optimization of OPA/ethanethiol derivatized amino acids using conventional bore columns of different lengths and reversed-phase particle sizes has been explored by others (Esl87). It would

be advantageous to decrease the gradient separation time for this automated system to increase the sample throughput.

The resolution equation in gradient elution is similar to that under isocratic conditions in which the resolution between two adjacent peaks is expressed using the following equation:

$$Rs = \sqrt{\frac{N}{16}} \cdot \left(\frac{\alpha - 1}{\alpha}\right) \cdot \left(\frac{k''}{k''+1}\right) \quad \text{Equation 4-1}$$

where R_s is the resolution between two adjacent zones, N is the efficiency of the column, α is the separation selectivity factor, and k'' is the average capacity factor. In many separations, the capacity factor term in the resolution equation is the most simple experimental variable to change since it is directly affected by mobile phase solvent strength. In LSS gradients, the mobile phase strength is linearly increased during the separation time causing the capacity factor of the analyte zone to continually decrease as the gradient progresses until the zone is eluted from the column. Therefore k" is representative of an average value of capacity factor (Syn79).

To optimize the resolution in gradient separations, the k" should fall between 2-10, similarly to isocratic elution (Syn79). In gradient separations, k" changes during the slope of the gradient profile or gradient steepness parameter (*b*) where *b* is related to k" by:

$$b = \frac{1}{1.15\, k''} \quad \text{Equation 4-2}$$

and

$$b = \frac{\Delta\Phi \cdot S \cdot V_0}{t_G \cdot F} \quad \text{Equation 4-3}$$

where $\Delta\Phi$ is the change in organic modifier during the gradient, S is the solvent strength of the organic modifier, V_0 is the void volume of the column, and t_G is the time over which the gradient is varied linearly. According to this theory, the optimal values for *b*, using optimal k" values of 2-10, range from 0.434 – 0.087 for a majority of applications. From these set of equations, the separation resolution increases asymptotically with $1/b$ or t_G. The OPA/*tert*-butyl derivatized amino acids are separated here on a 50 μm i.d. by 34.5 cm column (V_o= 474 nL, assuming a column porosity = ε = 0.7) using a column flow rate of 250 nL/min and a change in acetonitrile of 0.1825. The solvent strength of acetonitrile and other solvents are listed in Table 4-4 (Sny79). The current gradient slope of 2%B/min takes 14 mins to complete, resulting in *b*= 0.075 (k"=11.6), indicating that the separation time could be increased without loss in resolution by increasing *b*. To determine the gradient slope which provided the necessary resolution with lowest gradient time, 6 different gradient programs were used to separate a 16 component amino acid separation with a range of *b* from 0.038 to 0.2 (Table 4-5).

Table 4-4. Solvent Strengths of Various Organic Modifiers

Methanol	Acetonitrile	Ethanol	Acetone	Dioxane	Isopropanol	THF
3.0	3.1	3.6	3.4	3.5	4.2	4.4

Table 4-5: Gradients Tested for Amino Acid Separation

Gradient Steepness Parameter (b)	Gradient Time (t_G)	Gradient Slope (%B/min)	Gradient Slope (% acetonitrile /min)
0.038	27.9	1.0	0.65
0.075	14	2.0	1.3
0.09	11.78	2.36	1.53
0.1	10.6	2.64	1.72
0.15	7.0	4.0	2.6
0.2	5.3	5.28	3.43

The chromatograms using b=0.038, 0.075, and 0.15 are displayed in Figure 4-4A-C, and the data for peak variance, resolution, and peak height enhancement for all the gradients tested are displayed in Figure 4-5A-C. The change in gradient slope did not alter the peak elution order for any of the OPA/*tert*-butyl thiol derivatized amino acids. For the lowest gradient slope (b=0.038) that corresponds to a 1%B/min slope, the amino acid bands are well separated from each other (Figure 4-4A), but are quite broad (Figure 4-5A) which decreases the resolution between ARG-SER and O-PEA-THR to less than 1.5 (baseline resolution). As steeper gradients are used, both the zone spacing (difference in retention time) and zone variance decrease at disproportional rates, improving resolution between these adjacent pairs (Figure 4-5B). The decrease in peak variance (Figure 4-5A) which is proportional to peak width enhance the peak heights (Figure 4-5C), that improve the sensitivity of this method further (see below). For a majority of these studies, the early eluting amino acids ASP and GLU were not as affected by changes in the gradient slope as the later eluting peaks since they elute isocratically under the initial mobile phase conditions. However, at very steep gradient slopes ($b \geq 0.15$), the zone compression seen in the later eluting peaks (Figure 4-5A) is observed by both ASP and GLU. Also observed at high gradient slopes ($b \geq 0.2$) was the loss of resolution for β-ALA, TAU, and GABA (Figure 4-5) which were eluted out during the 65% acetonitrile wash-off step performed after each gradient run. This could possibly be solved by extending the gradient range to higher %B values or by incorporating a hold step at the final %B value to allow to these peaks to finish eluting prior to the wash off. From these gradient optimization studies using a 50 μm i.d. by 34.5 cm length columns packed with 5 μm particles, the 7 mins gradient time (b=0.15) produced the best results with regards to

resolution to the 14 min gradient and also generated a 40% enhancement in peak height. Prior to using this separation for analysis of biological samples, a three different amino acid test mixtures were spiked into a sample containing the 16 amino acid standard typically used to calibrate this system (Figure 4-6). Even when all 44 amines are present in the sample, all the major neurotransmitter amino acids are well resolved from and additional peaks, making this separation method suitable for amino acid analysis of biological samples.

While the 7 min reduction in duty cycle increased the throughput of the automated system by roughly 23%, the duty cycle (time necessary to perform 1 analysis) is 23.7 mins which is limited by the chromatography system. This is due to the 5 min wash-off and 10 min re-equilibration step required after each run. Since column wash-off and re-equilibration are volume-dependent processes, the time spent during these steps could be decreased by increasing the volumetric flowrate of the column either by increasing the operating backpressure during these steps or by using columns that operate with similar efficiencies at greatly increased flowrates. Increasing system backpressure only during these steps would necessitate steps that allow for the system to depressurize prior to performing the gradient run. Since this system is slow to depressurize through the splitting system and operates at half to maximum pressure load of the syringe pump piston seals, simply increasing the system backpressure is not a practical approach. The use of shorter columns packed with smaller diameter particles (< 5 μm) that possess similar efficiencies to the columns used in this work would permit higher volumetric flowrates to be used while maintaining the necessary separation efficiency. It should be noted that any increase in column efficiency should also allow steeper gradient slopes to

be used as well (Equation 4-1) further decreasing separation time. This could be accomplished using high efficiency capillary columns packed with 1-1.5 μm pellicular particles, however this approach requires ultra-high pressures that exceed the pressure limitations of the current pumping system.

Detection limits and reproducibility. After the gradient separation time as optimized, the system reproducibility and detection limits for the neurotransmitter amino acids were determined using the 25 nM, 16 amino acid standard solution. Prior to this study the high pressure syringe pump that had been leaking was disassembled, thoroughly cleaned, and a new high pressure seal was installed. With the new piston seal, the retention time and peak area RSD's (n=3) of the early eluting amino acids were significantly lower than those previously reported (Table 4-6). The detection limits ranged from 0.06 to 0.18 nM for most of the amino acids except GLY co-eluted with an amine contaminant (as reported previously). The detection limits for ASP and GLU were slightly higher than the other amino acids since the peak compression effect caused by the increased gradient slope does not affect these analytes as significantly as more higher retained amino acids. The lower detection limits for ARG and CIT have been observed previously and may be due to either a structural or transport effect.

Table 4-6: Reproducibility and Detection Limits for Faster Method

Amino Acid	Retention Time R.S.D	Peak Area R.S.D.	Detection limit (nM)	Detection limit (amol)
ASP	0.76	3.5	0.18	45
GLU	0.77	1.8	0.18	46
CIT	0.69	1.6	0.08	21
ARG	0.61	1.7	0.06	16
GLY	0.46	4.0	Background	Background
TAU	0.28	0.6	0.14	35
GABA	0.18	1.1	0.13	32

In conclusion, an automated method was developed that is analyzing micro- or nanoscale samples with both high precision and sub-nanomolar concentration limits of detection for the major neurotransmitter amino acids using a commercially available autosampler and 50 μm i.d. packed capillary columns. The problems associated with interfacing the 50 μm i.d. columns, autosampler, and high pressure gradient system were overcome by using large volume sample injections (0.25 μL) and by minimizing the gradient system dwell volume using 50 μm i.d. fused silica capillaries. This approach was possible only with the development of protocols to minimize amine contamination, clean derivatization chemistry, high resolution gradient separations, and high sensitivity electrochemical detection. Using a user-programmed sequence for sample handling and injection greatly reduced the sample consumed per analysis relative to a previously described manual method, permitting only 0.3 μL of sample be used per injection with good precision. In comparison to conventional size systems for automated amino acid analysis, this method obtains comparable levels of precision with 5-10-fold reduced sample volume requirements, 10-fold lower concentration detection limits, and greater than 100-fold lower mass detection limits. The overall duty cycle of the analyzer was reduced 22% by reducing the gradient separation time without compromising resolving power using the LSS theory. The resulting gradient time was reduced to 7 mins and permitted resolution of the major neurotransmitter amino acids including CIT and ARG from a 44 physiological amine standard.

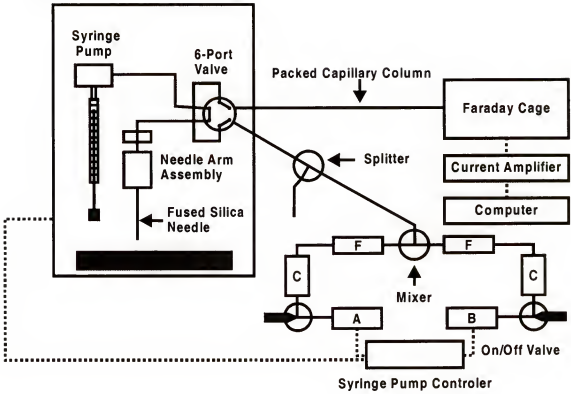

Figure 4-1. Schematic of the automated, amino acid analyzer. The fluid connection limes are represented by solid lines and communication lines are represented as dashed lines.

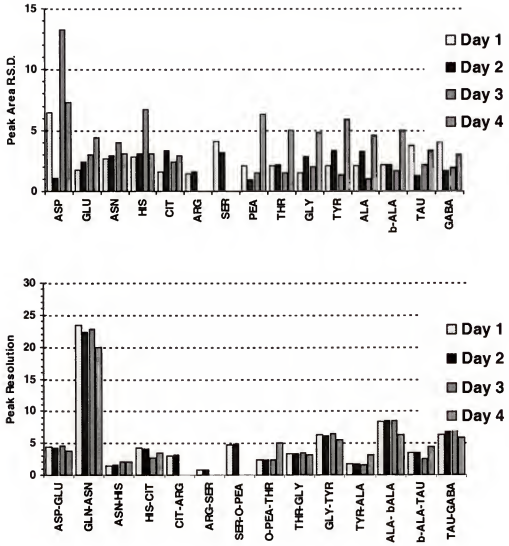

Figure 4-2. Results from the long term stability test of the automated instrument. Figure 4-2A shows the peak area RSD's for the 16 amino acids assayed. Figure 4-2B shows the peak resolution over the four day period. Due to a loss in resolution of ARG and SER after the second day, data for these peaks could not be determined on days 3 or 4. The resolution between the neighboring peaks (CIT and O-PEA) and the merged ARG-SER peak was unchanged on day 3 and 4.

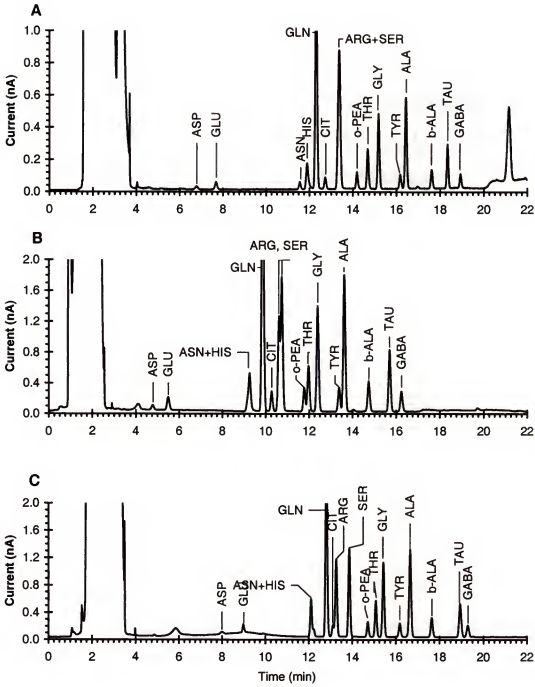

Figure 4-3: pH stable stationary phase particles

Figure 4-3. Amino acid separations of other pH- and phosphate stable columns. Chromatogram A is the amino acid separation using a 5 day old Alltima C8 columns where the resolution between ARG and SER had degraded. Chromatogram B was obtained using a 50 μm i.d. columns packed using MetaCapsil C8, 5 μm particles using the same gradient program and amino acid sample as in A. Chromatogram C was obtained using the Luna C5 phase but required an extended gradient for the elution of the later amino acids.

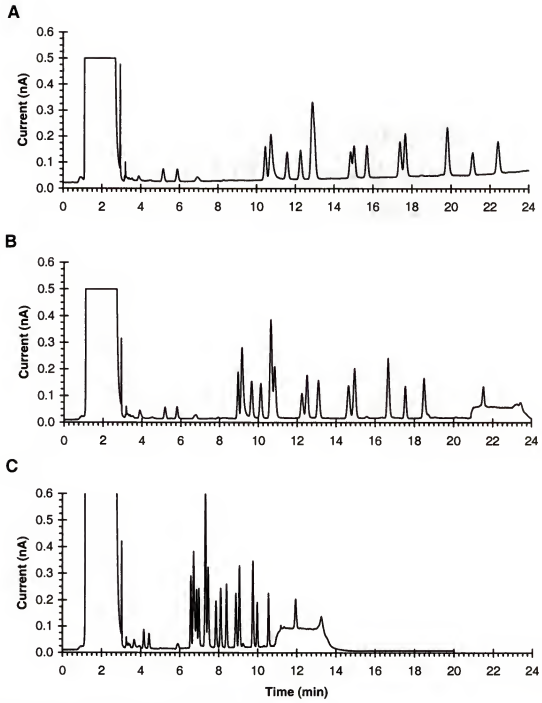

Figure 4-4: Optimization of gradient separation

Figure 4-4: Amino acid separations using different gradient steepness parameters (*b*). Chromatogram A used a gradient of 1% B/min (b=0.038), B used a gradient of 2% B/min (b=0.075), and C used a gradient of 4%B/min (b=0.15). The mobile phase gradient proceeded from 35-63% B for all experiments.

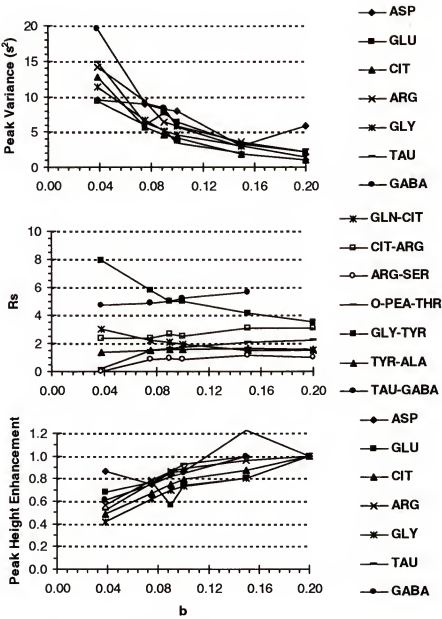

Figure 4-5: Effect of increasing b on peak zone variance (A), resolution of adjacent pairs (B), and peak height enhancement (C, ratio of peak height to maximum peak height obtained at either b=0.2 or 0.15). Since ASP and GLU are eluted under partially isocratic conditions, the changes in peak variance reduction and peak height enhancement are not as great as the more highly retained amino acids (CIT-GABA).

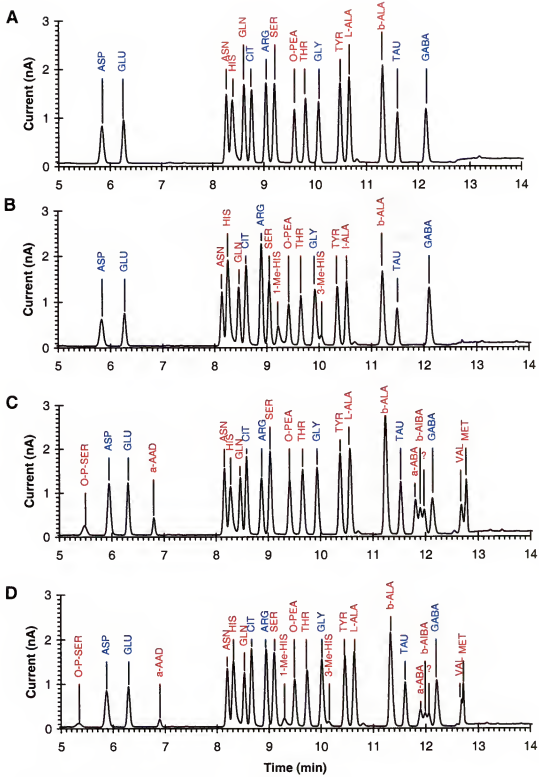

Figure 4-6: Resolution of optimized gradient separation

Figure 4-6: Resolving power of the new gradient separation. Chromatogram A shows that separation of a 500 nM 16 amino acid standard (ASP, GLU, ASN, HIS, GLN, CIT, ARG, SER, O-PEA, THR, GLY, TYR, L-ALA, β-ALA, TAU, AND GABA). Chromatogram B is a separation of the 16 amino acid standard with 125 nM basic amino acid standard containing (GABA, NH_4Cl, Anserine, ARG, Carnosine, Ethanolamine, Homocystine, HIS, δ-hydroxy-LYS, LYS, 1-methyl-HIS, 3-methyl-HIS, and PHE). Only the methyl-HIS peaks were elutes using this gradient. Chromatogram C is a separation of the 16 amino acid standard with 125 nM acidic and neutral amino acids standard containing (β-ALA, L-ALA, α-amino-n-butyric acid or α-ABA, α-aminoadipic acid or α-AAD, β-aminoisobutyric acid or β-AIBA, ASN, ASP, CIT, Cystathionine, Cystine, GLU, GLY, ILE, LEU, MET, O-P-SER, O-PEA, Sarcosine, SER, TAU, THR, TYR, Urea, and VAL). Chromatogram D combines all these amino acids and dopamine, noradrenaline, seratonin, and tyramine.

CHAPTER 5
PROFILING AMINO ACID SECRETION FROM SINGLE PANCREATIC ISLETS OF LANGERHANS

Introduction

In the brain, the amino acid neurotransmitters GABA and GLU have established roles as neurotransmitters. In various peripheral system including the gut, urinary bladder, heart, lung, ovary, and pancreas, the tissue levels of GABA and GLU are similar to that in the brain, however, several other characteristics must be met to classify these amino acids as neurotransmitters in the brain (Smi96a). The cell suspected of releasing a neurotransmitter must synthesize, store, and release it upon pre-synaptic stimulation. The neurotransmitter must also demonstrate that it can elicit the same post-synaptic response on target cells as pre-synaptic stimulation, and that this action can be blocked by pharmacological agents that block the post-synaptic response to exogenously applied putative neurotransmitter. The post-synaptic response should also terminate rapidly and the suspected transmitters must behave pharmacologically identical to the endogenous transmitter (Smi96a).

Within the pancreatic islets of Langerhans, some of these characteristics have been found, however, before GLU and GABA can be classified as neurotransmitters in islets, the glucose regulated secretion of these suspected neurotransmitters must be demonstrated. Islets are microorgans found in the pancreas that contain approximately

3,000 cells including α–cells that secrete glucagon and β-cells that secrete insulin (Figure 5-1). Secretion of these peptide hormones during different metabolic states are largely responsible for glucose homeostasis. Stimulation of β-cells with elevated levels of glucose directly increases the rate of insulin secretion, however, the mechanisms by which glucagon secretion from α-cells is inhibited by glucose is unknown (Ror89).

The regulation of islet hormone secretion by neurotransmitter amino acids has been reviewed in 3 recent articles that extensively outline the body of work done using electrophysiological and histochemical methods (Sor91, Mic92, Sat98). Since this work focuses on the possible neuroendocrine role of GABA and GLU in islets, the research pertinent to this work is breifly reviewed here. Other possible roles for GABA in islets, include a fuel for intracellular metabolism or GABA as a regulator of β-cell function (Mi92).

GABA and GLU receptors in islet cells. Functional, ionotropic $GABA_A$ receptors have been found on α-cells and functional, ionotropic GLU receptors have been found on β-cells (Ror89, Ina95). In electrophysiological studies using isolated α-cells (from guinea pig), exogenously applied GABA hyperpolarized (inhibited) the action potential of the cell and when removed, the cell again became depolarized (Ror89). The electrophysiological data obtained from the α-cells was similar to that obtained from other cells types possessing $GABA_A$ receptors (Ror89). In studies with isolated islets, the addition of GABA reduced stimulated glucagon release (Ror89). In similar studies using isolated β-cells, GLU receptor agonists, kainate, α-amino-3-hydroxy-5-methyl-4-isoxazole (AMPA), and *N*-methyl-D-aspartate (NMDA) all caused β-cell depolarization (Ina95). These agonists also stimulated insulin secretion from isolated islets (Ina95).

GABA and GLU synthesis. Glutamic acid decarboxylase (GAD) activity in islets was first discovered to be present at high levels in 1976, indicating that GABA could be synthesized within the islet (Oka76). Using immunohistochemistry, GAD was localized to be present only in β-cells (Gar88). Shortly after this, GAD was identified as the major autoantigen in type 1, insulin-dependent diabetes mellitus, a form of diabetes in which the β-cells are targeted and destroyed by autoimmune mechanisms (Bae90). The GABA metabolizing enzyme, 4-aminobutyrate-2-oxaglutarate aminotransferase (GABA-T), has also been found in the islets and localized to mitochondria in β-cells (Gar87a). The enzyme responsible for GLU synthesis in neuronal cells, phosphate activated glutaminase, was localized to α-cells within islets using enzyme labeled antibodies for this enzyme (Ina95).

GABA and GLU storage within islet cells. The large concentration of GABA within islets (Bri72, Ger79, Oka76) was found to be localized with GAD (Gar88) to β-cells (Gar87b). Synaptic-like microvesicles (SLMVs), with homologous structure to GABA containing synaptic vesicles, are present in β-cells and β-cells lines and were immunoreactive to antibodies against GABA and GAD (Ree91). SLMVs isolated from β-cell lines were found to contain a GABA transporter while SLMVs isolated from α-cell lines did not possess this transporter (Tho93).

GABA and GLU uptake by islet cells. Using radiolabeled GABA, uptake in islets was localized to the islet mantle in δ-cells, that secrete somatostatin (Gil89). In this study, the percentage of cells that take up GABA changed as the islet aged, which notable, but unexplainable at this time. A high affinity GLU/ASP transporter system has recently been reported in islets, and localized to non-β-cells within the islet (Wea98). Also, in this

study, when GLU uptake is blocked with L-*trans*-pyrrolidine-2,4-dicarboxylic acid, the rate of insulin secretion also increased, supporting the observations made by Inagaki (Wea98, Ina95).

GABA and GLU secretion by islet cells. Despite the amount of work done in this area, there is insufficient information to demonstrate that either GLU or GABA is secreted in a glucose dependent manner from islet cells. In the earliest study on glucose-stimulated GABA secretion, pieces of freshly dissected rabbit pancreas were transferred from a low glucose to high glucose media. When the media was analyzed, the high glucose media contained more GABA (Ger80), however, since whole pieces of pancreas were used, it was not possible to determine if the GABA released came from the acinar pancreas, endocrine pancreas, or nerves. In studies with isolated islets, GABA secretion from islets was detected, however, the secretion was not enhanced by glucose (Ror89). Using isolated islets, GLU secretion enhanced by glucose was reported, however, no quantitative information or statistical significance was reported (Wea98).

In studies using cell lines derived from mouse β-cells, similar glucose dependency experiments have been performed. Using the βTC3 line, potassium stimulated GABA secretion was observed from cells, however, basal levels and glucose stimulated levels could not be observed since the GABA concentration at these levels was at or below the detection limit of the analytical method used (Tho93). Using a more differentiated cell line, GABA secretion from βTC6 cells was demonstrated to be modulated by extracellular glucose (Gas96). In this study islets that were incubated in 10 mM glucose for 12 hours prior to secretion experiments secreted less GABA when the cell media was changed to 1 mM glucose during a 2 hour secretion experiment (Gas96). When cells that

were incubated in 1mM glucose during the 12 hour pre-incubation period were placed in 10 mM glucose, no significant change in GABA secretion was observed.

In a series of studies by Pipeleers, GABA secretion from rat β-cells was studied (Smi96b, Smi97). In the latter study, GABA secretion from these cells did not change with increasing extracellular glucose, however when the media was supplimented with 2.0 mM glutamine, the GABA release was observed to decrease with increasing glucose (Smi97). Since the cell content of GABA was also measured after the secretion studies, it was determined that the cells exposed to the elevated glucose levels during the 24 hour secretion test also contained ~28% less GABA at the end of the experiments. This indicated less GABA was produced by the cells in high glucose media, even when supplimented with 2.0 mM glutamine. Regardless of the extracellular media used in these experiments, the cells secreted 5 times their GABA content during the 24 hour period.

In this work, the automated, high sensitivity amino acid analyzer was used to profile amino acid secretion from single islets. The individual islets were placed in a microperfusion system and sampled with 2 minute temporal resolution. The islets were tested for both glucose and potassium dependent neurotransmitter amino acid secretion.

Experimental

Reagents. Amino acids, iodoacetamine (IAA), *o*-phthalaldehyde (OPA, >99% purity), 2-methyl-2-propanethiol (*tert*-butyl thiol), and boric acid were of the highest purity grade from Sigma or Aldrich (St. Louis, MO). All buffer salts and solvents were obtained from Fisher (Fairlawn, NJ). The phosphate buffer salts were enzyme grade while other salts

were certified A.C.S. grade. Water, acetonitrile, and methanol were HPLC grade. All solutions were made in clean glassware and filtered (as described in previous chapters). All derivatization reagents and reactions were prepared and preformed as described in Chapters 3 and 4.

Automated, amino acid analysis. The FAMOS-based, high pressure gradient elution, capillary liquid chromatography system has been described in detail previously. The precision of the amino acid analyzer was tested every two days by analyzing 3 replicate amino acid standards (50 nM) and calibration curves were constructed daily. The relative standard deviation of peak height and area using the amino acid analyzer was less than 5% for all the amino acids analyzed.

Biological buffers. Kreb-Ringer bicarbonate buffer (KRB) consisted of 120 mM NaCl, 4.8 mM KCl, 1.2 mM in $MgCl_2$ and Na_2HPO_4, 3 mM D-glucose, 2.5 mM $CaCl_2$, and 24 mM $NaHCO_3$ at pH 7.4 which was maintained by continual sparging with 95/5% air/CO_2 mix at 37° C. Higher glucose buffer (16.7 mM) were made by adding the appropriate mass of glucose to 100 mL of KRB. High potassium KRB was made to 60 mM KCl with 64.8 mM NaCl. The KRB buffers were continuously sparged during the day to maintain the necessary pH. Without sparging, the pH became basic within one hour. Due to the presence of trace level amines that interfered with the neurotransmitter analysis, "biological" buffers such as HEPES, TES, or TRIS could not be used in these studies. Interestingly, the ethane sulfonic acid-based buffers (HEPES, TES) contained ~ 0.001 % (% w/w/) amounts of an amine that co-eluted with TAU (amino-ethanesulfonic acid). Although not discussed in previous chapters, the use of the biological buffers could not

be used due to the trace levels amine contaminants present in every buffer tested (HEPES, TES, TRIS, TRICENE, MOPS, and MOPSO).

Microperfusion system. The microperfusion system used in this work is similar to that described by Tao98, but modified slightly. The flow control of the perfusion system was controlled using a CMA microsyringe pump (Sweden) and a flowrate of 1 μL/min (Figure 5-2). To incubate the islet chamber at the appropriate temperature (37 °C) a water bath was used to pre-heat 1.5 L of water to 50 °C. The heated water was mixed with tap water to obtain a final temperature of 37 °C that was maintained throughout the day using a heating element. The fluid connections were all made using 150 μm/360 μm (i.d./o.d.) capillary and Teflon connectors. A Cheminert 4-port valve was obtained from VICI and used to switch the perfusion flow from 3.0 mM glucose- KRB to the test stimulant. The outlets of the 4-port valve were matched to provide a steady backpressure to the syringe pumps which was required to maintain reproducible flowrates. The capillary used to connect the valve to the islet chamber was 11.4 cm in length (2.01 μL).

The void time of this system was measured by connecting the outlet of the system to a UV-absorbance detector (Spectra 100 model Spectra-Physics, San Jose, CA). Ascorbic acid was added to a KRB buffer and was monitored using λ_{abs}=260 nm. The void time using a flow rate of 1 μL/min was ~ 6 minutes, therefore all switching times were offset by this delay time.

The islet holder was constructed using a 250/360 μm capillary that was 5 cm in length. One end of the capillary was fitted with a sintered glass frit using 15 μm borosilicate glass beads (Duke Scientific, Palo Alto, CA). Due to the small bead size, the frits made in the 250 μm i.d. capillaries were longer than desired (> 500 μm), despite

efforts o reduce the frit size. The use of larger diameter beads for the frits was unsuccessful due to scattering of the particles during the frit sintering process. When similar frits were made using 150 μm i.d. capillary, much narrower frits could be made by inserting a 100 μm o.d. length of capillary to prevent beads from entering more than 100 μm into the capillary outlet during the frit making procedure. However, these capillaries could not accommodate some islets that were 200 μm in diameter.

These holders were designed to be easier to use the Teflon holder described previously (Tao98) and to have a greatly reduced dead volume. The islets could be removed directly from the media using a stereomicroscope since the holder outlet (360 μm) was of similar dimension to the islet. Using the Teflon holder, the outlet (1587.5 μm) obscured the islet during the pickup process making the process time consuming.

Islet procedure. Mouse islets were isolated and cultured using previously described techniques (Hua95). Islets were cultured in RPMI 1640 cell culture media supplemented with 10% fetal bovine serum, 1% penicillin, and 1% streptomycin. The islets remained in culture for either 1 or 24 hours in 6 or 10 mM glucose, as mentioned in the text. Individual islets were removed directly from culture media and placed into the microperfusion system for 30 minutes prior to collection of fractions. During this time, a 3 mM glucose supplemented KRB was used to perfuse the islet. Between islet experiments, the KRB solution in the syringe pumps were replaced with fresh KRB to maintain a pH and O_2 levels throughout the day. The experiments proceeded in the following order: basal, glucose stimulation, basal, potassium stimulation.

Results and Discussion

Performance of islet holder. The new islet holder made it considerably easier to manipulate single islets. Since the islet was also housed in the transparent fused silica holder, the physical appearance of the islet could be observed once the islet holder was installed on the microperfusion system (Figure 5-3). Since the islet is at the outlet of the perfusion system, there is a negligible pressure drop across the islet, which was a concern in the previous islet holder. Upon magnification, the finer features of the islet can be observed (Figure 5-4).

Amino acid secretion from single islets. In every islet tested, the same 16 amino acids present in the microdialysis samples were also present in the islet perfusates. The amino acid, HIS, was not analyzed in this studies since it often was at or below a signal-to-noise ratio of 10, the limit of quantitation (<0.6 nM). In all, 12 islets were tested for both glucose-dependent and potassium-dependent amino acid secretion (Figure 5-5 and Figure 5-6). The complied data indicated that although GABA secretion did increase for both glucose (3.4-fold) and potassium (3.9-fold) the variation between the islets reduced the significance of these changes (Figure 5-5 and Figure 5-6). The changes in GLU were also small, and not significant. Statistical analysis of the difference between matched sets of basal and sitmulated samples did not increase the statistical significance.

Of the 12 islets tested, only 4 demonstrated both glucose and potassium-dependent changes in GABA secretion (Figure 5-7 and Figure 5-8). This subset of islets also displayed glucose sensitive GLU secretion. However, the large islet-to-islet variation in basal level (<0.14 to 6 nM) and in glucose stimulated levels (44 – 110 nM) did not permit significant changes to be observed. Within this same subset, the change in

GABA secretion, expressed as percent basal, for glucose stimulation varied from 270 (islet 11) to 10,300% (islet 4) and for potassium stimulation 230 (islet 11) to 37,700% (islet 4). Since the data is time resolved for some islets, the relative change in amino acid concentration can be plotted as a function of perfusion time (Figure 5-9). The two islets shown in this plot are from two different sets of islet (figure caption).

The large variations in GABA secretion from islet to islet could be due to poor transport of the GABA secreted by the β-cells, which are present in the inner mantle of the islet. This requires the secreted GABA be transported through layers of cells, reducing the concentration of GABA inn the perfusion media. Another possibility for the observed heterogeneity could arise from digestion process used to isolate the islets. Transport properties in over-digested islets would be enhanced relative to lesser digested islets since some of the outer cell layers would be removed.

In conclusion, these experiments do not resolve the issue of glucose stimulated GABA or GLU secretion from islets of Langerhans. Comparison to the literature on this subject is difficult due to the absence of any quantitative data even though several different groups have attempted similar studies (Gar79b, Ror89, Tho93, Smi96b, Smi97, Wev98). Islets obtained from the same isolation were tested using ancillary techniques and found to be viable, therefore, the health of the islets was not questioned as a factor in these results. Since 4/12 of the islet expressed both glucose and potassium sensitivity, it is possible that there is heterogeneity of the islets within the pancreas.

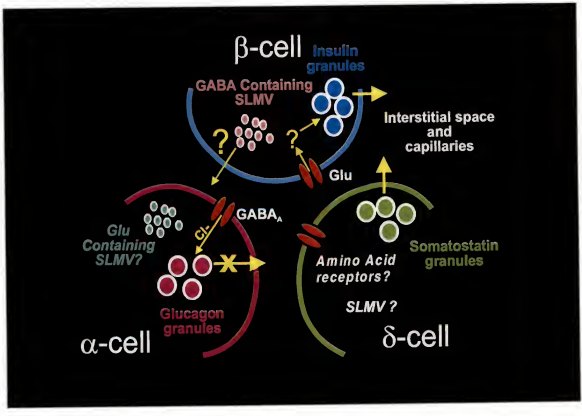

Figure 5-1: Representative cell types found in pancreatic islets of Langerhans.

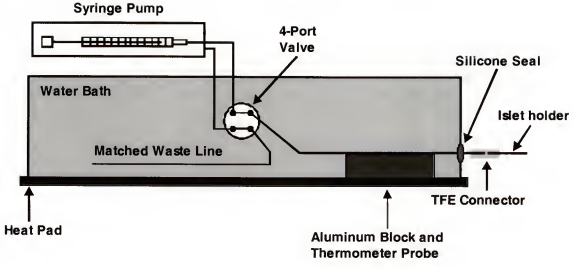

Figure 5-2: Microperfusion system.

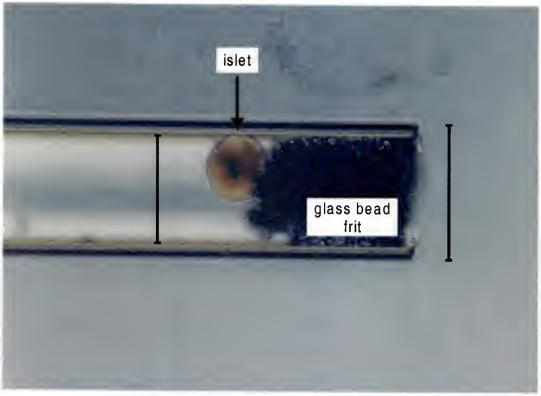

Figure 5-3: Islet holder with islet (full view). The scale bars within the capillary is 250 μm and the scale bar to the right of the capillary is 350 μm.

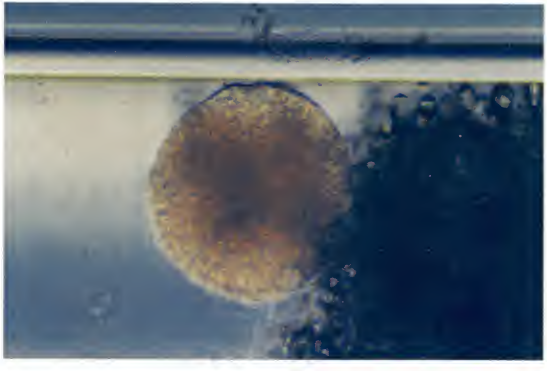

Figure 5-4: Islet holder with islet (islet only)

Amino Acid	3.0 mM Glucose ± S.E. (nM)	16.7 mM Glucose ± S.E. (nM)	P < from basal
ASP	25 ± 4	28 ± 6	0.389
GLU	20 ± 6	18 ± 5	0.399
ASN	15 ± 2	12 ± 3	0.184
GLN	59 ± 15	38 ± 10	0.149
CIT	2.6 ± 1	1.7 ± 0.4	0.148
ARG	110 ± 30	100 ± 20	0.390
SER	90 ± 20	69 ± 8	0.161
PEA	2.8 ± 1	2.1 ± 1	0.237
THR	23 ± 4	19 ± 3	0.253
GLY	100 ± 20	110 ± 20	0.452
TYR	8.6 ± 2	11 ± 4	0.324
ALA	44 ± 9	37 ± 7	0.246
β-ALA	4.1 ± 2	2.1 ± 1	0.228
TAU	14 ± 7	14 ± 6	0.489
GABA	2.2 ± 1	7.5 ± 5	0.136
ARG/CIT	78 ± 30	59 ± 10	0.277

Figure 5-5: Glucose stimulated amino acid secretion from 12 individual islets. For time resolved measurements, the mean (n=6) value for each islet is listed.

Amino Acid	3.0 mM Glucose ± S.E. (nM)	60 mM Potassium ± S.E. (nM)	P < from basal
ASP	25 ± 4	40 ± 10	0.081
GLU	20 ± 6	21 ± 5	0.413
ASN	15 ± 2	14 ± 4	0.439
GLN	59 ± 15	62 ± 40	0.469
CIT	2.6 ± 1	5.1 ± 2	0.114
ARG	110 ± 30	79 ± 20	0.195
SER	90 ± 20	95 ± 20	0.431
PEA	2.8 ± 1	2.7 ± 1	0.448
THR	23 ± 4	31 ± 6	0.150
GLY	100 ± 20	160 ± 30	0.083
TYR	8.6 ± 2	13 ± 3	0.149
ALA	44 ± 9	65 ± 20	0.131
β-ALA	4.1 ± 2	3.9 ± 2	0.469
TAU	14 ± 7	19 ± 10	0.358
GABA	2.2 ± 1	8.5 ± 5	0.107
ARG/CIT	78 ± 30	32± 9	0.076

Figure 5-6: Potassium stimulated amino acid secretion from 12 individual islets. For time resolved measurements, the mean (n=6) value for each islet is listed.

Amino Acid	3.0 mM Glucose ± S.E. (nM)	16.7 mM Glucose ± S.E. (nM)	P < from basal
ASP	18 ± 5	15 ± 5	0.346
GLU	15 ± 30	19 ± 8	0.364
ASN	16 ± 4	12 ± 4	0.219
GLN	91 ± 40	62 ± 30	0.301
CIT	1.4 ± 0.2	1.7 ± 0.3	0.308
ARG	180 ± 80	130 ± 50	0.337
SER	93 ± 90	63 ± 10	0.278
PEA	1.1 ± 0.3	2.0 ± 1	0.241
THR	21 ± 3	19 ± 5	0.369
GLY	67 ± 30	88. ± 40	0.322
TYR	4.7 ± 2	17 ± 10	0.168
ALA	32 ± 10	36 ± 10	0.406
β-ALA	0.7 ± 0.1	1.1 ± 0.2	0.135
TAU	13 ± 8	14 ± 2	0.459
GABA	1.8 ± 1	17 ± 10	0.139
ARG/CIT	150 ± 70	77 ± 10	0.190

Figure 5-7: Glucose stimulated amino acid secretion from 4 islets that were glucose sensitive. For time resolved measurements, the mean (n=6) value for each islet is listed.

Amino Acid	3.0 mM Glucose ± S.E. (nM)	60 mM Potassium ± S.E. (nM)	P < from basal
ASP	18 ± 5	17 ± 6	0.417
GLU	15 ± 30	21 ± 10	0.353
ASN	16 ± 4	8.1 ± 4	0.100
GLN	91 ± 40	30 ± 12	0.116
CIT	1.4 ± 0.2	2.9 ± 2	0.218
ARG	180 ± 80	90 ± 40	0.187
SER	93 ± 90	60 ± 20	0.270
PEA	1.1 ± 0.3	1.2 ± 1	0.477
THR	21 ± 3	23 ± 3	0.342
GLY	67 ± 30	54 ± 40	0.401
TYR	4.7 ± 2	11 ± 8	0.225
ALA	32 ± 10	23 ± 10	0.302
β-ALA	0.7 ± 0.1	0.8 ± 0.5	0.448
TAU	13 ± 8	12 ± 10	0.491
GABA	1.8 ± 1	21 ± 10	0.112
ARG/CIT	150 ± 70	40 ± 10	0.111

Figure 5-8: Potassium stimulated amino acid secretion from 4 islets that were glucose sensitive. For time resolved measurements, the mean (n=6) value for each islet is listed.

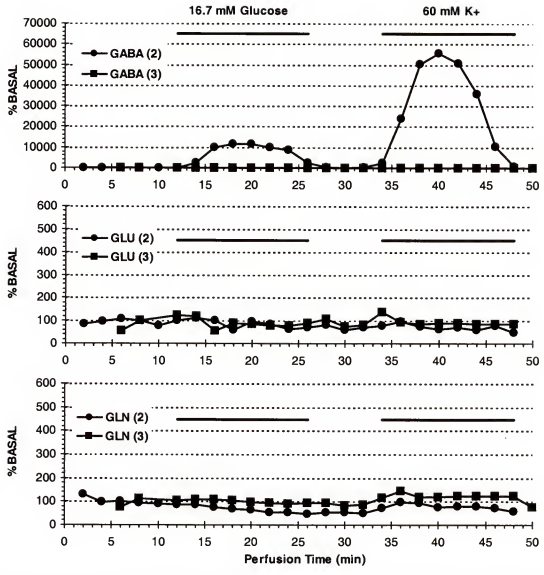

Figure 5-9. Time resolved measurements of amino acid secretion from single islets. The levels of GABA (A), GLU (B), and GLN (C) are shown for two different islets (islet 2 from set 1 and islet 3 from set 2). The data is plotted using %basal (([data point]/[basal])*100). The basal concentration is calculated from the first 4-5 points from each islet (8-10 minutes) after a 30 minute pre-incubation using 3.0 mM glucose supplemented KRB. The bars (16.7 mM glucose and 60 mM K^+) indicate which stimulant is interrogating the islet.

CHAPTER 6
RAPID, HIGH SENSITIVITY ASSAY FOR HUMAN CREATINE KINASE ISOENZYMES USING CAPILLARY ELECTROPHORESIS

Introduction

The creatine kinase enzymes are found in many different tissues in the human body and play a major role in the production of ATP for cellular energy and can also be used to assess traumatic injuries to these tissues. There are three different forms of the CK enzyme, CK-MM which is specific to skeletal muscle, CK-BB which is found predominantly in the brain, and CK-MB which is found specifically in the myocardium (heart tissue). During acute myocardial infarction (AMI), the blood supply to the heart from the coronary arteries is partially or fully blocked, causing diminished blood supply to myocardium resulting in cell death. As a result, the internal contents of the cell, including CK-MB and other cardiac specific proteins, are released into the blood stream. However, a majority of the other enzymes released during AMI such as myoglobin, aspartate aminotransferase, or lactate dehydrogenase are not cardiac-specific and can be released during non-cardiac injury such as trauma to skeletal muscle (Pul90). Furthermore, the time course of release and clearance for these enzymes are such that they will not show a significant increase in serum levels until 6-48 hours after the onset of AMI (Tie87, App92). Since thrombolytic therapy is most effective when administered

in the initial hours after the onset of AMI, it is necessary to develop assays that will accurately diagnose AMI in its early stages (Pul90, App92).

During AMI, the myocardium-specific isoenzyme, CK-MB2, is released into bloodstream where a plasma-based carboxypeptidase-*N* converts it to CK-MB1. Monitoring the plasma ratio of MB2/MB1 (Pul89) is a better early indicator of AMI than the commonly used total CK-MB since small changes in MB2 cause significant changes in the ratio that occur before the total plasma level of CK-MB passes the upper limit of normal. Currently, the only method of monitoring both the MB1 and MB2 isoenzymes is gel electrophoresis which uses the product of an enzymatic cascade (NADPH) for detection and quantitation of the isoenzyme in 25 minutes with a linear dynamic range of 0-30 U/l (Figure 6-1).

Capillary electrophoresis-based enzyme assays have recently been described by several groups (Bao92, Avi93, Har93, Xue94). In one permutation of the electrophoretically-mediated microanalysis (EMMA) format, a narrow, enzyme containing sample zone is introduced into the separation capillary (< 75 μm inner diameter) that contains the necessary reagents for the enzymatic production of a product. As the enzyme migrates along the separation capillary under an electric field (E) at one velocity (ν_E), the product of the enzymatic reaction is produced and migrates at its inherent velocity (ν_p).

$$\nu_e = \mu_e E \quad \text{and} \quad \nu_p = \mu_p E \qquad \text{equation 6-1}$$

$$\mu_e \propto z_e / M_e^{2/3} \quad \text{and} \quad \mu_p \propto z_p / M_p^{2/3} \qquad \text{equation 6-2}$$

Since the electrophoretic mobilities, or charge (z) to mass (M) ratio, of the product (μ_p) differs significantly from the much larger enzyme (μ_e), broad product zones are produced

(Bao92). In an alternative mode called the zero potential assay, the migration of the enzyme zone in the capillary can be stopped by removing the electric field (E) (Wu93, Har94,Xue94). This on-column incubation can be used to generate larger product signals, thereby increasing the sensitivity of the assay. Once the incubation time is complete, the electric field is restored and the product zone is migrated past the on-column detector (Figure 6-2). Assays performed using this format predominately use enzymes that produce a product that is spectrochemically different than the substrate, which fills the capillary column, greatly limiting the practicality of this approach for real biological applications. Using high sensitivity fluorescence detectors and enzymes with large turnover rates that produce fluorescent products such as alkaline phosphatase or lactate dehydrogenase (LDH), single enzyme molecules can be detected (Cra97, Xue95).

The specificity of the EMMA format permits certain enzymes to be detected, however, by performing an electrophoretic separation prior to the enzyme assay, individual isoenzymes of these enzymes can detected. After the isoenzyme separation, the isoenzyme zones can be assayed using the EMMA technique. Using separation conditions that separated 3 out of 5 total LDH isoenzymes prior to the enzymatic turnover step, the activity of 3 LDH isoenzymes was determined in single human erythrocytes (Xue94).

The goal of this work is to develop an enzyme assay for CK-MB1 and CK-MB2 that is based on a capillary electrophoresis isoenzyme separation prior to enzymatic turnover of adenosine diphosphate (ADP) to adenosine triphosphate (ATP) which is used for detection and quantification. This required the enzymatic turnover reaction be optimized for the capillary format, and the determination of separation conditions to

resolve the CK-MB1 and CK-MB2 isoenzymes. The enzyme product zones were detected by displacement using an ultraviolet-absorbance detector (UV). The optimization of the turnover reaction allowed 1.4 nM (~ 80 U/l) of both MB1 and MB2 to be detected using a UV detector in a total analysis time of 12 minutes for a zero potential assay. To enhance the sensitivity of this assay, the bioluminescent reaction of ATP and firefly luciferase was explored using post-column detection.

Experimental

Reagents. ATP, ADP, creatine (C), phosphocreatine (PC), *N*-acetyl cysteine (NAC), ethylenediaminetetraacetic acid (EDTA), acrlyamide, *N',N',N',N'*-tetrramethylethylenediamine (TEMED), β-mercaptoethanol (β-ME), and γ-methacryoxytripropyl silane (MAPS) were obtained from Sigma/Aldrich (St. Louis, MO). The acetic acid (HAc), hydrochloric acid (HCl), potassium persulfate, trishydroxy-amino-methane (tris), phosphate buffers, and other salts were or A.C.S. or enzyme grade from Fisher Scientific (Fairlawn, NJ). The human CK-MB isoenzyme were obtained from Scripps Laboratories (La Jolla, CA) as a gift from Soane BioSciences (Hayward, CA). Phosphate buffers were made from concentrated solutions of monobasic and dibasic phosphate stocks (0.5 M).

Enzyme storage solutions. All enzyme dilutions were made using a 5 mM succinate, 1 mM EDTA, 5 mM β-ME, and 10 mM NaCl solution buffered at pH 7.0. This was done at the manufacturers suggestion (Scripps). Enzyme standards diluted to nanomolar concentrations in the buffer were observed to maintain their activity over a period of two days.

Off-column assay. In these experiments the substrate mixture to be tested (100 μL) was placed in a 500 μL polypropylene centrifuge tube. To initiate the reaction, 500 nM of a CK isoenzyme mix (1 μL, CK-Isotrol, Sigma) was spiked into the substrate and this reaction was sampled every 60 s. CK Isotrol was used for these experiments since it is significantly less expensive then the purified CK-MB isoenzymes. However, as a control after the substrate buffer was optimized, the turnover rate was tested with CK-MB1 to test for any derivations. No difference was observed.

Electrophoresis was performed using an effective separation length of 4 cm (minimum distance that can be used using this absorbance detector) and a polyacrylamide coated capillary to reduce electroosmotic flow and prevent fouling of the capillary surface by the enzyme mixture (which was 5 % bovine serum albumin). This separation took 45 s using 30 kV potential.

On-column assay. After optimization the substrate containing buffer used for the on-column assay was made as follows: 3 mM PC, 5 mM NAC, 2.5 mM $MgCl_2$, and 0.5 mM ADP in a 50 mM phosphate buffer pH 6.8. To use higher potentials without increasing Joule Heating, a 25 μm i.d. capillary (30 cm total length) was used with a 9 cm effective separation distance. This allowed 30 kV be applied using this substrate buffer while maintaining a power dissipation of < 0.02 W/cm. For all the on-column assays, data acquisition began when the separation voltage was re-applied after the on-column incubation, or zero-potential step.

Linear polyacrylamide coated capillaries. Prior to coating, the fused silica capillaries (25 or 50 μm inner diameter) were cut to the desired final length and a small segment of polyimide coating was removed to form an on-capillary detection window. The capillary

was then rinsed with successive washes of 1 N HCl (1 hour), de-ionized water (0.5 hour), 1 N NaOH (1 hour), de-ionized water (0.5 hour), and 5% HAc (0.5 hour). The HCl and NaOH washes were performed to produce as many surface silanol groups as possible and reduce the number of vicinal lone silanol groups which will not react with the silane. The HAc rinse was performed to protonate the silanol groups which is required to bond the MAPS to the fused silica capillary wall. The coating procedure is similar to that of Hjerten (Hje85). Briefly, a 3% (v/v) solution of MAPS (90 μL) was prepared in a matrix of 50% (v/v) ethanol and 5% HAc (3 mL) and passed through the capillary for 5 minutes (~ 20 μL) and then left to incubate under static conditions for 1 hour. After this step, a 4% (w/v) acrylamide aqueous solution was degassed for 10 minutes using He (g) sparging. After degassing, 1 μL/mL TEMED and 2 mg/mL potassium persulfate were added and the solution was flushed through the capillary for 5 minutes to pass several column volumes, and then left to incubate under static conditions for 1 hour. After this last incubation, the extremely viscous acrylamide solution was removed from the capillary using a 5% HAc solution and washed for several minutes. The capillary was then conditioned with the electrophoresis buffer for 30 minutes prior to use.

Capillary electrophoresis. The data acquisition system was identical to those described in all the previous chapters except the output of the digital-to-analog converter (DAC OUT) from the National Instruments AT-MIO-16 board (Austin, TX) was connected to the voltage control input on a Spellman CZE-100 (Plainview, NY) high voltage power supply to remotely control the high voltage power supply (Figure 6-3). A Spectra-Physics model Spectra 100 ultraviolet-visible absorbance detector (San Jose, CA) was used for on-column detection. The backpanel switches of this detector were set to a 1 V

full-scale setting and the analog-to-digital converter gain on the AT-MIO-16 was set on 10 to reduce the amount of bit noise observed at high detector gain settings. For experiments to directly detect the CK-MB isoenzymes, an absorbance wavelength of 210 nm was used and for detection of ATP and/or ADP a wavelength of 260 nm was used for more sensitive and selective monitoring. All of this work was done using high sensitivity detector settings (0.001 absorbance units, full-scale or 0.001 AU/V) and a rise time setting of 0.1 s.

Results and Discussion

Isoenzyme separation conditions. Attempts to separate the CK-MB isoenzymes using unmodified fused silica capillaries resulted in very broad and tailing peaks, indicating that the enzymes were adsorbing to the capillary surface. To reduce protein adsorption, the separation capillary was coated with a hydrophilic coating previously described (Hje85). This significantly improved the peak shape of the isoenzymes and permitted the separation of the major isoenzymes using a field strength of 350 V/cm (Figure 6-4). The effective separation distance (distance from inlet to on-column detection window) in these experiments was 9 cm. Analysis of the resulting peaks from the isoenzyme separation indicate that there are other forms of protein present in the sample and are seen as the shoulder between the two peaks and smaller peaks at ~3.5 minutes. The identity of these peaks is not known, but they do exhibit enzymatic activity similar to the primary CK-isoenzymes (see below). The presence of "atypical" CK-isoforms has been noted before using slab gel isoelectric focusing (Kan94).

Optimization of the enzymatic reaction. Using the EMMA format for the CK-MB assay, it was necessary to optimize the proportions of the ATP turnover reaction to make the final substrate solution compatible with the necessary electrophoresis and detection conditions. To maintain high separation efficiency in capillary electrophoresis, it is necessary to minimize the Joule heating generated during the separation. It was also necessary to reduce the amount of ADP present in the electrophoresis buffer to 0.5 mM to minimize disturbances in the detector's baseline (see below for explanation).

In addition to the required substrates for the ATP turnover reaction (ADP and phosphocreatine, PC) the reaction performs best at pH 6.8 (Ros67), and both magnesium and a free sulfhydryl group is also required since the actual substrate for the CK reaction is a ADP/Mg complex. The thiol is required to serve as a scavenger to prevent fouling of the enzymes active site (which contains a sulfhydryl group) (Ros67).

The reaction was optimized using off-column reactions that were sampled at 60 s intervals using capillary zone electrophoresis. The magnesium concentration was the first variable to be tested since it was the major contributor to the overall current generated during the separation (data not shown). After the minimum concentration of magnesium was added to the substrate buffer (0.1 mM), the enzyme turnover rate ($moles_{ATP} \bullet moles_{CK\text{-}MB}^{-1} \bullet min^{-1}$) stabilized quickly and did not increase with higher concentrations of magnesium (Figure 6-5).

Since the substrate buffer must also act as the isoenzyme separation buffer, the isoenzyme separation was tested using the Tris buffer and found to be quite poor. Therefore, the compatibility of the phosphate buffer (the best buffer for the isoenzyme separation) with the turnover reaction (Figure 6-5). Surprisingly the turnover reaction at

short incubation times performed significantly better using the phosphate buffer relative to the Tris buffer. Since this on-column incubation times this assay will be quite short, the heightened turnover reaction will greatly reduce the total analysis time significantly. This could be due to species present in the Tris buffer that fouled the active site of the enzyme. In all further experiments, the phosphate buffer was used in place of the Tris buffer.

Next the minimum amount of excess thiol (referred to as an activator in the literature) was determined. While very high concentrations are used in commercial preparations of this substrate mixture (24 mM), as little as 5 mM could be used without a noticeable decrease in turnover rate (Figure 6-5). The minimum concentration of PC required for these reaction demonstrated a similar independence at concentration greater than 3 mM (data not shown).

The final substrate buffer used in all subsequent on-column assays as follows: 0.5 mM ADP, 3.0 mM PC, 2.5 mM $MgCl_2$, and 5 mM NAC in a 50 mM phosphate buffer pH 6.8.

On-column assay. In these preliminary experiments, an absorbance detector was used to monitor the production of ATP by the CK-MB isoenzymes. This detection scheme is complicated somewhat, since ADP and ATP have very similar ultraviolet absorption characteristics, with λ_{max} of 260 nm. Since the capillary is filled with the substrate buffer that contains 0.5 mM ADP, there is a large continuous background absorbance. However, during the enzyme reaction, the ADP concentration in the enzyme zone is depleted and ATP is formed. Since the electrophoretic mobilities of ATP is larger than that of ADP, when the electric field is turned on after the on-column incubation, these

zones will migrate quickly into an region of the capillary containing ADP, producing an additive signal composed of ATP and ADP, appearing as a series of peaks on top of the ADP background. The enzyme depleted regions will then appear dips in the ADP background. Monitoring the ATP formation will then be based on displacement of the ATP zones from the ADP-depleted zones. Characteristic electropherograms of an ATP and ADP separation and an on-column enzyme assay are displayed in Figure 6-2.

Electrokinetic injections were used to introduce small sample volumes (0.5 nL) into the capillaries for the enzyme assay. To perform these injections, the capillary inlet was dipped into a 10 μL sample containing the enzyme sample, a platinum electrode was inserted, and a potential of 25 kV was applied for a present period of time. Using a 2 s injection time and 25 kV field (60 cm capillary length) from a sample containing 5.7 nM CK-MB1 and 11 nM CK-MB2, an isoform separation time of 120 s at 30 kV, and a zero-potential incubation time of 120 s, the resulting ATP peaks from each isoenzyme are clearly visible (Figure 6-6). Although the sample concentration of CK-MB2 was twice that of CK-MB1, the lower electrophoretic mobility of CK-MB2 resulted in less CK-MB2 being injected onto the capillary. This made it difficult to calculate the mass injected since the enzyme is not directly detected. Using the electrophoretic mobility calculated from the Figure 6-4, it is estimated that 3.0 amol and 4.2 amol of CK-MB1 and CK-MB2 were injected into the capillary during this injection. The reproducibility for these assays are listed in Table 6-1. The resolution between the CK-MB1 and CK-MB2 ATP peaks was 1.3 ± 0.106 (n=4).

Table 6-1: Reproducibility of the on-column, zero-potential assay (n=4)

Enzyme	Migration Time R.S.D.	Peak Height R.S.D.	Height ratio (MB2/MB1)
5.7 nM CK-MB1	0.23	3.99	6.64
11.0 nM CK-MB2	0.30	3.45	

To determine the best isoenzyme separation time, the separation time was varied from 120 to 240 s using a 30 kV potential (Figure 6-7). The best results were obtained using a 120 s separation step. Although the major isoenzymes better separated at longer isoenzyme separation times, this also increased the resolution of the "atypical" isoenzymes present in this enzyme preparation. This suggests that the small peaks present in the Figure 6-4 that have electrophoretic velocities between that of the major CK-MB isoenzymes also possess similar enzymatic activities to that of the major isoenzymes.

Due to the enzymatic nature of the sample, the ATP signal can be increased for a given concentration by increasing amount of time the enzyme zones are permitted to incubate on the column after the isoenzyme separation. An example is seen in Figure 6-8, where the signal from a mixture of 2.85 nM CK-MB1 and 5.5 nM CK-MB2 is amplified 3-fold by increasing the zero-potential or incubation step 3-fold. Since the noise is not affected by the increased incubation time, detection limits are also increased 3-fold. However, in this reagent system, the ADP recycling that occurs in multiple enzymes systems is not present (Figure 6-1), therefore at excessively long incubation times all the ADP present in the enzyme zones will be depleted. Due to the large turnover rate of this enzyme in this optimized reagent buffer, the same 2.85 nM CK-MB1

and 5.5 nM CK-MB2 sample depleted the ADP in the sample zone in less than 8 minutes (Figure 6-8).

The linear dynamic range of this assay, using a 2 minute incubation time, ranges from 1.4 – 11 nM for CK-MB1 (r^2=0.990) and 2.75 – 22 nM for CK-MB2 (r^2=0.977) with the upper limit limited to the available ADP in the substrate buffer and the lower limit limited by the poor concentration sensitivity of the UV-absorbance detector used in this work (Figure 6-9). Even at the detection limits, the patterns of ATP peaks (large plateau generated during sample injection, isoenzyme separation, and the peaks generated during the on-column incubation) and ADP dips are clearly visible (Figure 6-10).

Improving detection limits. To improve the detection limits of this assay, a more sensitive detector is needed for ATP. The firefly luciferase (FFL) enzyme catalyzes the oxidation of D-luciferin in the presence of ATP and Mg^{2+} to produce light and several other products (Figure 6-11). One problem with this reaction is the very low turnover number associated with FFL, which has been estimated to be 6 min^{-1} due to the tight binding of the FFL*P product that causes end-product inhibition and the inhibition of the light producing reaction by pyrophosphate (PP) (Sel60, Del74).

Using a FFL reagent obtained from Sigma, a post-column bioluminescence detector was constructed. The effluent from the capillary exited into a stagnant solution containing the FFL reagent. The detection limits obtain using this system were nearly identical to the detection limits for detecting ATP using absorbance detection (~ 1.3 fmol). While detection limits of 0.1 fmol for ATP were obtained using a similar post-column detector and reagents, these detection were not obtainable using a microscope based bioluminescence detector (Dad94, Lad97).

The development of a highly sensitive assay for creatine kinase has been described. Using an optimized substrate buffer to maximize the turnover reaction, a relatively insensitive UV-absorbance detector could be used to obtain 1.4 nM (~ 700 zeptomoles/0.5 nL injection or 420,00 enzyme molecules) detection limits for CK-MB1, with a relative short total analysis time (12 min).

This method was originally developed for use on microfabricated analytical devices in collaboration with Soane BioSciences. Since the microfabricated devices were constructed out of a plastic which possess significant self-fluorescence, traditional methods of laser-induced fluorescence detection were not explored. For use in other analytical system, it would be interesting to explore the use of the enzyme cascade (Figure 6-1). Since no other species necessary for these reactions absorb at 340 nm, it should be possible to obtain lower detection limits than the previously described system. Another advantage of this approach is that ATP is recycled back to ADP in step 2, thereby eliminating the ADP depletion experiences in these studies, permitting the use of longer incubation times and lower detection limits. While the eletrophoretic mixing steps may be more complicated due to the larger number of substrates and enzymes required, the electrophoretic mobilities of these enzymes and substrates has been described previously (Avi93).

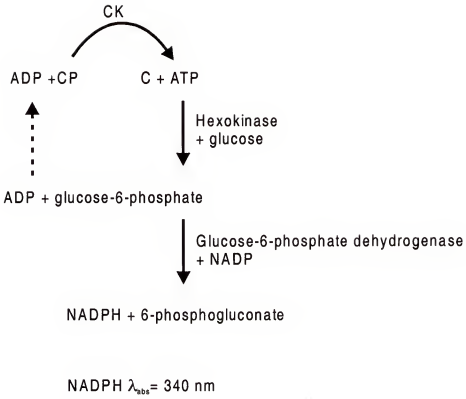

Figure 6-1: Detection of CK isoenzymes using a multiple enzyme cascade. The reactions to form the reporter molecule (NADPH) are solid. The dotted line is included to show the recycling of ADP after the hexokinase reaction.

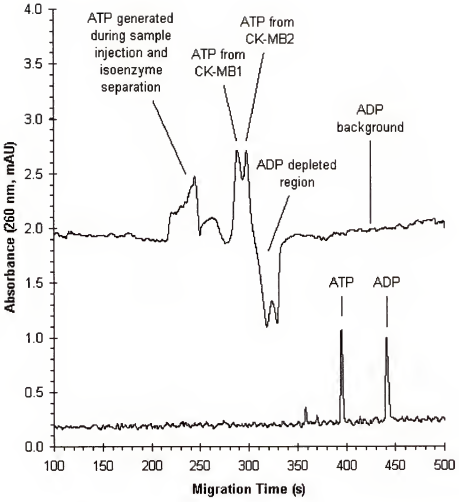

Figure 6-2: Electropherograms obtained during and zero-potential EMMA experiment and CZE separation of ADP and ATP standards

.

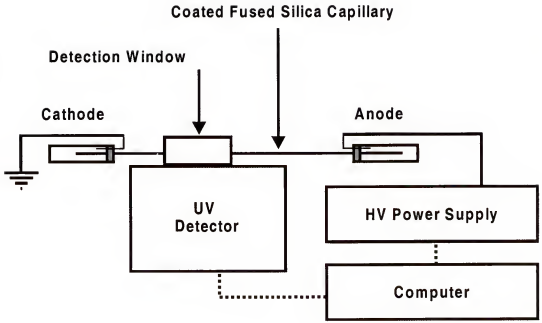

Figure 6-3: Schematic of the capillary electrophoresis system.

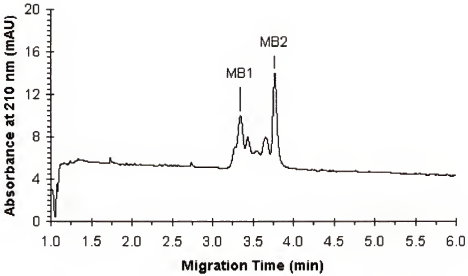

Figure 6-4: Separation of CK-MB isoenzymes using a polyacrylamide coated capillary. This separation was performed using a 50 mM phosphate buffer pH 6.8, in a 50 μm i.d. by 30 cm capillary. The effective separation distance was 9 cm, and the field strength was 350 V/cm (3.15 kV).

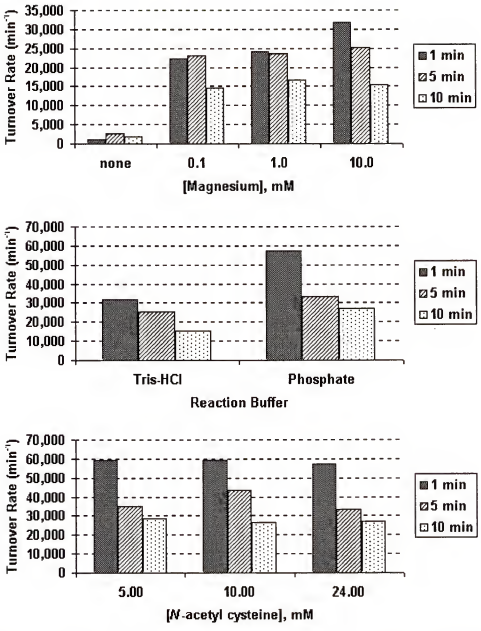

Figure 6-5: Effect of different reaction parameters on turnover rate. Top graph: concentration of magnesium, Tris buffer pH 6.8. Middle graph: Comparison of different reaction buffers. Bottom graph: Effect of excess thiol on turnover reaction rate.

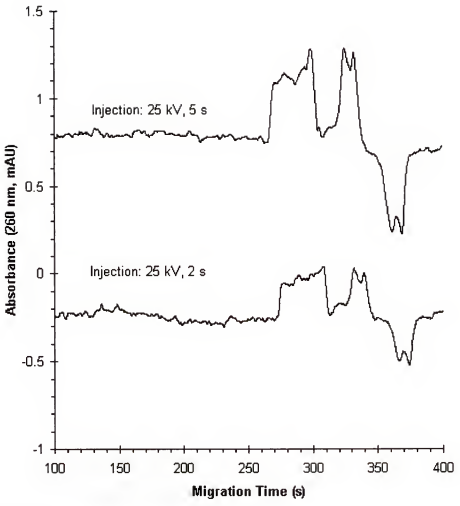

Figure 6-6: Varying sample injection time to increase the mass of enzyme loaded on the capillary.

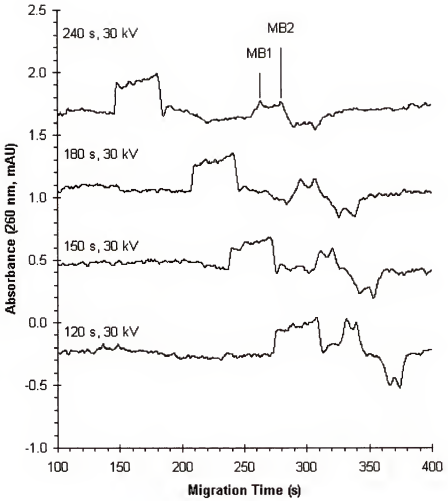

Figure 6-7: Isoenzyme separations at30 kV using different separation times. For each experiment 3.0 amol of CK-MB1 and 4.5 amol of CK-MB2 was injected using a 2 s injection time and 25 kV injection voltage. To minimize Joule heating a 25 μm i.d. capillary was used for these experiments.

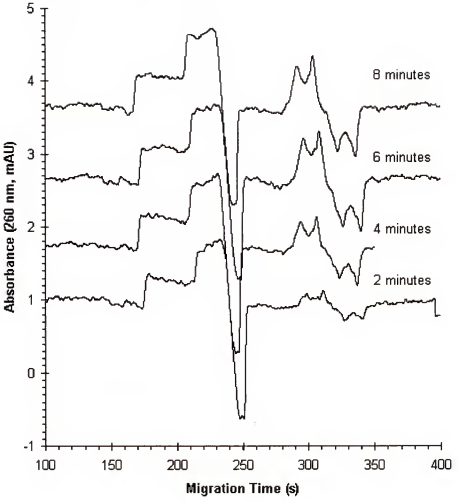

Figure 6-8: Signal amplification using longer incubation times.

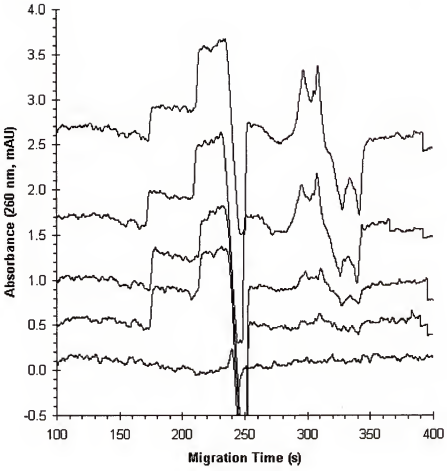

Figure 6-9: Electropherograms obtained from detection limit study.

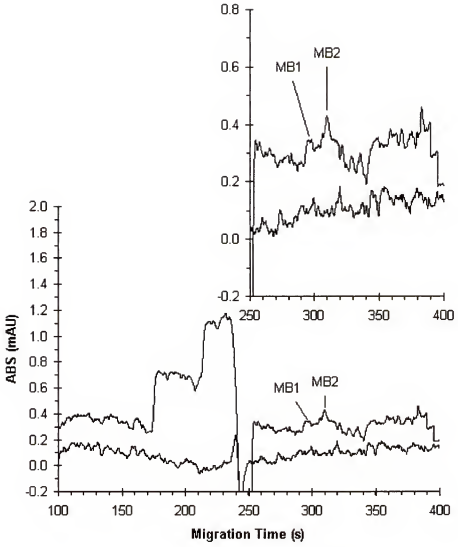

Figure 6-10: Electropherograms of blank and 1.4 nM CK-MB1 and 2.75 nM CK-MB2 isoenzymes. Even at the detection limit, the pattern of ATP generated during sample injection and isoenzyme separation and peaks and dips denote the presence of both isoenzymes.

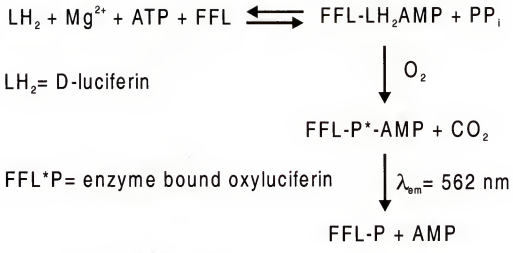

Figure 6-11: Firefly luciferase reaction

CHAPTER 7
CONCLUSIONS

In bioanalytical chemistry, the complex nature of the samples typically push conventional methods of analysis to their limits with regards to sensitivity and selectivity. While development of new, higher sensitivity detection strategies (Che88, Wei98), instrumental technology (Jac96a,Jac96b), and chemical reagents (Dem87) will push bioanalysis to new limits, the methods developed using these advances must be rigorously evaluated to ensure accuracy or precision are not compromised.

In this work, the cornucopia of methods used for amino acid analysis were thoroughly evaluated to determine the necessary characteristics required to develop a rugged, accurate method of amino acid analysis using microcolumn liquid chromatography and optimized electrochemical detector. The resulting method utilized a quantitative derivatization reaction and was tested using a wide range of biological samples. The use of sample preconcentration techniques permitted low concentration limits of detection to be obtained and permitted the analysis of nanoscale sample. The concentration limits of detection were realized only once amine contamination was reduced and the chemical background associated with the derivatization reaction was minimized. Nanoscale analysis was performed using conventional microdispensors by diluting the sample to microliter volumes prior to sample handling. The precision of the

method was increased using automated sample derivatization and injection. The sample throughput was increased by optimizing the separation to reduce analysis time.

The amount of chemical information obtained from the biological samples can be expanded further to include other neurotransmitters such as dopamine, noradrenaline, and seratonin, all of which possess primary amines that can be derivatized using the OPA reagent. However, due to the appreciable hydrophobicity of these derivatized amines, the elution window of the current method must be expanded by either using a less hydrophobic thiol in the derivatization reaction or by decreasing the hydrophobicity of the stationary phase used in these separations.

The separation time can also be reduced by using smaller particles, shorter columns, and higher flow rates. Since both column efficiency (N) and backpressure (ΔP) increase with decreasing stationary phase particle diameter (d_p):

$$N \propto 1/d_p^2 \qquad \text{and} \qquad \Delta P \propto 1/d_p^2$$

Mobile phase pumping system with higher backpressure are required to operate smaller particle columns at similar flowrates to larger particle columns. This requirement can be lessened by using shorter columns packed with small, pellicular particles that provide comparable efficiency to the longer, larger particle columns. The higher efficiency separation should also allow faster, steeper gradient to be used (Syn79).

Vigilant searches of the literature should also be made to continually assess the properties of new derivatization reagents. In addition to amine reactive reagents, the emergence of fluorogenic reagents selective for catecholamines offers great promise (Keh94). The development of labeling reagents that possess electroactive moieties that are electrochemically reversible are also enticing since recycling electrochemical

detection strategies could be used to amplify the signal-to-noise ratio thereby increasing sensitivity (Cox92, Ros99).

APPENDIX A
CONSTRUCTION OF PACKED CAPILLARY COLUMNS

Column blanks with recessed frits for in-column electrochemical detection were constructed using a packing technique in place of the ram-rod method. In the ram-rod method, glass beads used to make frits are first placed in the column by tapping the capillary end into a vial cap containing frit material (for 50 μm i.d. capillaries, 7.8 – 8 μm borosilicate glass beads) and then puching the beads the desired distance using a 20 μm o.d. tungsten wire (the ram-rod). The beads are then sintered in place using a flame or micro-arc. The ram-rod method produces very thin (3-5 bead length) frits but is time consuming (until mastered) and requires the use of micromanipulaltors. An alternative method was developed that is based on packing the frit material into a column blank using a high pressure bomb.

Capillary columns were cut to their desired length and 2 cm of polyimide was removed from each end. One end of the column was fritted by tapping the outlet end into a conical microvial containing 15.5 μm borosilicate glass beads. These beads were sintered by quickly tapping the end of the capillary into he cool region of a flame. This formed a temporary frit at the column outlet. Next a short length (2-3 cm) was packed with 7.8 μm borosilicate glass beads by placing the column inlet into a slurry (10 mg/mL beads in 2-propanol) contained in a gas pressurized high pressure bomb (300 psi). The bomb was quickly pressurized (10-30 s) until 1 cm of the column was observed to be

packed. At this point the bomb was de-pressurized, the inlet lifted above the level of the slurry, and then the pressure was re-applied. This served to transport the beads in the column to the outlet end and also dried out the packed bed which was 2-3 cm long after drying.

After constructing the packed bed, the outlet of the column (with the inlet still placed inside the bomb) was positioned between the two electrodes of a micro-arc. There are several variables to be considered when making the final frit. The sintering process is dependent on the current of the arc, the time spent in the arc, the dryness of the packed bed, and whether the high pressure bomb is pressurized. The first two variables can be tested by sintering a section of the packed bed near the temporary frit, which will be removed after the final frit is made. Partially wet beads will scatter the packed bed during the sintering process and should be avoided. It was also found that the sintering process can be slowed down by passing helium through the column during sintering. For identical arc setting and times, the sintering process is much faster in larger bore columns (> 150 μm i.d.) since the fused silica wall of the capillary is much thinner. Dissipating the heat by forcing helium through the column slows down this process making it more controllable. When the proper arc setting and time had been determined, the column was moved to place the very end of the packed bed, which was still coated with polyimide, between the electrodes. It was observed that the amount of time required to char the ploy imide from the capillary was similar to the required sintering time for 50 μm i.d. columns. Once the final frit was sintered, the bomb was pressurized, the temporary frit cut, and unsintered material removed from the capillary. If beads remained in the column, the outlet was placed into a beaker containing water and sonicated (Sonic Dismembrator).

The final frits produced by this method were observed to be 0.05 – 0.1 mm in length. While these frits are longer than those produced in the previous method, there was no observed decrease in separation efficiency. While adequate for derivatized amino acid analysis, effects of non-specific absorption due to the increased frit surface area for protein and peptide anlaysis should be considered. If non-specific adsorption is observed, these effects could be minimized by using dichlorodimethyl silane (DCMS).

The column blanks were slurry packed using Alltima C8 (5 μm diameter) particles. A slurry of 10 mg/mL in acetone was prepared and loading into a high pressure packing bomb. Columns of 40 cm were packed in 30 minutes using a pneumatic amplifer pump (Alltech) filled with propanol pressurized to 4000 psi. After packing, the pressure was bled from the bomb by slowly opening the prime/purge valve inline with the pump. If columns were to be stored prior to use, slurry solvent was left in the column and a small frit (15.5 μm beads) placed in the column inlet to prevent unpacking, and the ends dipped in propanol. Immediately prior to use, the column was fitted with the appropriate fitting and flushed with a 90% acetonitrile solution at 5000 psi for 20 minutes. Pressure was bled off by closing the prime/purge valve inline with the pump. After this final flushing step, the packed bed had compacted by 2-3 cm. The blank fused silica was trimmed from the column head and then placed in the chromatography system.

APPENDIX B
FAMOS USER PROGRAM

STEP	VOL. (μL)	COMMAND	LOCATION	SPEED	HEIGHT (mm)
1.		Inj. valve: load			
2.		Syringe valve: needle			
3.		Wait: 5 s			
4.	50	Wash			
5.	2.0	Aspirate	C	1	4
6.	1.0	Dispense	Waste	1	
7.	0.4	Dispense	Sample	1	4
8.		Wait: 5 s			
9.	1.8	Aspirate	Sample	1	4
10.	1.8	Dispense	Sample	1	4
11.	0.6	Dispense	Sample	1	4
12.	50.0	Wash	Waste	1	
13.		Wait: 5 min			
14.	2.0	Aspirate	D	1	4
15.	1.0	Dispense	Waste	1	
16.	0.4	Dispense	Sample	1	4
17.		Wait: 5 s			
18.	1.8	Aspirate	Sample	1	4
19.	1.8	Dispense	Sample	1	4
20.	0.6	Dispense	Sample	1	4
21.	50.0	Wash	Waste	1	
22.		Wait: 3 min			
23.	5.0	Aspirate	B	1	4
24.	2.0	Dispense	Waste	1	
25.	1.0	Aspirate	Sample	1	4
26.		Wait: 5 s			
27.	0.0	Aspirate	Sample	1	4
28.	2.4	Aspirate	B	1	4
29.		Wait: 5s			
30.	0.0	Aspirate	B	1	4
31.		Inj. Valve: inject			
32.		Marker: inj. pulse ON			

33.		Wait: 1 min
34.		Inj. Valve: load
35.	150.0	Wash
36.		Wait: 7 min
37.		End user program

This user program was written to perform 2-step derivatization (with 1 mixing step between reagent additions) of 2.0 μL sample contained in 0.25 μL tapered, polypropylene microvials. A modified micro-pickup injection is used to sandwich a small plug of sample (Step 25) between plugs of transport fluid (Reagent B). The reproducibility of this program is cited in Chapter 4.

A couple of unusual steps were included in the program to prevent air bubbles from being formed during the reagent addition steps and micro-pickup steps. Before the fused silica sample capillary comes in contact with the sample, an excessive amount of either derivatization reagent or transport fluid is aspirated through the system (2 μL for derivatization reagent, 5 μL for transport fluid). Typically, one half of this volume is dispensed to waste prior to addition to the sample. This is step was incorporated after it was observed that 25% of the samples derivatized without this step had very small bubbles in the remaining solution after the injection step. These bubbles adversely affected precision and were introduced by the sample capillary. These flushing steps eliminated these bubbles. Step 33 corresponds to the injection time and can be varied as necessary. Step 36 is the offset time between the beginning of the next derivatization reaction and the end of the gradient program.

APPENDIX C
PCR PLATE ADAPTER

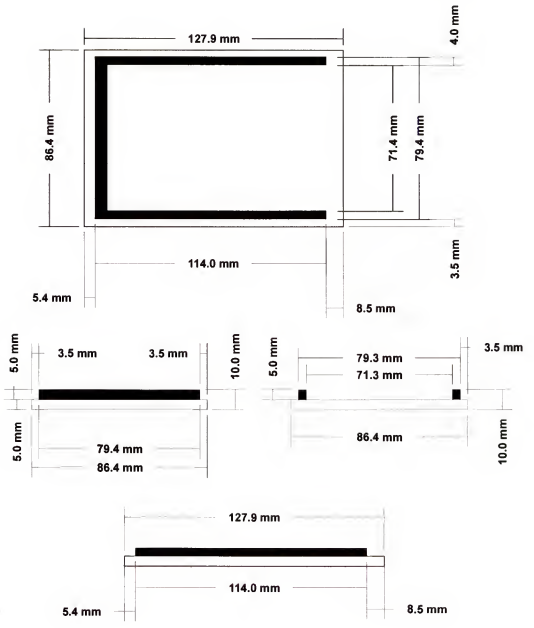

REFERENCES

All84 Allison, L.A., Mayer, G.S.; Shoup, R.E. *Anal. Chem.* **1984**, 56, 1089-1096

All96 Allin, S.M.; Hodkinson, C.C.; Taj, N *Synlett* **1996**, Aug, 781-782

Alv89 Alvarez-Coque, M.G.; Medina Hernández, M.J.; Villanueva Camañas, M.; Mongay Fernandez, O. *Anal. Biochem.* **1989**, 178, 1-7

And90 Anderson, J.J.; DiMicco, J.A. *J. Pharmac. Exper. Therap.*, **1990**, 255, 1399-1407

And92 Anderson, J.J.; DiMicco, J.A. *Life Sci.*, **1992**, 51, 623-630

App92 Apple, F.S., *Amer. Clin. Path.*, **1992**, 97, 217-225

Arr95 Arriaga, E.A.; Zhang, Y.; Dovichi, N.J. *Anal. Chim. Acta* **1995**, 299, 319-326

Asw84 Aswad, D.W. *Anal. Biochem.*, **1984**, 137, 405-409

Avi93 Avila, L.Z.; Whitesides, G.M. *J. Org. Chem.*, **1993**, 58, 5508-5512

Bae90 Baekkeskov, S.; Aanstoot, H.J.; Christgau, S.; Reetz, A.; Solimena, M.; Cascalho, M.; Folli, F.; Richter-Olesen, H.; De Camilli, P. *Nature*, **1990**, 347, 151-156

Bao92 Bao, J.; Regnier, F.E. *J. Chromatogr.*, **1992**, 608, 217-224

Bar97 Bardelmeijer, H.A.; Waterval, J.C.M.; Lingeman, H.; van't Hof, R.; Bult, A.; Underberg, W.J.M. *Electrophoresis*, **1997**, 18, 2203-2213

Bea90 Beal, S.C.; Hsieh, Y.-Z.; Wiesler, D.; Novotny, M. *J. Chromatogr.* A **1990**, 499, 579-587

Beq94 Berquist, J; Gilman, S.D.; Ewing, A.G.; Ekman, R. *Anal. Chem.* **1994**, 66, 3512-3518

Beq96 Berquist, J.;Vona, M.J.; Stiller, C.-O.; O'Connor, W.T.; Falkenberg, T.; Ekam, R. *J.Neurosci. Meth.* **1996**, 65, 33-42

Ber96a Bert, L.; Robert, F.; Denoroy, L.; Renaud, B. *Electrophoresis* **1996**, 17, 523-525

Ber96b Bert, L.; Robert, F.; Denoroy, L.; Stoppini, L.; Renaud, B. *J. Chromatogr.* A **1996**, 755, 99-111

Ber98 Bianchi, L.; Colivicchi, M.A.; Bolam, J.P.; Della Corte, L. *Neurosci.* **1998**, 87, 171-180

Bia99 Bianchi, L.; Della Corte, L.; Tipton, K.F. *J. Chromatogr. B*, **1999**, 723, 47-59

Bjo98 Björklund, J.; Einarsson, S.; Engström, A.; Grzegorczyk, A.; Becker, H.-D.; Josefsson, B. *J. Chromatogr.* A **1998**, 798, 1-8

Bou91 Bourdelais, A.; Kalivas, P.W. *J. Neurosci. Meth.* **1991**, 39, 115-121

Bov94 Bovingdon, M.E.; Webster, R.A. *J. Chromatogr.* B, **1994**, 659, 157-183

Boy98 Boyd, B.W.; Kennedy, R.T. *Analyst* **1998**, 123, 2119-2124

Bri72 Briel, G.; Gylfe, E.; Hellman, B.; Neuhoff, V. *Acta Physiol.* **1972**, 84, 247-253

Bri96 Britton, P.; Whitton, P.S.; Fowler, L.J.; Bowery, N.G. *J. Neurochem.* **1996**, 67, 324-329

Bru89 Bruckner, H.; Witter, R.; Godel, H. *J. Chromatogr.*, **1989**, 476, 73-82

Buc84 Buck, R.H.; Krummen, K. *J. Chromatogr. A*, **1984**, 315, 279-285

Buc87 Buck, R.H.; Krummen, K. *J. Chromatogr. A*, **1987**, 387, 255-256

But87a Butcher, S.P.; Hamberger, A. *J. Neurochem.*, **1987**, 48, 713-721

But87b Butcher, S.P.; Sandberg, M.; Hagberg, H.; Hamberger, A. *J. Neurochem.*, **1987**, 48, 722-728

Che79 Chen, R.F.; Scott, C.; Trepman, E. *Biochim. et Biophys. Acta*, **1979**, 576, 440-455

Che88 Cheng, Y.F.; Dovichi, N.J. *Science*, **1988**, 242, 562-564

Chi98 Chiu, D.T., Lillard, S.J.; Scheller, R.H.; Zare, R.N.; Rodriguez-Cruz, S.E.; Williams, E.R.; Orwar, O.; Sandberg, M.; Lundqvist, J.A. *Science* **1998**, 279, 1190-1193

Coh93 Cohen, S.A.; Michaud, D.P. *Anal. Biochem.* **1993**, 211, 279-287

Coh94 Cohen, S.A.; De Antonis, K.M. *J. Chromatogr.* A **1994**, 661, 25-34

Cox92 Cox, R.L.; Schneider, T.N.; Koppang, M.D. *Anal. Chim. Acta*, 262, 145-159

Cra97 Craig, D.B.; Arriaga, E.; Wong, J.C.Y.; Lu, H.; Dovichi N.J. *Anal. Chem.* **1997**, 69, 39A-43A

Dad94 Dadoo, R., Seto, A.G.; Colon, L.A.; Zare, R.N. *Anal. Chem.* **1994**, 66, 303-306

Dai97 Dai, F.; Burkert, V.P.; Singh, H.N.; Hinze, W. *Microchem. J.* **1997**, 57, 166-198

Das89 Dasgutpta, P.K.; Genfa, Z. *Anal. Chem.* **1989**, 61, 408-412

Del74 DeLuca, M.; McElroy, W.D. *Biochemistry*, 1974, 13(5), 921-925

Del90 Delanghe, J.R.; De Mol, A.M.; De Buyzere, M.L.; De Scheerder, I.K.; Wieme, R.J., *Clin. Chem.*, **1990**, 36(1), 149-153

Dem87 de Montigny, P.; Stobaugh, J.F.; Givens, R.S.; Carlson, R.G.; Srinivasachar, K.; Sternson, L.A.; Higuchi, T. *Anal. Chem.* **1987**, 59, 1096-1101

Dem90 DeMontigny, P.; Riley, C.M.; Sternson, L.A.; Stobaugh, J.F. *J. Pharm. Biomed. Anal.*, **1990**, 8, 419-429

Dim92 DiMicco, J.A.; Anderson, J.J. *Life Sci.* **1992**, 51, 623-630

Don88 Donzanti, B.A.; Yamamoto, B.K. *Life Sci.* **1988**, 43, 913-922

Dur88 Durkin, T.A.; Anderson, G.M.; Cohen, D.J. *J. Chromatogr. B* **1988**, 428, 9-15

Ein87 Einarsson, S.; Folestad, S.; Josefsson, B. *J. Liq. Chromaogr.*, **1987**, 10, 1589-1601

Erd86 Erdo, S.L.; Bowery, N.G. (Editors), *GABAergic Mechanisms in the Mammalian Periphery*, Raven Press, New York, **1986**

Esl87 Eslami, M.; Stuart, J.D.; Cohen, K.A. *J. Chromatogr.*, **1987**, 411, 121-138

Ewi94 Ewing, A.G.;Mesaros, J.M.;Gavin, P.F. *Anal. Chem.* **1994**, 66, 527A-537A

Fek96 Fekkes, D *J. Chromatogr.* A **1996**, 682, 3-22

Flo98 Floyd, P.D.; Moroz, L.L.; Gillette, R.; Sweedler, J.V. *Anal. Chem.*, **1998**, 70, 2243-2247

Fur90 Fürst, P.; Pollack, L.; Graser, T.A.; Godel, H.; Stehle, P. *J. Chromatogr.* A **1990**, 499, 557-569

Gar87a Garry, D.J.; Coulter, H.D.; McIntee, T.J.; Wu, J.Y.; Sorenson, R.L. *J. Histochem. Cytochem.*, **1987**, 35, 831-836

Gar87b Garry, D.J.; Sorenson, R.L.; Coulter, H.D. *Diabetologia*, **1987**, 30, 115-119

Gar88 Garry, D.J.; Appel, N.M.; Garry, M.G.; Sorenson, R.L. *J. Histochem. Cytochem.*, **1988**, 36, 573-580

Gas95 Gaskins, H.R., Baldeon, M.E.; Selassie, L.; Beverly, J.L. *J. Bio.Chem.*, **1995**, 270, 30286-30289

Ger79a Gerber, J.C. III; Hare, T.A. *Diabetes*, **1979**, 28, 1073-1076

Ger79b Gerber, J.C.; Hare, T.A. *Brain Res. Bull.* **1979**, 5, 341-346

Gid91 Giddings, J.C. *Unified Separation Science*, John Wiley and Sons, **1991**

Gil89 Gilon, P.; Remacle, C. *J. Histochem. Cytochem.* **1989**, 37, 1133-1139

Gil95 Gilman, D.S.; Ewing, A.G. *Anal. Chem.*, **1995**, 67, 58-64

Glo91 Globus, M.Y.T..; Busto, R.; Martinez, E.; Valdes, I.; Dietrich, W.D.; Ginsberg, M.D. *J. Neurochem.*, **1991**, 57, 470-478

God84 Godel,H.; Graser, T.; Földi, P.; Pfaender, P.; Fürst, P *J. Chromatogr.* A **1984**, 297, 49-61

God97 Godschalk, M.H.; Voerman, A.J.; Ooms, J.A.; Vissers, J.P.C. *Presented at The Pittsburgh Conference*, Atlanta, GA, March **1997** 102P

Gra85 Graser, T.A.; Godel, H.G.; Albers, S.; Földi, P; Fürst, P. *Anal. Biochem.* **1985**, 151, 142-152

Gyl73 Gylfe, E.; Hellman, B. *Endocrin.*, **1973**, 94, 1150-1156

Har80 Hare, T.A.; Manyam, N.V.B. *Anal. Biochem.*, **1980**, 101, 349-355

Har93 Harmon, B.J.; Patterson, D.H.; Regnier, F.E. *Anal. Chem.*, **1993**, 65, 2655-2662

Har94 Harmon, B.J; Leesong, I.; Regnier, F.E. *Anal. Chem.*, **1994**, 66, 3797-3805

Hje85 Hjerten, S. *J. Chromatogr. A,* **1985**, 347, 191-198

Hor95 Horn, T.; Bauce, L.; Landgraf, R.; Pittman, Q.J. *J. Neurochem.* **1995**, 64, 1632-1644

Hos86 Hoskins, J.A.; Holliday, S.B.; Davies, F.F *J. Chromatogr. B* **1986**, 375, 129-133

Hua95 Huang, L.; Shen, H.; Atkinson, M.A.; Kennedy, R.T. *Proc. Natl. Acad. Sci. USA*, **1995**, 92, 9608-9611

Ina95 Inagaki, N.; Kuromi, H.; Gonoi, T.; Toshimasa, O.; Ishida, H.; Seino, Y.; Kaneko, T.; Iwanaga, T.; Seino, S. *FASEB*, **1995**, 9, 686-691

Jac86 Jacobs, W.A.; Leburg, M.W.; Madaj, E.J. *Anal. Biochem.* **1986**, 156. 334-340

Jac87 Jacobs, W.A. *J. Chromatogr. A* **1987**, 392, 435-441

Jac94a Jacobson, S.C.; Koutny, L.B.; Hergenröder, R.; Moore, A.W.; Ramsey, J.M. *Anal. Chem.*, **1994**, 66, 3472-3476

Jac94b Jacobson, S.C.; Hergenröder, R.; Moore, A.W.; Ramsey, J.M. *Anal. Chem.*, **1994**, 66, 4127-4132

Jar86 Jarrett, H.W.; Cooksy, K.D.; Ellis, B.; Anderson, J.M. *Anal. Biochem.* **1986**, 153, 189-198

Jon81 Jones, B.N; Pääbo, S.; Stein, S *J. Liq. Chromatogr.* **1981**, 4, 565-586

Jon83 Jones, B.N.; Gilligan, J.P. *J. Chromatogr.*, **1983**, 266, 471

Jor81 Jorgenson, J.W.; Lukacs, K.D. *Anal. Chem.* **1981**, 53, 1298

Jos83 Joseph, M.H.; Davies, P. *J. Chromatogr. A* **1983**, 277, 125-136

Kam92 Kam, J.A.; Mohabbat, T.; Greenhagen, R.D.; C.J. Decedue; Lunte, S.M. *Current Sep.* **1992**,

Kan94 Kanemitsu, F.; Okigaki, T., *Clin. Chim. Acta*, **1994**, 229, 161-169

Kar74 Karger, B.L.; Martin, M.; Guiochon, G. *Anal. Chem.* **1974**, 46, 1640-1647

Kaw89 Kawasaki,; Higuchi, T.; Imani, K.; Wong, O.S. *Anal. Biochem.* **1989**, 180, 279-285

Kaw93 Kawagoe, K.T.; Zimmerman, J.B.; Wightman, R.M *J. Neurosci. Meth.* **1993**, 48, 225-240

Keh88 Kehr, J; Ungerstedt, U. *J. Neurochem.* **1988**, 51, 1308-1310

Keh94 Kehr, J. *J. Chromatogr. A*, **1994**, 661, 137-142

Keh94 Kehr, J. *J. Chromatogr. A* **1994**, 661, 137-142

Keh98a Kehr, J. *J. Chromatogr. B* **1998**, 708, 27-38

Keh98b Kehr, J. *J. Chromatogr. B* **1998**, 708, 49-54

Ken89a Kennedy, R.T.; Oates, M.D., Cooper, B.R.; Nickerson, B.; Jorgenson, J.W. *Science*, **1989**, 246, 57

Ken89b Kennedy, R.T.; Jorgenson, J.W. *Anal. Chem.* **1989**, 61, 1128-1135

Ken89c Kennedy, R.T, PhD. Dissertation, University of North Carolina at Chapel Hill, **1989**

Ken89d Kennedy, R.T.; Jorgenson, J.W. *Anal. Chem.* **1989**, 61, 436-441

Kil98 Kilkenny, M.L.; Slavik, M.; Riley, C.M.; Stobaugh, J.F. *J. Pharm. Biomed. Anal.*, **1998**, 17, 1205-1213

Kne84 Knecht, L.A.;Guthrie, E.J.;Joregenson, J.W. *Anal. Chem.* **1984**, 56, 479-482

Kwa90 Kwakman, P.J.M.; Koelewijn, H.; Kool, I.; Brinkman, U.A.Th.; De Jong, G.J. *J. Chromatogr. A* **1990**, 511, 155-166

Lad97 Lada, M.W.; Vickroy, T.W.; Kennedy, R.T. *Anal. Chem.* **1997**, 69, 4560-4565

Lau98 Lau, S.K.; Zaccardo, F.; Little, M.; Banks, P. *J. Chromatogr. A* **1998**, 809, 203-210

Lee96 Lee, T.T.; Yeung, E.S. *Meth. Enzmol.* **1996**, Chap. 19, 419-449

Lee98 Lee, I.H.; Pinto, D.P.; Arriaga, E.A.; Zhang, Z.; Dovichi, N.J *Anal. Chem.* **1998**, 70, 4546-4548

Lin79 Lindroth, P.; Mopper, K. *Anal. Chem.* **1979**, 51, 1667-1674

Liu91 Liu, J.; Hsieh, Y.-Z.; Wiesler, D.; Novotny, M. *Anal. Chem.* **1991**, 63, 408-412

Liu99 Liu, Y.-M.; Moroz, T.; Sweedler, J.V. *Anal. Chem.*, **1999**, 71, 28-33

Lo97 Lo, E.H., Pierce, A.R.; Matsumoto, K.; Kano, T.; Evans, C.J.; Newcomb, R. *Neurosci.* **1997**, 83, 449-458

Mat87 Matuszewski, B.K.; Givens, R.S.; Srinivasachar, K.; Carlson, R.G.; Higuchi, T. *Anal. Chem.* **1987**, 59, 1102-1105

Mch76 McHugh, W.; Sandmann, R.A.; Haney,W.G.; Sood, S.P.; Wittmer, D.P. *J. Chromatogr. A*, **1976**, 89, 361

Mic92 Michalik, M.; Erecinska, M. *Biochem. Pharmac.,* **1992**, 44 (1), 1-9

Mif89 Mifune, M.; Krehbiel, D.K.; Stobaugh, J.F.; Riley, C.M. *Chrombio.*, **1989**, 378, 56-70

Mol98 Molnár-Perl, I.; Bozor, I. *J. Chromatogr. A* **1998**, 798, 37-46

Mol99 Molnár-Perl, I.; Bozor, I. *J. Chromatogr. A* **1999**, 835, 73-91

Moo93 Moore, Jr.,A.W.; Joregenson, J.W. *Anal. Chem.* **1993**, 65, 188-191

Mor93 Moriari, M.; O'Connor, W.T.; Ungerstedt, U.; Fuxe, K. *J. Neurochem.* **1993**, 60, 1884-1893

Mor98 Mort, A.J.; Zhan, D.; Rodriguez, V. *Electrophoresis* **1998**, 19, 2129-2132

Nic86 Nickerson, B.;Jorgenson, J.W. *J. High Res. Chromatogr. & Chromatogr. Commun.* **1986**, 11, 878-881

Nov96 Novotny, M.V. *Methods Enzymol.* **1996**, Chapter 5, 101-132

Nus92 Nussbaum, M.A.; Przedwiecki, J.E., Staerk, D.U.; Lunte, S.M.; Riley, C.M. *Anal. Chem.* **1992**, 64, 1259-1263

Oat89 Oates, M.D.; Jorgenson, J.W. *Anal. Chem.* **1989**, 61, 432-435

Oat90 Oates, M.D., Cooper, B.R., Joregenson, J.W. *Anal. Chem.* **1990**, 62, 1573-1577

Ohk94 Ohkura,Y.; Kai, M.; Nohta, N. *J. Chromatogr. B* **1994**, 659, 85-107

Oka76 Okada, Y.; Taniguchi, H.; Shimada, C. *Science*, **1976**, 194, 620-622

Old97 Oldenburg, K.E.; Xi, X.; Sweedler, J.V. *Analyst* **1997**, 122, 1581-1585

Orw91 Orwar, O.; Folestad, S.; Einarsson, S.; Andiné, P.; Sandberg *J. Chromatogr. A* **1991**, 566, 39-55

Orw94 Orwar, O.; Sandberg, M.; Jacobson, I.; Sundahl, M.; Folestad, S. *Anal. Chem.* **1994**, 66, 4471-4482

Osh92 O'Shea, T.J.; Greenhagen, R.D., Lunte, S.M.; Lunte, C.E.; Smyth, M.R.; Radzik, D.M.; Watanabe, N. *J. Chromatogr. A* **1992**, 593, 305-312

Pal87 Pallister, D. *Current Sep.*, **1987**, 8, 53-57

Phi97 Phillips, Jr., J.B.; Cox, B.M. *J. Neurosci. Meth.* **1997**, 77, 211-220

Pul89 Puleo, P.R.; Guanagno, P.A.; Roberts, R.; Perryman, M.B. *Clin. Chem.*, **1989**, 35 (7), 1452-1455

Pul90 Puleo, P.R.; Guanagno, P.A.; Roberts, R.; Scheel, M.V.; Marian, A.J.; Churchill, D.; Perryman, M.B. *Circulation*, **1990**, 82(3), 759-764

Qu98 Qu, Y.; Arckens, L.; Vandenbussche, E.; Geeraerts, S.; Vandesande, F. *J. Chromatogr. A* **1998**, 798, 19-26

Ree91 Reetz, A.; Solimena, M.; Matteoli, M.; Folli, F.; Takei, K.; De Camilli, P. *EMBO*, **1991**, 10(5), 1275-1284

Rei94 Reinhoud, N.J.; Tjaden, U.R.; van der Greef, J. *J. Chromatogr. A* **1994**, 673, 255-266

Roa87 Roach, M.C.; Harmony, M.D. *Anal. Chem.* **1987**, 59, 411-415

Rob95 Robert, F.; Bert, L.; Denoroy, L.; Renaud, B. *Anal. Chem.* **1995**, 67, 1838-1844

Rob96 Robert, F.; Bert, L.; Lambãs-Señas, L.; Denoroy, L.; Renaud, B. *J. Neurosci. Meth.* **1996**, 70, 153-162

Rob98 Robert, F.; Bert, L.; Parrot, S.; Denoroy, L.; Stoppini, L.; Renaud, B. *J. Chromatogr. A* **1998**, 817, 195-203

Ror89 Rorsman, P.; Berggren, P.O.; Bokvist, K.; Ericson, H.; Mohler, Hanns, Ostenson, C.G.; Smith, P.A. *Nature*, **1989**, 341, 233-236

Ros67 Rosalki, S.B. *J. Lab. & Clin. Med.*, 1967, 69 (4), 696-705

Ros88 Rose, D.J.; Jorgenson, J.W. *J. Chromatogr.*, **1988**, 447, 117-131

Ros99 Rose, M.J.; Lunte, S.M.; Carlson, R.G.; Stobaugh, J.F. *Anal. Chem.*, **1999**, 71, 2221-2230

Rot71 Roth, M. *Anal. Chem.* 1971, 43, 880-882

Row95 Rowley, H.L.; Martin, K.F.; Marsden, C.A. *J. Neurosci. Meth.* **1995**, 57, 93-99

Sai94 Saito, K.; Horle, M.; Nakazawa, H. *Anal. Chem.* **1994**, 66, 134-138

Sat98 Satin, L.S.; Kinard, T.A. *Endocrine*, **1998**, 8(3), 213-223

Sel90 Seliger, H.H.; McElroy, W.D. *Archives of Biochem. And Biophys.*, 1960, 88, 136-141

Sem95 Semba, J.; Kito, S.; Toru, M. *J. Neural Transm.*[GenSect], **1995**, 100, 39-52

She97 Shen, H.; Lada, M.; Kennedy, R.T. *J. Chromatogr. B.* **1997**, 689, 43-52

Shi93 Shibanoki, S.; Kogure, M.; Sugahara, M.; Ishikawa, K. *J. Neurochem.*, **1993**, 61, 1698-1704

Shi95 Shirotani, T.; Shima, K.; Chigasaki, H. *Stroke*, **1995**, 26, 878-884

Sim77 Simons, Jr., S.S.; Johnson, D.F. *Anal. Biochem.* **1977**, 89, 251-255

Sim78a Simons, Jr., S.S.; Johnson, D.F. *Anal. Biochem.* **1978**, 90, 705-725

Sim78b Simons, Jr., S.S.; Johnson, D.F. *J. Org. Chem.* **1978**, 43, 2886-2891

Sko92 Skoog, D.A.; Leary, J.L. *Principles of Instrumental Analysis*, Saunders College Publishing, **1992**

Slo93 Sloss, S.;Ewing, A.G. *Anal. Chem.* **1993**, 65, 577-581

Smi96a Smith, C.U.M. (Ed.) *Elements of Molecular Neurobiology*, John Wiley and Sons, England, **1996**

Smi96b Smismans, A.; Devos, A.; Smolder, I.; Schuit, F.; Pipeleers, D. *Diabetologia*, **1996**, 39, SUPPL.1, 261-261

Smi97 Smismans, A.; Schuit, F.; Pipeleers, D. *Diabetologia*, **1997**, 40, 1411-1415

Smo95 Smolders, I.; Sarre, S.; Michotte, Y.; Ebinger, G. *J. Neurosci. Meth.* **1995**, 57, 47-53

Smt97 Smith, J.T. *Electrophoresis*, **1997**, 18, 2377-2392

Sny79 Snyder, L.R.; Dolan, J.W.; Gant, J.R. *J. Chromatogr. A*, **1979**, 165, 3-30

Sor91 Sorenson, R.L.; Garyy, D.G.; Brelje, T.C. *Diabetes*, **1991**, 40, 1365-1374

Spa58 Spackman, D.H.; Stein, W.H.; Moore, S. *Anal. Chem.*, **1958**, 30, 1190-1206

Stc85 St. Claire, R.L.; Jorgenson, J.W. *J. Chromatogr. Sci.* **1985**, 23, 186-191

Sto83 Stobaugh, J.F., Repta, A.J., Sternson, L.A.; Garren, K.W. *Anal. Biochem.* **1983**, 135, 495-504

Sve93 Sved, A.F.; Curtis, J.T. *J. Neurochem.* **1993**, 61I, 2089-2098

Swa98 Swanek, F.D.; Anderson, B.B.; Ewing, A.G. *J. Microcol. Sep.* **1998**, 10, 185-192

Tao98 Tao, L, Ph.D. Dissertation, University of Florida, 1998

Tho93 Thomas-Reetz, A.; Hell, J.W.; During, M.J.; Walch-Solimena, C.;Jahn, R. and De Camilli, P. *Proc. Natl. Acad. Sci. USA*, **1993**, 90, 5317-5321

Tho94 Thomas-Reetz, A.; De Camilli, P. *FASEB*, **1994**, 8, 209-216

Tie87 Tietz, N.W. (Ed.) *Fundamentals of Clinical Chemistry*, W.B. Saunders Co., US, **1987**

Tim95 Timmerman, W.; Westernik, B.H.C. *Neurosci. Letts.* **1995**, 197, 21-24

Tot93 Toth, E.; Vizi, E.S.; Lajtha, A. *Neuropharm.*, **1993**, 32, 827-832

Tuc97 Tucci, S.; Rada, P.; Sepúlveda, M.J.; Hernandez, L. *J. Chromatogr. B* **1997**, 694, 343-349

Uch94 Uchiyama-Tsuyuki, Y.; Araki, H.; Yae, T.; Otomo, S. *J. Neurochem.*, **1994**, 62, 1074-1078

Uhe91 Uhe, A.M.; Collier, G.R.; McLennan, E.A.; Tucker, D.J.; O'Dea, K. *J. Chromatogr A.*, **1991**, 564, 81

Und72 Undenfriend, S.; Stein, S.; Bohlen, P.; Dairman, W.; Leimgruber, W.; Weigele, M *Science*, **1972**, 178, 871-872

Ung84 Ungerstedt, U. *Measurement of Neurotransmitter Release In Vivo*, Marsden, C.A. (Ed.), John Wiley and Sons, **1984**

Van93 van Eijk, H.M.H, Rooyakkers, D.R.; Deutz, N.E.P. *J. Chromatogr. B* **1993**, 620, 143-148

Vis96 Vissers, J.P.C.;Arnoud, H.de R.;Ursem, M.;Chervet, J.-P. *J. Chromatogr. A* **1996**, 746, 1-7

Vis97 Vissers, J.P.C.;Claessens, H.A.;Cramers, C.A. *J. Chromatogr. A* **1997**, 779, 1-28

Wan97 Wang, Z.; Yeung, E.S. *J. Chromatogr. B*, **1997**, 695, 59-65

Wea98a Weaver, C.D.; Partridge, J.G.; Yao, T.L.; Moates, J.M.; Mangnuson, M.A.; Verdoorn, T.A. *Mol. Pharm.*, **1998**, 54, 639-646

Wea98b Weaver, C.D.; Gundersen, V.; Verdoorn, T.A. *J. Bio. Chem.*, **1998**, 273 (3), 1647-1653

Web88 Weber, S.G.;Long, J.T. *Anal. Chem.* **1988**, 60, 903A-913A

Wei98 Wei, J.; Gostkowski, M.L.; Gordon, M.J.; Shear, J.B. *Anal. Chem.* **1998**, 70, 3470-3475

Won85 Wong, O.S., Sternson, L.A.; Schowen, R.L. *J. Am. Chem. Soc.* **1985**, 107, 6421

Wu93 Wu, D.; Regnier, F.E. *Anal. Chem.*, **1993**, 65, 2029-2035

Xue94 Xue, Q.; Yeung, E. *Anal. Chem.*, **1994**, 66, 1175-1178

Xue95 Xue, Q.; Yeung, E. *Nature* **1995**, 373, 681-682

Zha95 Zhao, M.; Bada, J.L. *J. Chromatogr. A*, **1995**, 690, 55-63

Zho95 Zhou, S.Y.; Zuo, H.; Stibaugh, J.F.; Lunte, C.E., Lunte, S.M. *Anal. Chem.*, **1995**, 67, 594-599

BIOGRAPHICAL SKETCH

Brendan William Boyd was born on 27 March 1972 in Norfolk, Virginia. As a chemistry major at Furman University in Greenville, South Carolina, he conducted undergraduate research using capillary electrophoresis and capillary isotachophoresis under the direction of Dr. Jon F. Wheeler. The Bachelor of Science degree was conferred to him in June 1994. As post-graduate researcher at Furman, he developed methods to analyze the flavenoid compounds in fermented beverages using liquid chromatography with electrochemical and absorbance detection. This research combined two favorite pastimes, consuming fermented beverages and analytical chemistry. In the Fall of 1994, he began graduate studies in bioanalytical chemistry at the University of Florida under the direction of Dr. Robert T. Kennedy, in the Division of Analytical Chemistry within the Chemistry Department. There, his research focused on improving the concentration sensitivity of microscale separation-based analytical techniques used to analyze amino acids, peptides, and proteins.

I certify that I have read this study and that in my opinion it conforms to acceptable standards of scholarly presentation and is fully adequate, in scope and quality, as a dissertation for the degree of Doctor of Philosophy.

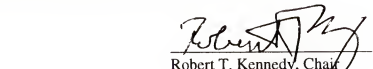

Robert T. Kennedy, Chair
Professor of Chemistry

I certify that I have read this study and that in my opinion it conforms to acceptable standards of scholarly presentation and is fully adequate, in scope and quality, as a dissertation for the degree of Doctor of Philosophy.

Richard Yost, Co-chair
Professor of Chemistry

I certify that I have read this study and that in my opinion it conforms to acceptable standards of scholarly presentation and is fully adequate, in scope and quality, as a dissertation for the degree of Doctor of Philosophy.

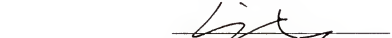

Weihong Tan
Assistant Professor of Chemistry

I certify that I have read this study and that in my opinion it conforms to acceptable standards of scholarly presentation and is fully adequate, in scope and quality, as a dissertation for the degree of Doctor of Philosophy.

Benjamin A. Horenstein
Associate Professor of Chemistry

I certify that I have read this study and that in my opinion it conforms to acceptable standards of scholarly presentation and is fully adequate, in scope and quality, as a dissertation for the degree of Doctor of Philosophy.

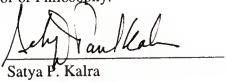

Satya P. Kalra
Professor of Neuroscience

This dissertation was submitted to the Graduate Faculty of the Department of Chemistry in the College of Liberal Arts and Sciences and to the Graduate School and was accepted as partial fulfillment of the requirements for the degree of Doctor of Philosophy.

August, 1999

Dean, Graduate School